UNIVERSITY OF CALIFORNIA,
IRVINE

Understanding ENSO Transition Complexity and its Underlying Dynamics

DISSERTATION

submitted in partial satisfaction of the requirements
for the degree of

DOCTOR OF PHILOSOPHY

in Earth System Science

by

Shih-Wei Fang

Dissertation Committee:
Professor Jin-Yi Yu, Chair
Professor Gudrun Magnusdottir
Professor Francois Primeau
Assistant Professor Michael Pritchard

2020

DEDICATION

To my parents, sisters, friends

and other significances along this journey

TABLE OF CONTENTS

LIST OF FIGURES

LIST OF TABLES

ACKNOWLEDGEMENTS

I would like to express my sincere appreciation to my advisor Prof. Jin-Yi Yu, who introduced me into the field of Earth Science and spent vast amount of time and effort on me throughout these years. His convincing guidance encouraged me to be professional and continue on my research journey. Without his persistent help, the goal of this dissertation would not have been realized.

I would like to thank my committee members, Professor Gudrun Magnusdottir, Professor Francois Primeau, and Professor Mike Pritchard for their constructive suggestions to excellent my thesis work. I also thanks Professor Kuolin Hsu being my Ph.D. advancement committee members. And I wish to express my gratitude to Doctor Yohe Tony Song, who recommended me to enter the climate research and being my Ph.D. advancement committee member.

I acknowledge all the professors with whom I participated in teaching assistant and with whom I took courses at University of California, Irvine: Elizabeth Crook, Claudia Czimczik, Julie Ferguson, Saewung Kim, Katherine Mackey, Gudrun Magnusdottir, Adam Martiny, Mathieu Morlighem, Francois Primeau, Mike Pritchard, James Randerson, Isabella Velicognia, Jin-Yi Yu, and Charles Zender. I am grateful to Jaycee Chu, Melanie Nakanishi, Morgan Sibley, and other administrative staff of the department who are always willing to help.

Thanks the past and current members in Jin-Yi's group whom I have worked with: Mengyan Chen, Shan He, Ting-Ting Zhu, Ji-Won Kim, Yu-Chiao Liang, Yong-Fu Lin, Kewei Lyu, Houk Paek, Pengfei Tuo, and Li Xu. Thanks to my cohorts: Yongmin Choi, Megan Fowler, Emily Kane, Zackary Labe, Christian Lewis, Johann Lopez, Romain Millan, Blanca Rodriguez, and Daniel Ruiz. And thanks to all other people that have contributed to this dissertation in any ways.

I wish to express my thank to my parents, sisters, and other family members for their kind supports throughout my life. Finally, I thank my friends at Irvine, Taiwan, and other places, who always show their generosities to keep me on this journey.

I want to thank the financial support provided by the Jenkins family, University of California, Irvine (UCI), Nation Science Foundation's (NSF's) Climate and Large-scale Dynamics Program under Grants Atmospheric and Geospace Sciences-1505145 and 1833075. I also thank American Geophysical Union provided me permission to use my publications as part of my dissertation. I am grateful to have computational resources supported by Cheyenne of NCAR and Greenplanet of UCI for conducting analyses and climate model simulations.

VITA

Shih-Wei Fang

Education

2015-2020	Ph.D., Earth System Science, University of California, Irvine.
2015-2017	M.S., Earth System Science, University of California, Irvine.
2012-2015	M.S., Computer Science, California State Polytechnic University, Pomona
2005-2010	B.S., Mathematical Science, National Chengchi University, Taiwan

Publications

- **Fang, S. W.** & Yu, J. Y. ENSO Transition Complexity and its underlying dynamics in CMIP5/6 models. (To be submitted)
- **Fang, S. W.** & Yu, J. Y. A Control of ENSO Complexity by Tropical Pacific Mean SSTs through Tropical-Subtropical Interactions. *Geophysical Research Letters*, in press.
- Chen, M., T-H Chang, C-T Lee, **S-W Fang**, & J-Y Yu. A Study of Climate Model Responses of the Western Pacific Subtropical High to El Niño Diversity. (Review in *Climate Dynamics*)
- He, S., J.-Y. Yu, S. Yang, & **S. W. Fang**, (2019). Why does the CP El Niño less frequently evolve into La Niña than the EP El Niño? *Geophysical Research Letters*, in revision.
- He, S., J.-Y. Yu, S. Yang, & **S.-W. Fang**, (2020). ENSO's impacts on the tropical Indian and Atlantic Oceans via tropical processes: CMIP5 simulations versus observations. *Climate Dynamics.*
- Yu, J. Y., & **Fang, S. W.** (2018). The Distinct Contributions of the Seasonal Footprinting and Charged-Discharged Mechanisms to ENSO Complexity. *Geophysical Research Letters*, *45*(13), 6611-6618.
- Liang, Y. C., Mazloff, M. R., Rosso, I., **Fang, S. W.**, & Yu, J. Y. (2018). A Multivariate Empirical Orthogonal Function Method to Construct Nitrate Maps in the Southern Ocean. *Journal of Atmospheric and Oceanic Technology*, *35*(7), 1505-1519.
- **Fang, S. W.**, Portante, A., & Husain, M. I. (2015). Moving target defense mechanisms in cyber-physical systems. *Securing Cyber-Physical Systems*, 63.

- **Fang, S. W.**, Rajamanthri D., & Husain M. I. (2015). Facebook Privacy Management Simplified. *12th International Conference on Information Technology-New Generations*. *IEEE*.

Presentations

Oral:

- **Fang, S. W.**, Understanding ENSO Transition Complexity and its underlying dynamics, *CASPO Seminar in Scripps Institution of Oceanography, UCSD*, San Diego, CA, USA (Invited Oral, 2020)
- **Fang, S. W.**, & Yu, J. Y., ENSO Transition Complexity in CMIP5/6 Models, *2020 American Meteorological Society Annual Meeting*, Boston, MA, USA (Oral, 2020)
- **Fang, S. W.**, A Constraint on ENSO Transition Complexity as the Pacific Warms, *The 2nd Climate Hotpots In Action (CHIA) Forum*, Taipei City, Taiwan (Oral, 2019)
- **Fang, S. W.**, A Constraint on ENSO Transition Complexity as the Pacific Warms, *Institute of Oceanography in National Taiwan University*, Taipei City, Taiwan (Oral, 2019)

Poster:

- **Fang, S. W.**, & Yu, J. Y., ENSO Transition Complexity in CMIP5/6 Models, *2020 AGU Ocean Science meeting*, San Diego, CA, USA (Poster, 2020)
- **Fang, S. W.**, & Yu, J. Y., ENSO Transition Complexity in CMIP5/6 Models, *2019 Annual Fall Meeting of American Geophysical Union*, San Francisco, CA, USA (Poster, 2019)
- **Fang, S. W.** & Yu, J. Y., Can the Pacific Meridional Mode Represent the Seasonal Footprinting Mechanism? *2018 Annual Fall meeting of American Geophysical Union*, Washington D. C., USA (Poster, 2018)
- **Fang, S. W.** & Yu, J. Y., A Physical Mode Decomposition Study of the ENSO Predictability Before and After 1990s. *2016 Annual Fall meeting of American Geophysical Union*, San Francisco, USA (Poster, 2016)

Outreach

- **Fang, S. W.**, Understanding El Niño-Southern Oscillation and Its Complex Behaviors. *North America Taiwanese Professors' Association*, CA, USA (Oral, 2019)

Award

- **Fang, S. W.**, Lai Y. C., Wu B. Team "EleMon". *2nd place for "App of Energy" Hackathon San Diego*, San Diego, CA, USA (02/2014)
- **Fang, S. W.**, Lai Y. C., Wu B. Team "DrunkenEye". *2nd place for HackPoly 2014*, Pomona, CA, USA (01/2014)

ABSTRACT OF THE DISSERTATION

Understanding ENSO Transition Complexity and its Underlying Dynamics

by

Shih-Wei Fang

Doctor of Philosophy in Earth System Science

University of California, Irvine, 2020

Professor Jin-Yi Yu, Chair

No two El Niño-Southern Oscillation (ENSO) events evolve the same way. Transitions from one ENSO event to another occur in various ways and constitute a key component of ENSO complexity. While ENSO complexity in amplitude, periodicity, and spatial patterns has been frequently studied, ENSO transition complexity has not yet been systematically explored in either the observations or climate model simulations. This dissertation uses statistical analyses and numerical modeling experiments to develop a dynamical framework that can explain how three key transition patterns of ENSO (i.e., episodic, cyclic, and multi-year ENSOs) are produced, and further applies this framework to examine these ENSO transitions in contemporary climate models and to project future changes of the transition complexity.

This dissertation finds that the occurrence of the three ENSO transitions depends on two primary onset mechanisms of ENSO. The tropical Pacific onset (TP-onset) mechanism initiates sea surface temperature (SST) anomalies in the equatorial eastern Pacific through thermocline variations, while the subtropical Pacific onset (SP-onset) mechanism brings the subtropical SST anomalies into the equatorial central Pacific through a series of subtropical couplings. The TP-

onset mechanism is found to mainly produce the cyclic ENSO transition and, as a result, contributes to reduced ENSO transition complexity. In contrast, the SP-onset mechanism is found to be capable of producing all three transitions and is a key source of the transition complexity. While the TP-onset mechanism has maintained its strength in the past six decades, the SP-onset mechanism became more important in producing ENSO events since the early-1990s. The intensified SP-onset mechanism increases ENSO complexity and can be a factor for the changing ENSO properties observed in the 21st century.

By further focusing on the SP-onset mechanism, this dissertation finds that the tropical mean state of SSTs can control the occurrence of cyclic and multi-year ENSO transitions. Specifically, the mean SST in the eastern equatorial Pacific controls the frequency of cyclic transitions related to the SP-onset mechanism, while the mean SST in the central equatorial Pacific is responsible for the multi-year transitions. This control arises from the fact that the mean state SST determines how easily the anomalous warming/cooling from an ENSO event can excite deep convective heating in each region to activate the SP-onset mechanism and trigger another ENSO event in the following year. In a future warmer world, this mean state control is projected to increase the cyclic transition but decrease the multi-year transition of ENSO.

In this dissertation, ENSO transition complexity is also compared between observations and contemporary climate model simulations. The El Niño transition complexity is found to be dominated in order by the episodic transition, cyclic transition, and multi-year transition. Interestingly, the reversed order is discovered for the La Niña transition complexity (multi-year, cyclic, and then episodic La Niña). This asymmetry between El Nino and La Niña transitions results from two reasons: 1) the SP-onset mechanism generates episodic El Niño more than the episodic La Niña due to the nonlinear growth of the equatorial wind anomalies it induces, 2) the

nonlinear responses of the SP-onset mechanism to tropical Pacific mean SSTs favor more multi-year La Niña than multi-year El Niño. Contemporary models realistically produce the observed transition complexity for El Niño but fail to simulate the reversed order of La Niña transitions. These deficiencies arise from a weak subtropical onset mechanism in the models and a cold bias in tropical Pacific mean-state.

Findings from this dissertation offer a novel perspective to understand and study ENSO complexity dynamics, which is a new area of ENSO research. The dynamical framework developed has the potential to branch a critical new direction of understanding ENSO dynamics, properties, and activities in present, past, and future climates.

Chapter 1

Introduction

1.1 Complex Behaviours of ENSO

El Niño-Southern Oscillation (ENSO) is one of the most influential phenomena in our Earth system, causing climate and weather extremes, massive ecosystem impacts, and tremendous economic losses (McPhaden et al. 2006; Donnelly and Woodruff 2007; Coelho and Goddard 2009; Power et al. 2013). However, no ENSO event evolves the same as another (see the equatorial sea surface temperature (SST) evolutions in Fig. 1.1). The complex behaviours of ENSO impede the predictions of its occurrence and results in difficulties in mitigating its global impacts (Fedorov et al. 2003; Vecchi and Wittenberg 2010; Collins et al. 2010; Cai et al. 2014; Sohn et al. 2016). The underlying causes of these complex behaviours have still not been fully understood.

ENSO complexity, coined in recent years to study the complex behaviours (Timmermann et al. 2018), appears in several key aspects of ENSO properties: intensity, spatial pattern, and temporal evolution. Earlier studies on these behaviours had focused on the intensity—the magnitude of the SST anomalies during the peak phase of ENSO. The ENSO intensity influences the scale of global impacts it produces, but the impacts are not related to the intensity in a linear way (Barnston et al. 1999; Nakagawa et al. 2000; Jin et al. 2003; Ñiquen & Bouchon 2004; Santoso et al. 2017). Strong El Niño events, such as the 1982-83 El Niño, produce disproportionally larger global impacts than moderate events, including a severe reduction of marine life in the eastern-central equatorial Pacific (Philander 1983) and an increase of precipitation over the southern U.S. (Quiroz 1983). ENSO events have been separated according to their intensity to study their climate

impacts, underlying dynamics, and changes in the future warming world (Cai et al. 2014; Cai et al. 2015).

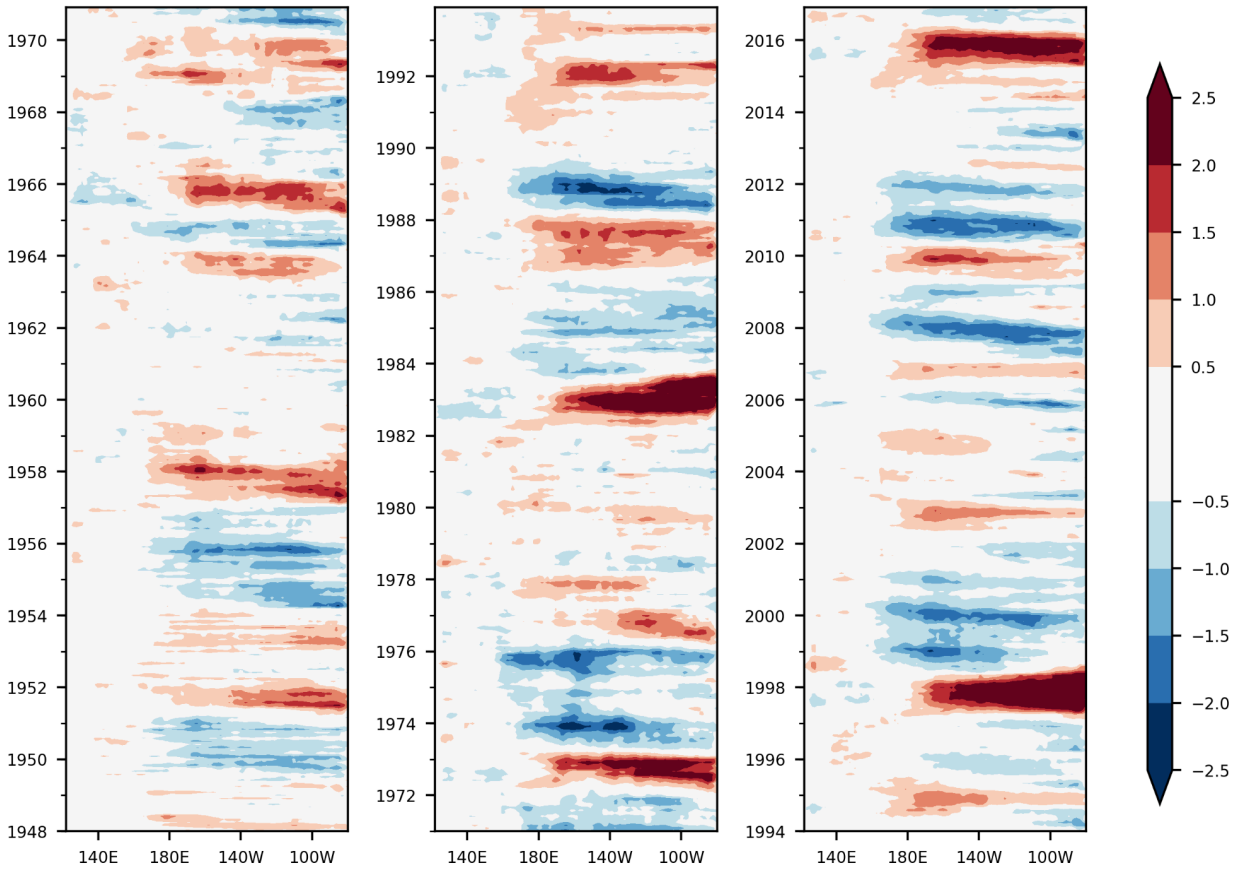

Figure 1.1 Evolution of the equatorial SST anomalies (averaged between 5°S-5°N) over the Pacific from 1948-2016. The SST data are from Hadley Center Sea Ice and Sea Surface Temperature data set (HadiSST; Rayner et al., 2003)

During the past two decades, studies of ENSO complexity in its spatial structures have attracted lots of attention. This is partially caused by the notion that the location of peak ENSO SST anomalies appears to have shifted from the eastern equatorial Pacific to the central equatorial Pacific in the 21st century (Yu and Kao 2007; Kao and Yu 2009; Yeh et al. 2014; Xu et a. 2016).

These two types (or flavors) of ENSO structures have been mostly referred to as the Eastern Pacific (EP) type and the Central Pacific (CP) type of ENSO (shown in Fig. 1.2; Yu and Kao 2007; Kao and Yu 2009), though multiple terms have been introduced (Dateline ENSO from Larkin and Harrison (2005), Modoki ENSO from Ashok et al. (2007), and Warmpool ENSO from Kug et al. (2009)). The longitudinal difference in ENSO locations have been successfully used to explain the climate impacts from different ENSO events even when they were of comparable intensities (Li et al. 2011; Zhang et al. 2011; Graf & Zanchettin 2012; Yuan & Yang 2012; Yeh et al. 2014). For example, the EP El Niño affects winter temperatures mostly over the Northeast and Southwest US, while the CP El Niño affects the temperatures mostly in the northwestern and southeastern U.S. (Yu et al. 2012).

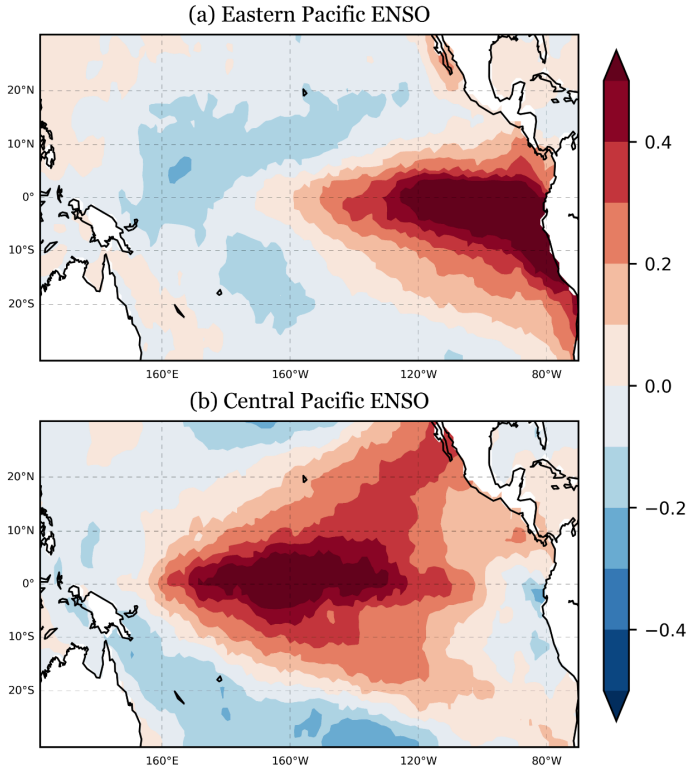

Figure 1.2 Regression of (a) the eastern Pacific index and (a) the central Pacific index onto the tropical SST anomalies (1948-2016 of HadiSST).

By separating ENSO events into these two types, the ENSO research community has obtained new insights into the dynamics of ENSO (Captondi et al. 2015; Yu et al. 2017). One key advancement is an increased understanding of the role of subtropical Pacific processes in ENSO dynamics (Chiang & Vimont 2004; Yu and Kao 2007). While the conventional view focused on ocean-atmosphere coupling in the tropical Pacific to explain ENSO properties, a new view has emerged and emphasizes the possibility of subtropical Pacific forcing to initiate the coupling processes and further generate an ENSO event (see Yu et al. 2017 for a review of this new perspective). The new perspective suggests that the subtropical Pacific processes are essential to the generation of the CP ENSO, which may be a source for the weaker skill of ENSO prediction experienced over the 21st century (Ham & Kug 2012; Yeh et al. 2014; Pillai et al. 2017; Lee et al. 2018).

In recent years, studies of ENSO complexity have shifted the focus to their temporal evolution of ENSO (An & Kim 2017; Lee et al. 2017; An & Kim 2018; Wang et al. 2019; Wu et al. 2019). That focus is built upon the observation that the ENSO can transition from one event to the other in complex ways. An El Niño event, for example, is often followed by a La Niña event in the following year. However, it has also been observed that some El Niño events are followed by another El Niño event. And some events are produced from a neutral condition in the tropical Pacific. Do these different transition patterns occur only by chance? Or are there specific dynamics that control what pattern should occur? This issue, to our knowledge, has not been systematically addressed in the research community but has stressed on the importance for a better understanding on ENSO. Therefore, ENSO transition complexity and its associated dynamics are the focus of this dissertation.

The focus on ENSO transitions is fundamentally different from the earlier emphases on ENSO complexities in intensity and spatial type. The latter are related to peak-phase characteristics of ENSO, while the former is related to onset-phase characteristics of ENSO. Unlike the classification in intensity (strong versus weak) and spatial pattern (EP versus CP types), there has not been a generic way to classify the temporal evolution of ENSO and to investigate its underlying dynamics. The goal of this dissertation is to develop a classification method and to form a dynamical framework to explain varied ENSO transitions.

1.2 ENSO Transition Complexity

ENSO Transition Complexity is a term we coined to study different ways that ENSO transitions from one event to another. Traditionally, ENSO is considered a semi-periodic phenomenon that oscillates between its warm (i.e., El Niño) and cold (i.e., La Niña) phases. Therefore, one ENSO event is expected to transition to an opposite-phase event in the following year, resulting in a cyclic transition (i.e., El Niño-to-La Niña or La Niña-to-El Niño; Fig. 1.3). The recharged oscillator, for example, was developed to explain how this cyclic transition can be produced from a lagged response of the ocean to the ENSO-induced wind forcing (Wyrki 1975; Jin 1997a; Jin 1997b). Studies of this oscillatory nature of ENSO have laid the foundations of ENSO dynamics (Suarez and Schopf 1988; Schneider et al. 1995; Kirtman 1997; Wang et al. 1999; Wang 2000).

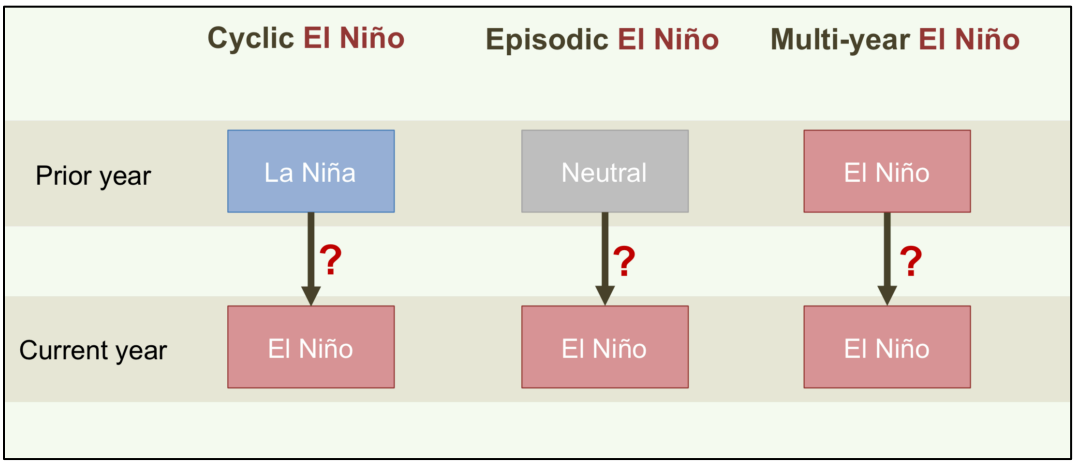

Figure 1.3 Schematic of the three types of ENSO transition patterns.

However, not every ENSO event follows this cyclic pattern. For example, studies have observed a significant number of ENSO events that can transition to another same-phase event (i.e., El Niño-to-El Niño or La Niña-to-La Niña) (Okumura et al. 2011; Ohba & Watanabe 2012; McGregor et al. 2013; Choi et al. 2013; Dommenget et al. 2013; DiNezio & Deser 2014; Chen 2016; An & Kim 2017; Okumura et al. 2017). We refer to this transition as multi-year transition. Other ENSO events were not produced by a prior ENSO event (Chen et al. 2015; Thual et al. 2016; Chen & Majda 2016), which we refer to as the episodic transition. Therefore, ENSO transitions can intuitively be separated into three types: cyclic, episodic, and multi-year ENSO (Fig. 1.3). To reiterate, an El Niño event can be preceded by a La Niña event to form a cyclic El Niño; by a neutral condition to become an episodic El Niño; or by another El Niño event resulting in a multi-year El Niño. The same classification can also be applied to La Niña. Differing from the cyclic transition, the episodic and multi-year transitions do not exhibit an oscillating characteristic. Therefore, in order to fully explain the ENSO transition complexity, the traditional theories of ENSO onset need to be re-investigated and/or additional theories need to be developed.

It should be noted that understanding the causes of the transition patterns is important not only to the studies of ENSO dynamics but also to the studies of predicting ENSO impacts. For instance, multi-year La Niña events can shift the region of reduced precipitation to more southeast in the U.S. than other La Niña events (Okumura et al. 2017). Also, the prior seasons (summer or fall) before the ENSO peak phase (winter) are found to be critical to predicting the ENSO impacts. The summer of the cyclic La Niña, for example, can generate distinct atmospheric wavetrains to the extratropical Pacific and cause a significant warming signal over the Midwest in the U.S., compared to the multi-year La Niña (Jong et al 2020).

1.3 Mechanisms for ENSO Onset

Multiple onset processes of ENSO have been developed by the ENSO research community. They can be separated into two major groups: a group that emphasizes tropical Pacific processes and another group that emphasizes subtropical Pacific processes (see reviews in Capotondi et al. 2015; Yu et al.; 2017; Wang et al. 2017; Yang et al. 2018). We refer to them as the tropical Pacific onset (TP-onset) mechanism and subtropical Pacific (SP-onset) mechanism.

The TP-onset mechanism suggests that thermocline variations along the equatorial Pacific control the onset of ENSO events. The mechanism described by the recharge oscillator theory (Wyrki 1975; Jin 1997a and 1997b) is one included in the TP-onset mechanism. This theory emphasizes that an El Niño (La Niña) event can shallow (deepen) the thermocline depth via surface wind stress anomalies it induces, which then bring anomalous cold (warm) water to surface to onset a La Niña (El Niño) event in the subsequent year. The delayed oscillator theory (Battisti & Hirst 1989; Zebiak & Cane 1987) is another example of the TP-onset mechanism. This theory suggests that oceanic Rossby waves excited by ENSO events via surface winds can propagate and

reflect along the equatorial Pacific to vary the thermocline depth and to onset another ENSO event. The western Pacific oscillator theory (Weisberg and Wang 1997; Wang et al. 1999) also invokes wind-induced thermocline variations to explain how ENSO transitions from one event to another. Physical processes involved in these theories (Suarez and Schopf 1988; Schneider et al. 1995; Kirtman 1997; Wang et al. 1999; Wang 2000) all reside within the tropical Pacific and, therefore, should be together referred to as the TP-onset mechanism.

The SP-onset mechanism, on the other hand, suggests that initial SST anomalies of ENSO can be established by subtropical processes that bring SST anomalies from the northeastern Pacific into the equatorial Pacific. The subtropical processes involve the coupling between the northeasterly trade winds and SSTs from off the coast of Baja California to the equatorial central Pacific (Vimont et al. 2003). Anomalies of these two quantities, induced by the extratropical atmospheric disturbance, can sustain and intensify each other through the coupling carried by surface latent heat flux, known as the wind-evaporation-SST feedback (Xie and Philander 1994; Chang et al. 1997; Xie 1999). As a result of this coupling, wind and SST originating from the subtropical Pacific can self-sustain and propagate toward the equatorial central Pacific (Yu et al. 2010; Yu & Kim 2011).

This series of coupling processes is described as the seasonal footprinting mechanism (Vimont et al. 2003; Kao & Yu 2009; Alexander et al. 2010) and the SST anomalies extending from Baja California to the equatorial Pacific are described as the Pacific Meridional mode (PMM; Chiang & Vimont 2004; Chang et al. 2007; Larson and Kirtman 2013; Stuecker 2018; Amaya 2019). Conventionally, the positive phase of the SP-onset mechanism is characterized by warm SST anomalies coupled with the decrease of trade winds extending from the ocean outside Baja California to the equatorial central Pacific (i.e., a positive PMM; Fig. 1.4). A trade wind charging

theory (Anderson et al. 2013; Anderson & Perez 2015) has also been proposed to suggest how subtropical Pacific wind anomalies can produce the warming in the equatorial central Pacific through an oceanic pathway.

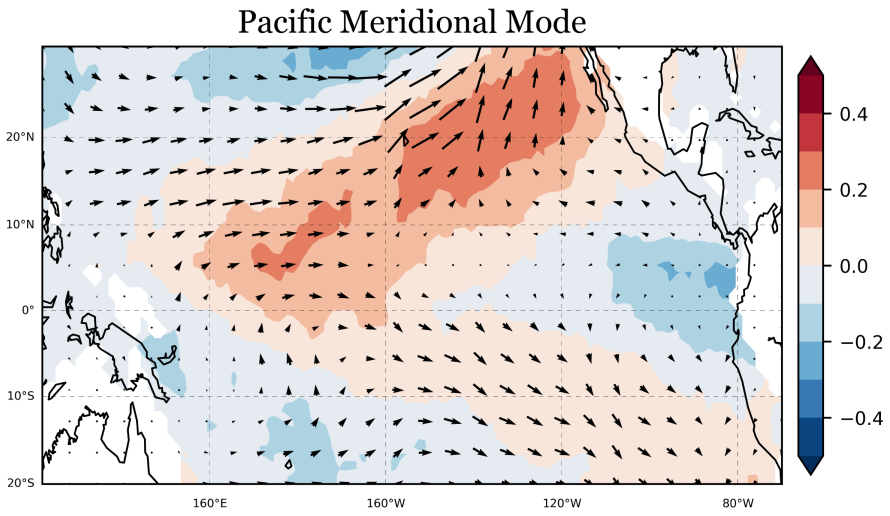

Figure 1.4 Regression of the Pacific Meridional Mode onto the tropical SST (HadiSST) and surface wind anomalies (1948-2016). The surface wind data are from the National Centers for Environmental Prediction-National Center for Atmospheric Research (NCEP-NCAR) reanalysis (Kalnay et al., 1996).

The TP-onset mechanism has been the central focus of ENSO research over the past few decades, but the SP-onset mechanism has started attracting more and more attention in recent years. This is because ENSO properties have noticeably changed after the 1990s (Yeh et al. 2009; Lee & McPhaden 2010; Takahashi et al. 2011; Newman et al. 2011; Dewitte et al. 2012) and these changes seem to be related to the SP-onset mechanism (Yu et al. 2017). Also, there is evidence that the strength of the SP-onset mechanism has intensified since the early-1990s when the Atlantic Multi-decadal Oscillation (AMO) changed to its positive phase (Yu et al. 2015). However, how

these two onset mechanisms affect the ENSO transition and its complexity has not been systematically studied. In this dissertation, we have developed a dynamical framework that uses these two onset mechanisms to study the ENSO transition complexity in observations and contemporary climate models.

1.4 Limited Complexity in Contemporary Climate Model Simulations

Model representation of the ENSO transition complexity is another focus of this dissertation. Contemporary climate models are able to reproduce several observed properties of ENSO events (Ham & Kug 2012; Kim & Yu 2012), but the ENSO transition complexity in model simulations has yet to be examined in detail. For example, previous studies have examined how well Climate Model Intercomparison Project phase 3 and 5 (CMIP3 and CMIP5) models can simulate extreme and moderate ENSOs and the EP and CP types of ENSOs, but there has not been much effort to examine the transition patterns of models (Yeh et al. 2014; Xu et a. 2016). Whether or not contemporary models can reproduce the observed ENSO transition patterns, the complexity, and the related underlying dynamics affect how well we can use the models to perform ENSO predictions and projections (Larson & Kirtman 2013; Thomas & Vimont 2016; DiNezio et al. 2017). Therefore, it is one critical issue to address for ENSO complexity studies.

The ENSO research community has long been aware that asymmetries exist between the El Niño and La Niña phases of ENSO (An & Jin 2004; Frauen & Dommenget 2010; Okumura & Deser 2010; Santoso et al. 2013; Chen et al. 2016). The properties of La Niña are not exactly an inverse of those of El Niño. For example, strong El Niño events are mostly in the EP-type, while strong La Niña events are in the CP-type in observations (Lee & McPhaden 2010). Also, the SST anomalies for El Niño prefer to propagate eastward, while the La Niña tends to propagate to the

west in observations (McPhaden & Zhang 2009; Santoso et al. 2013). Model simulations can simulate the similar propagation preference for La Niña but not for the El Niño (Chen et al. 2016). The El Niño-La Niña asymmetry is another aspect of ENSO complexity that needs to be better understood and that contemporary models have to be able to reproduce.

This dissertation develops a framework for studying ENSO transition complexity and further applies this framework to examine the ENSO transition complexity in CMIP models. Model performance and the causes of model deficiencies are identified.

1.5 Outline of the Dissertation

In this dissertation, ENSO transition complexity and its relationship with the two ENSO onset mechanisms are studied through statistical analyses and climate model experiments. The organization of this dissertation thesis is as follows:

In Chapter 2, the relations between the two ENSO onset mechanisms and the ENSO transitions are examined. The possible controls of ENSO transitions from the two ENSO onset mechanisms are studied by composite analyses and a unique statistical approach. In contrast to previous studies considering only one onset mechanism, the finding in this chapter introduces a possibility of simultaneously investigating the two ENSO onset mechanism, which provides a framework to further study ENSO transition complexity with a focus on the onset stage of ENSO. In addition, the two onset mechanisms are also applied to understand the changing ENSO issue. This chapter develops a framework of studying the ENSO transition complexity and can be applied to study various issues related to ENSO.

In Chapter 3, the tropical regulations of the SP-onset mechanism are investigated. The physical processes of how anomalous warming/cooling in the equatorial Pacific can activate the SP-onset

mechanism to trigger an ENSO event (i.e. the cyclic and multi-year transitions) are studied by analyzing reanalysis products and climate model simulations and by conducting atmospheric general circulation model experiments. Future projections of ENSO transition complexity are also addressed. The finding from this chapter first proposes a tropical control of the subtropical forcing on the ENSO onset and expands the possible tropical-subtropical interactions that may contribute to the ENSO triggering processes.

In Chapter 4, the transition complexity of El Niño and La Niña is examined in both reanalysis products and the contemporary climate model simulations. Combining the results from the first few chapters, this chapter summarizes the current understanding of ENSO transition complexity and targets the causes of the deficiencies of transition complexity found in the state-of-art model simulations. The finding guides a direction of improving the current model simulations that may shed light on the model predictions and future projections of ENSO events.

Chapter 5 summarizes the main results found in this dissertation and introduces possible implications and future directions based on our findings. Parts of the results in Chapters 2 and 3 are published works, each of which can be read independently.

Chapter 2

The Control of ENSO Onset Mechanisms on ENSO Transitions

2.1 Abstract

This chapter finds the SP-onset mechanism to be a key source of ENSO complexity, whereas the TP-onset mechanism acts to reduce complexity. The TP-onset mechanism forces El Niño and La Niña to follow each other, resulting in a more cyclic and less complex ENSO evolution, while the SP-onset mechanism involves subtropical forcing and results in an ENSO evolution that is more episodic and irregular. The SP-onset mechanism also has a tendency to produce multiyear La Niña events but not multiyear El Niño events, contributing to El Niño-La Niña asymmetries. The strength of TP-onset mechanism has been steady, but SP-onset mechanism has intensified during the past two decades, making ENSO more complicated. Most Climate Model Intercomparison Project version 5 models overestimate the strength of the TP-onset mechanism but underestimate the strength of the SP-onset mechanism, causing their simulated ENSOs to be too regular and symmetric. It is noted that the TP-onset mechanism is termed as the charged-discharged onset mechanism and the SP-onset mechanism is termed as the seasonal footprinting mechansim in my published paper (Yu & Fang 2018) that are used in the figures in this chapter.

2.2 Introduction

Not all ENSO events are the same. Some noticeable changes in ENSO properties observed during recent decades have motivated efforts to better understand the sources/causes of ENSO complexity (Capotondi et al., 2015; Wang et al., 2017). A significant component of ENSO

complexity is manifested in the way one ENSO event transitions to another. Some events are followed by events of the opposite phase (i.e., El Niño to La Niña or La Niña to El Niño) to give rise to ENSO cycles; others are followed by neutral years to become episodic events, and still others are followed by events of the same phase to become multi- year El Niño or La Niña events. In this chapter, we examine how the different onset mechanisms of ENSO may affect these event-to-event transitions and thus ENSO complexity.

Studies on ENSO dynamics have identified two key onset mechanisms for events: the TP-onset and SP-onset mechanisms. The TP-onset mechanism describes how the lagged response of the equatorial Pacific thermocline to ENSO wind forcing can result in alternations between El Niño and La Niña phases (Jin, 1997a, 1997b; Wyrtki, 1975). The SP-onset mechanism describes how subtropical Pacific SST anomalies initially induced by atmospheric disturbances can be sustained through several seasons and, at the same time, spread equatorward via subtropical ocean-atmosphere coupling to trigger ENSO events (Vimont et al., 2003). Recent studies suggest that these two mechanisms can trigger events at different locations to produce the Eastern Pacific and Central Pacific types (Kao & Yu, 2009; Yu & Kao, 2007) of ENSO (Yu et al., 2010, 2012, 2017). However, it is not yet fully understood whether or not these two mechanisms impose any particular constraints on the event-to-event transitions and how they contribute to ENSO complexity.

In this chapter, we first show that the strengths of these two onset mechanisms can be determined from observations by applying a Multi-variate Empirical Orthogonal Function (MEOF) analysis to combined atmospheric and oceanic anomalies. The event-to-event transitions are then separately composited and analyzed for the two onset mechanisms using reanalysis products during the period 1958–2014. The same analyses are also performed with the preindustrial simulations produced by Climate Model Intercomparison Project version 5 (CMIP5) models

(Taylor et al., 2012) to understand how simulations of these two onset mechanisms affect the properties of the model ENSOs

2.3 Datasets and Methods

Monthly mean values of SST, surface wind, and sea surface height (SSH) were used and regridded to a common 1.5° × 1° longitude-latitude grid for analysis. The SST data are obtained from Hadley Center Sea Ice and Sea Surface Temperature data set (Rayner et al., 2003), the surface wind data are from the National Centers for Environmental Prediction-National Center for Atmospheric Research reanalysis (Kalnay et al., 1996), and the SSH data are from the German contribution of the Estimating the Circulation and Climate of the Ocean project (Köhl, 2015). Anomalies in this study are defined as the deviations from the seasonal cycle averaged over the analysis period after removing the linear trend. The same procedures were applied to the last 100 years of the preindustrial simulations produced by 34 CMIP5 models (Table 2.1).

To identify the dominant ocean-atmosphere coupling processes associated with ENSO, we applied an MEOF analysis to the combined anomalies of SST, surface wind, and SSH within the tropical Pacific (20°S–20°N, 122°E–70°W) during the period 1958–2014. Following Xue et al. (2000), a two-step procedure was used to perform the MEOF analysis. The first step is to apply a spatial EOF analysis separately to the SST, wind, and SSH anomalies to obtain their individual leading EOF modes. The second step is to apply a temporal EOF analysis to the combined principal components (PCs) of the leading spatial EOF modes of each variable to obtain the leading coupled modes among the variables. The leading modes obtained from the final step of the MEOF analysis are referred to as the leading MEOF modes. The same MEOF analysis was applied to CMIP5 model simulations.

Model	Modeling Center	Model	Modeling Center
ACCESS1-0	Commonwealth Scientific and Industrial Research Organization (CSIRO) and Bureau of Meteorology (BOM), Australia	GISS-E2-R	NASA Goddard Institute for Space Studies
ACCESS1-3		GISS-E2-R-CC	
bcc-csm1-1	Beijing Climate Center, China Meteorological Administration	HadGEM2-CC	Met Office Hadley Centre (additional HadGEM2-ES realizations contributed by Instituto Nacional de Pesquisas Espaciais)
bcc-csm1-1-m		HadGEM2-ES	
CanESM2	Canadian Centre for Climate Modelling and Analysis	inmcm4	Institute for Numerical Mathematics
CCSM4	National Center for Atmospheric Research	IPSL-CM5A-LR	Institut Pierre-Simon Laplace
CESM1-BGC	Community Earth System Model Contributors	IPSL-CM5A-MR	
CESM1-CAM5		IPSL-CM5B-LR	
CESM1-FASTCHEM		MIROC-ESM	Japan Agency for Marine-Earth Science and Technology, Atmosphere and Ocean Research Institute (The University of Tokyo), and National Institute for Environmental Studies
CESM1-WACCM		MIROC-ESM-CHEM	
CMCC-CESM	Centro Euro-Mediterraneo per I Cambiamenti Climatici	MIROC5	Atmosphere and Ocean Research Institute (The University of Tokyo), National Institute for Environmental Studies, and Japan Agency for Marine-Earth Science and Technology
CMCC-CM		MPI-ESM-LR	Max-Planck-Institut für Meteorologie (Max Planck Institute for Meteorology)
CMCC-CMS		MPI-ESM-MR	
CNRM-CM5	Centre National de Recherches Météorologiques / Centre Européen de Recherche et Formation Avancée en Calcul Scientifique	MPI-ESM-P	
CNRM-CM5-2		MRI-CGCM3	Meteorological Research Institute
GFDL-ESM2G	NOAA Geophysical Fluid Dynamics Laboratory	NorESM1-M	Norwegian Climate Centre
GFDL-ESM2M		NorESM1-ME	

Table 2.1. The names of the 34 CMIP5 models used in chapter 2.

For the analysis of El Niño-La Niña asymmetries, we need to identify multi-year ENSO events. A multi-year event is considered to occur if one of the following criteria is met: (1) an ENSO event is preceded by another event with the same phase or (2) an ENSO event has a duration longer than 18 months. Here, an El Niño (La Niña) event is defined as one whose 3-month average of Niño3.4 index (sea surface temperature anomalies averaged between 5°S-5°N and 170°W-120°W) are larger (smaller) than 0.5°C (-0.5°C) for more than 5 consecutive months. Based on these criteria, one multi-year El Niño (1976) event and four multi-year La Niña events (1970, 1983, 1998, and 2010) events were identified during the analysis period. The same identification method was applied to the CMIP5 model simulations to identify multi-year ENSO events, except we chose ±0.7 standard deviation (instead of ±0.5°C that may identify extreme amounts of ENSO events when models having different amplitudes) of Niño3.4 index as the threshold for an event.

2.4 Two ENSO Onset Mechanisms

Figure 2.1 shows the structures of the first three leading MEOF modes, which are similar to the MEOF modes obtained by Xue et al. (2000). The first mode (MEOF1) explains a large percentage (32%) of the coupled variance among surface wind, SST, and SSH. This mode represents the Bjerknes (BJ) feedback process that is well known as a positive feedback mechanism that can cause ENSO to grow in intensity (Bjerknes, 1969). This mode is characterized by warm SST anomalies in tropical central-to-eastern Pacific (Fig. 2.1a) that are coupled with westerly anomalies to the west (Fig. 2.1b) and an east-west sloping of thermocline (represented by SSH) along the tropical Pacific (Fig. 2.1c).

The second mode (MEOF2; explaining 7.3% of variance) represents the SP-onset mechanism and is characterized by positive SST anomalies extending from the subtropical northeastern Pacific

into the equatorial central Pacific (Fig. 2.1d) that assumes a pattern similar to the Pacific meridional mode (Chiang & Vimont, 2004). This meridional structure of SST anomalies is overlaid by surface southwesterly anomalies (Fig. 2.1e) that are opposite in direction from the climatological trade winds. These anomalies thus weaken surface winds, reduce surface evaporation, and help maintain the positive Pacific meridional mode anomalies through the wind-evaporation-SST feedback (Xie & Philander, 1994). Meanwhile, the wind anomalies can deepen the thermocline in the central Pacific (Figure 1f), triggering the onset of an El Niño (Anderson & Perez, 2015). Conversely, the negative phase of the SF mechanism can trigger the onset of La Nina events (Yu & Kim, 2011).

The third mode (MEOF3; explaining 5.3% of the variance) represents the TP-onset mechanism that is characterized by an increase in SSH (i.e., ocean heat content) along the entire equatorial Pacific and a decrease in SSH along most of an off-equatorial Pacific belt at about 10°N (Figure 1i). The increase (decrease) of the equatorial SSH, which represents the charging (positive) or discharging (negative) of the ocean heat content, is driven by the ENSO-associated wind anomalies in the tropical Pacific. The charging of the ocean heat content deepens the thermocline to onset positive SST anomalies in the tropical eastern Pacific (Fig. 2.1g). The MEOF analysis clearly identifies one development mechanism (i.e., the BJ mechanism) and two onset mechanisms (the SP-onset and TP-onset mechanisms) for ENSO. Although the second and third MEOF modes are not distinguishable from the higher modes based on the analysis of their eigenvalues (North, 1984), their robustness was examined by applying the same MEOF analyses separately to the first and second halves of the analysis period (Figs. 2.2 and 2.3) and using other sets of SST, SSH, and surface wind data (Fig. 2.4; Balmaseda et al., 2013; Kobayashi et al., 2015; and Smith et al, 2008).

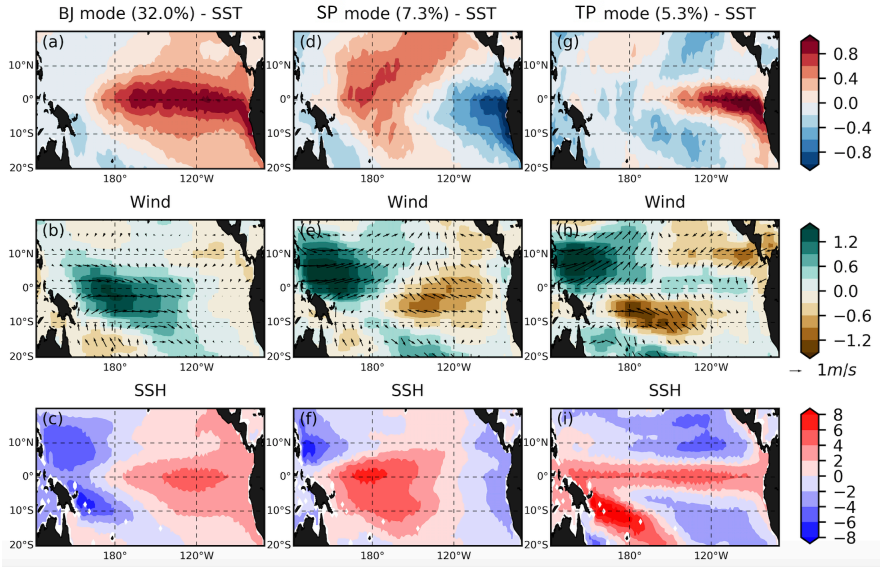

Figure 2.1. The anomaly patterns in SSTs (upper row), surface winds (middle row), and SSHs (lower row) associated with the MEOF modes for the BJ mechanism (MEOF1; left column), SP-onset mechanism (MEOF2; middle column), and TP-onset mechanism (MEOF3; right column).

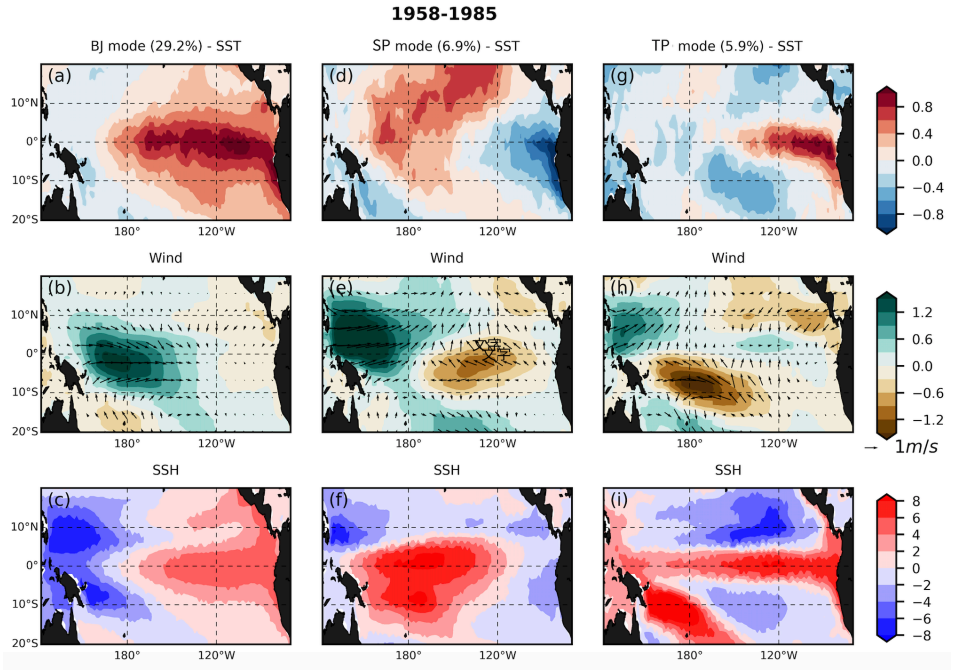

Figure 2.2. As in Figure 1, except for period 1958-1985.

To examine the robustness of the MEOF modes shown in Figure 2.1, we conducted two additional MEOF analyses. In the first one, the MEOF analysis was applied separately to the first and second halves of the analysis period: 1958-1985 and 1986-2014. Figure 2.2 and 2.3 show that SP-onset and TP-onset modes obtained from both of the half periods are similar to those obtained from the full period. In the second additional analysis (see Fig. 2.4), we repeated the MEOF analysis but using SST, SSH, and surface winds obtained from different reanalysis datasets: the Extended Reconstructed Sea Surface Temperature (ERSST) v3 for SST (Smith et al. 2008), the Japanese 55-year Reanalysis Project (JRA55) for wind (Kobayashi et al. 2015), and the Ocean Reanalysis System 4 (ORAS4) for SSH (Balmaseda et al. 2013). The MEOF modes obtained are similar to the original MEOF modes. The correlation coefficients between the PCs of the new and original MEOF modes are larger than 0.95 for all three MEOF modes. These two additional analyses indicate that the SP-onset and TP-onset modes obtained from the original MEOF analysis are robust.

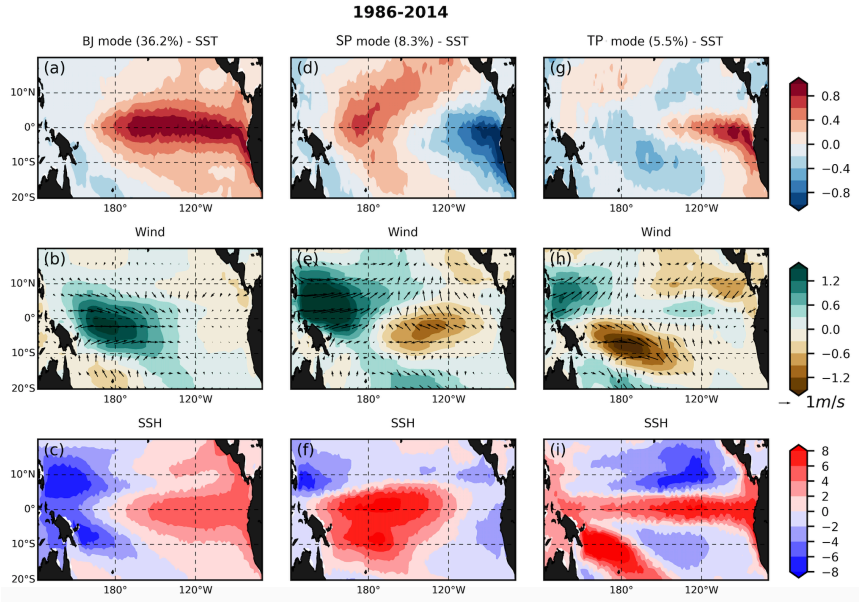

Figure 2.3. As in Figure 1, except for period 1986-2014.

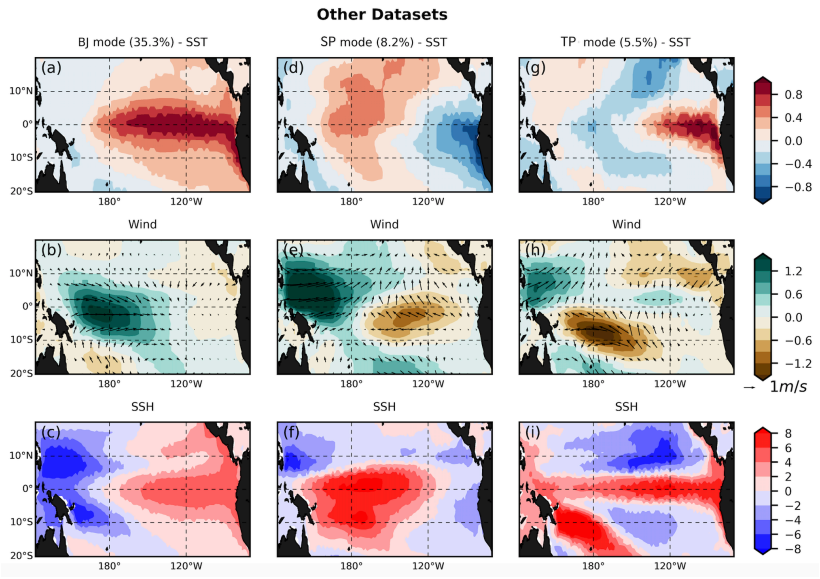

Figure 2.4. As in Figure S1, except the MEOF analysis is applied to other datasets: the ERSST v3 for SST, the JRA55 for wind, and the ORAS4 for SSH

To confirm the relationships between the first three MEOF modes and ENSO, we performed a lead–lag correlation analysis between the PCs of the three modes and the Niño3.4 index (Fig. 2.5a). Being an ENSO development mechanism, the PC of the BJ mode (i.e., PC1) evolves together with the Niño3.4 with the largest correlation at lag 0. The PC of the SP-onset mode (i.e., PC2) has its largest correlation with the Niño3.4 index when it leads Niño3.4 by about 9 months, indicating that the SP-onset mode is an ENSO onset mechanism. The 9-month lead time is also consistent with the fact that the SP-onset mechanism is usually at its strongest strength in boreal spring (Vimont et al., 2003), while ENSO typically peaks in boreal winter. The PC of the TP-onset mode (i.e., PC3) has its largest positive correlation with Niño3.4 when it leads the index by 5–6 months and the largest negative correlation when it lags the index by 7–8 months. These two extreme values of correlation correspond to the charging (discharging) of ocean heat content before the El Niño (La Niña) onset and the discharging (charging) of the ocean heat content after the ENSO

fully develops. A lead-lagged regression analysis of Pacific SST anomalies onto PC2 and PC3 also confirms that an ENSO event develops after the TP-onset and SP-onset modes peak (Fig. 2.6).

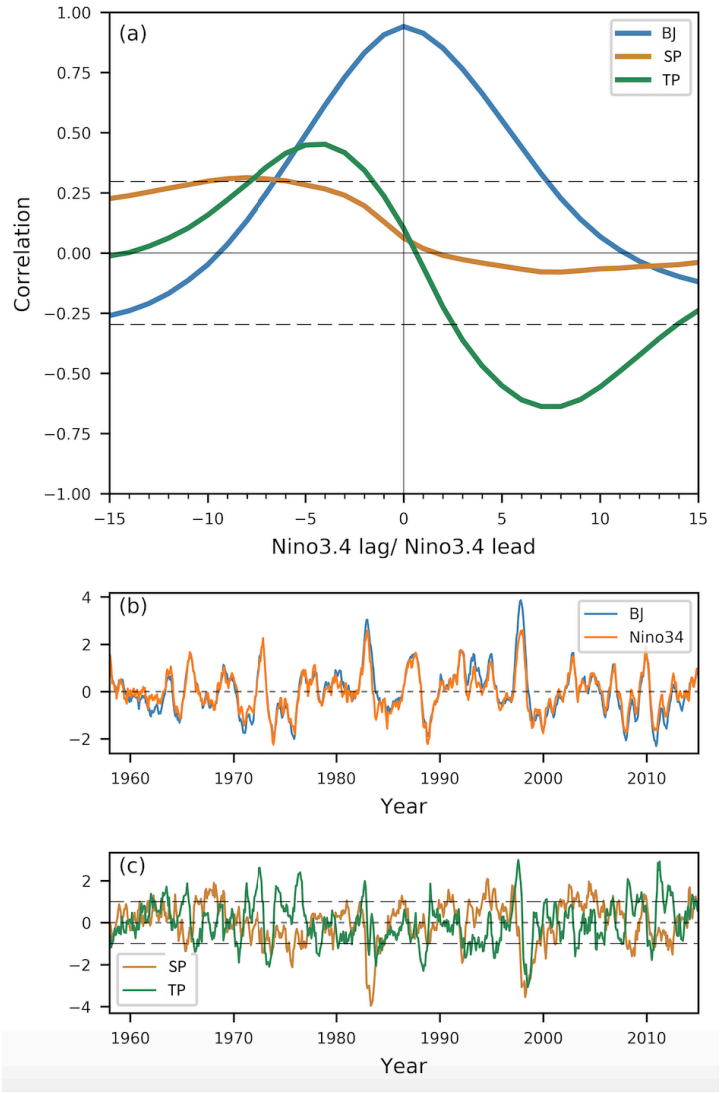

Figure 2.5. (a) The lead/lag correlations between the monthly PCs of the first three leading MEOF modes and the Niño3.4 index. The brown line is the first MEOF (the BJ mode); green is the second MEOF (the SP-onset mode) and blue is the third MEOF (the TP-onset mode). The light gray dashed line denotes the 95% confidence level. (b) The PC of the BJ mode and the time series of Niño3.4 index. (c) The normalized PC of the SP-onset and TP-onset modes. The gray dashed lines denote one standard deviation.

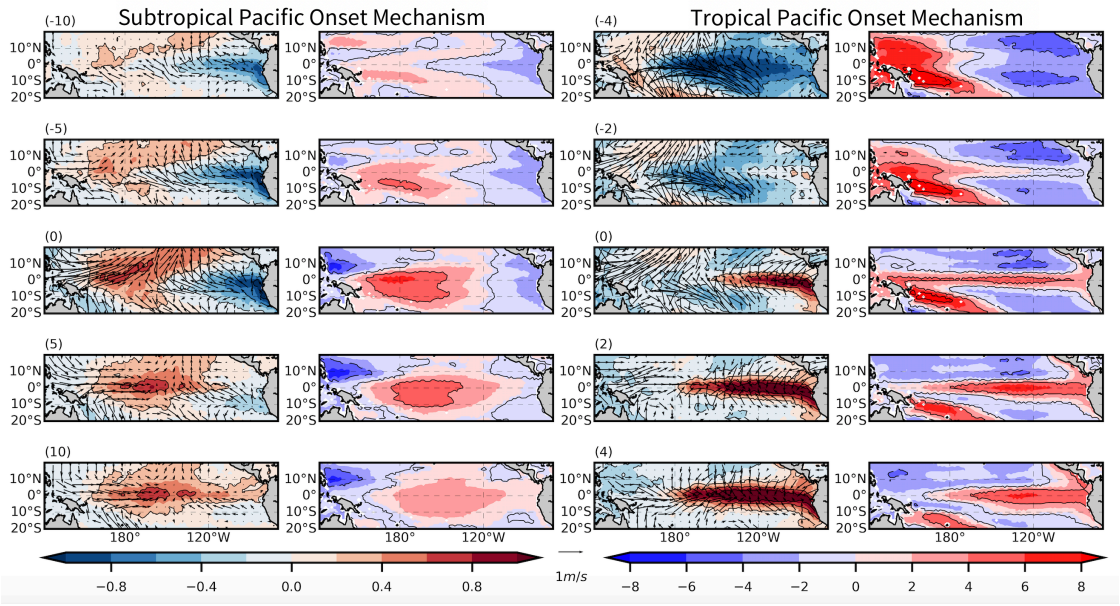

Figure 2.6. The lead/lag regressions onto the PCs of the SP-onset and TP-onset modes of the anomalies in sea surface temperature, wind (together in first and third columns), and sea surface height anomalies (second and fourth columns). The regressions are shown for different lead/lag months for the SP-onset and TP-onset modes, which are indicated by the number shown above the upper left of each panel.

2.5 ENSO Onset Mechanisms on ENSO Transitions

To examine the degree of ENSO complexity produced by the TP-onset and SP-onset mechanisms, we performed a composite analysis that investigates the SST evolution associated with these two mechanisms. We first selected the months in which the PC2 (PC3) values are larger than one standard deviation for the composite of the positive SP-onset (TP-onset) mechanisms. Conversely, the months of negative SP-onset (TP-onset) mechanisms are chosen when the PC2 (PC3) values were smaller than ±1 standard deviation. Figures 2.7a-d show the evolutions of the composited SST anomalies along the equatorial Pacific (5°S–5°N) during a period of 12 months before to 12 months after the peak of the two onset mechanisms The composite evolution for the

TP-onset mechanism (Figs. 2.7a and 2.7b) is relatively simple and characterized by oscillatory transitions: A positive TP-onset mode is preceded by a La Niña and followed by an El Niño event and vice versa for the negative TP-onset mode. This is consistent with the existing view that a La Niña event produces a wind stress pattern that tends to charge the equatorial Pacific thermocline (i.e., a positive phase of the TP-onset mechanism), which later onsets an El Niño event and vice versa for the negative TP-onset mechanism. The evolution shows little asymmetry during ENSO transitions between positive and negative phases. It should be noted that previous studies have found that the charging associated with La Niña and the discharging associated with El Niño can be asymmetric in amplitude (Chen et al., 2015; Hu et al., 2017); however, this asymmetry differs from the transition asymmetry discussed here.

For the SP-onset mechanism, the composite evolution is less oscillatory (Figs. 2.7c and d). This is particularly clear for the positive SP-onset mechanism, where the El Niño event it induces is not preceded by a La Niña. Also, the El Niño onset is in the tropical central Pacific rather than in the tropical eastern Pacific as is the case for the ENSO induced by the TP-onset mechanism (cf. Figs 2.7a and b). As for the positive SP-onset mechanism, the composite for the negative SP-onset mechanism also shows that the La Niña develops in the tropical central Pacific with cold anomalies lingering in the region for many months before the onset. However, the evolution for the negative SP-onset mechanism is not symmetric with respect to the positive SP-onset mechanism. The negative SP-onset composite is preceded by a strong El Niño, which has the magnitudes larger than the subsequent La Niña. We noticed that a number of the preceding months used in this composite are associated with the 1982–1983 and 1997–1998 El Niño events. Apparently, the ENSO evolution is very different between the positive and negative phases of the SP-onset mechanism. The event-to-event evolution is more complex for the SP-onset mechanism than for

the TP-onset mechanism and is also more asymmetric between the positive and negative phases of the SP-onset mechanism.

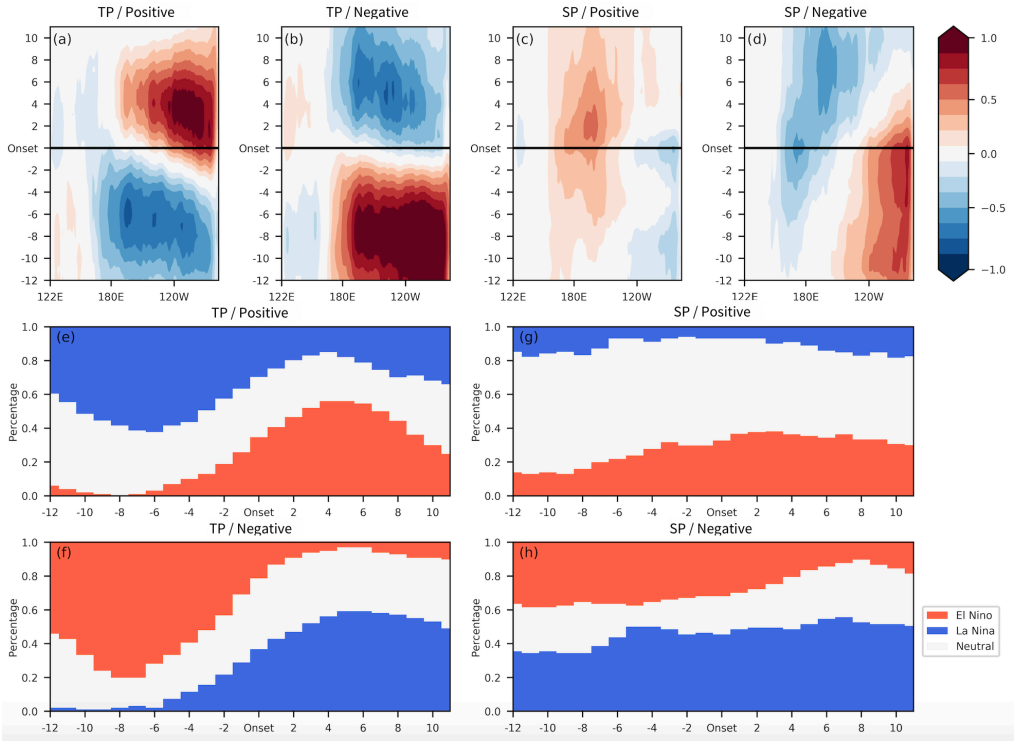

Figure 2.7. (a)-(d) The evolution of equatorial Pacific (5°S-5°N) SST anomalies composited for (a) the positive TP-onset mechanism, (b) the negative TP-onset mechanism, (c) the positive SP-onset mechanism, and (d) the negative SP-onset mechanism. (e)-(h) The percentages of the composited months that are in an El Niño (red), La Niña (blue), or neutral (white) state during the period 12 months before to 12 months after the positive and negative phases of the TP-onset mode (e and f) and the SP-onset mode (g and h) reach their peak (at lag 0). A composited month is determined to be in an El Niño (La Niña) state if the Niño3.4 index in that month is greater (smaller) than or equal to (-)0.5°C. Otherwise, it is in a neutral state. The total number of months in each composite is shown above the upper-right corner of each panel.

We performed another analysis with the same set of months selected for the composite SST analysis but focused on how the El Niño, La Niña, and neutral states evolve from one to another (Figs. 2.7e-h). A month is determined to be in an El Niño (La Niña) state if the Niño3.4 index in that month is greater (smaller) than or equal to (–)0.5 °C. Otherwise, it is in a neutral state. We also used different thresholds (0.5, 0.8, and 1.0 standard deviation) to define strong onset mechanisms and found the composite results not sensitive to these thresholds (see Fig. 2.8). Figure 2.7e shows the percentages of ENSO states before and after the positive TP-onset mechanism peaks (i.e., at lag 0). The figure shows that, 5–6 months after the strong positive TP-onset phase, close to 50% of the months are characterized by an El Niño state. The figure also indicates that the strong positive TP-onset phase is preceded mostly (>60%) by a La Niña state. The composite for the strong negative TP-onset phase (Fig. 2.7f) shows a similar oscillatory evolution, except that the negative TP-onset phase is preceded by an El Niño and fol- lowed by a La Niña. Figures 2.7e and f confirm that the TP-onset mechanism strongly (>50–60%) regulates the transitions between El Niño and La Niña phases. Therefore, the TP-onset onset mechanism acts to reduce ENSO complexity.

Figure 2.7g shows that a strong positive SP-onset phase tends (about 40% of the time) to be followed by an El Niño state, as we expect from the SF mechanism (e.g., Chang et al., 2007; Yu et al., 2010). However, this SP-onset phase is mostly (>80%) preceded by a neutral state. This is consistent with the understanding that the initial subtropical Pacific SST anomalies associated with the SP-onset mechanism are often induced by subtropical or extratropical atmospheric disturbances, particularly the North Pacific Oscillation (NPO; Vimont et al., 2003; Yu & Kim, 2011). The NPO can be an internal mode of the atmosphere and is not necessarily forced by ENSO (Linkin & Nigam, 2008). Figure 2.7h shows that the negative SP-onset phase tends (about 50%)

to be followed by a La Niña state. Interestingly, the negative SP-onset phase is mostly preceded by an El Niño (about 38%) or La Niña (51%) state but not the neutral state. The transition from a La Niña to another La Niña results in a multiyear La Niña event. That is, the negative phase of the SP-onset mechanism is forced by ENSO, which is very different from the positive phase of the SP-onset mechanism that is mostly not related to ENSO forcing.

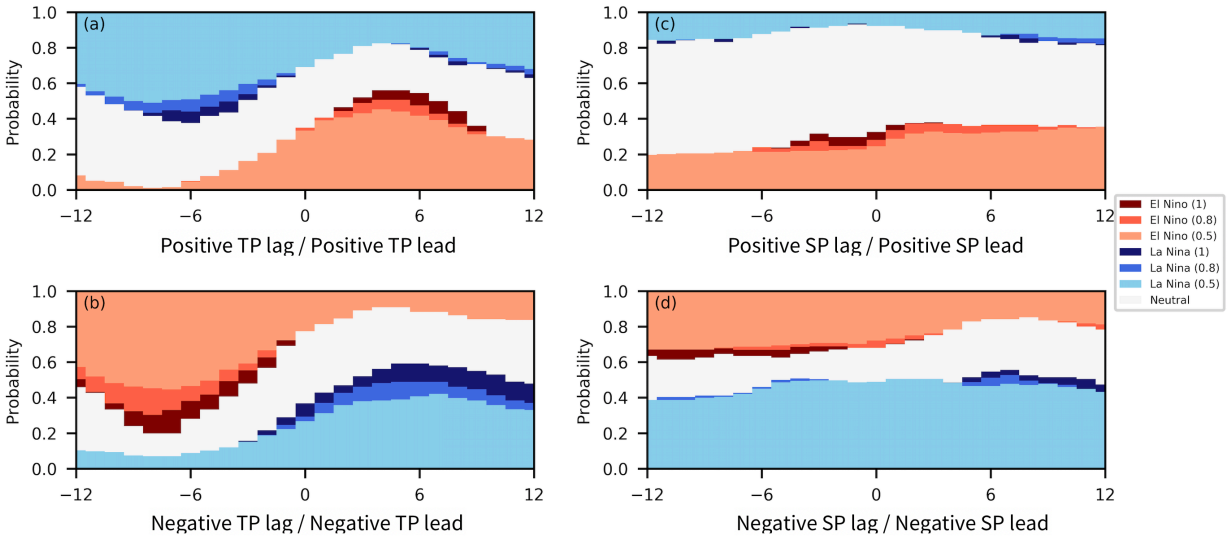

Figure 2.8. Similar to Figure 2.7e-h, but using different values of the threshold to define the ENSO states (i.e., El Niño, La Niña, or neutral). The light, normal, and dark colors are the ENSO states determined, respectively, using 0.5, 0.8 and 1.0 of the standard deviation of the PCs as the threshold.

As noted in Figure 2.7h, the negative SP-onset mechanism is often preceded by an El Niño or La Niña event. The preceding El Niño months are related to the extreme El Niño events, including the 1982–1983 and 1997–1998 El Niño events. Yu and Kim (2011) have shown that these extreme El Niño events can induce the positive phase of NPO via teleconnections to turn on the negative SP-onset mechanism, which then onsets La Niña events in the tropical central Pacific. In fact,

Figure 2.7h indicates that the negative SP-onset onset mechanism is more often preceded by a La Niña event, resulting in multiyear La Niña events. No such tendency for multiyear El Niño events can be found in the positive SP-onset mechanism. All four multiyear La Niña events we identified (see Section 2.3 for a description of the methodology) in the analysis period maintained negative PC values of the SF mode throughout these events, but the PC values of the TP-onset mode fluctuated from positive values in year 1 to negative values in year 2 (Fig. 2.9). The asymmetry between the positive and negative phases of the SP-onset mechanism is one possible reason why multiyear La Niña events occur more often than multiyear El Niño events (Hu et al., 2014; Ohba & Ueda, 2009; Okumura & Deser, 2010). The cause of this asymmetry associated with the positive and negative phases of the SF mechanism needs to be investigated but is beyond the scope of this chapter.

We next use the CMIP5 preindustrial simulations to examine two of our main findings so far: (1) That the SF mechanism increases ENSO complexity while the TP-onset mechanism decreases complexity and (2) that the SP-onset mechanism increases El Niño-La Niña asymmetries. Based on the eigenvalues of the TP-onset and SP-onset modes (Fig. 2.10), we find that most (26 out of the 34) CMIP5 models are dominated by the TP-onset mechanism. Only eight of the models are dominated by the SP-onset mechanism. Since the observation during the analysis period is dominated by the SP-onset mechanism, this simple analysis indicates that contemporary climate models in general overestimate the strength of the TP-onset mechanism but underestimate the strength of the SF onset mechanism. Based on the observational composite analysis, we expect the models dominated by the TP-onset mechanism to produce more regular and less complex ENSO evolutions compared to the models dominated by the SP-onset mechanism. The power spectra of the Niño3.4 index produced by these two groups of models confirm this speculation. Figure 2.11a

reveals that the mean spectrum averaged from all the TP-dominated models shows a sharp peak in power centered around 3–4 years indicating a very regular ENSO evolution, whereas the mean spectrum of the SP-dominated models shows large values of the power spread out over 2 to 6 years indicating a less-regular and more-complex evolution of their simulated ENSOs.

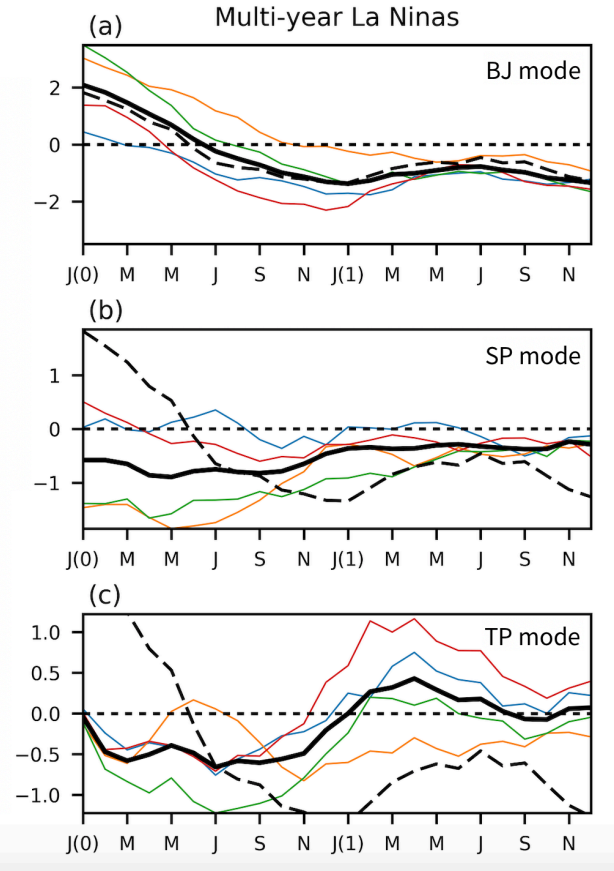

Figure 2.9. The PCs of the BJ mode (a), SP-onset mode (b), and TP-onset mode (c) during four multi-year La Niña events (i.e., 1970, 1983, 1998, and 2010). The thick-solid lines are the means of the four events, whereas the colored thin lines are for the individual events. The long-dashed lines are the mean values of Niño3.4 index averaged over all four events.

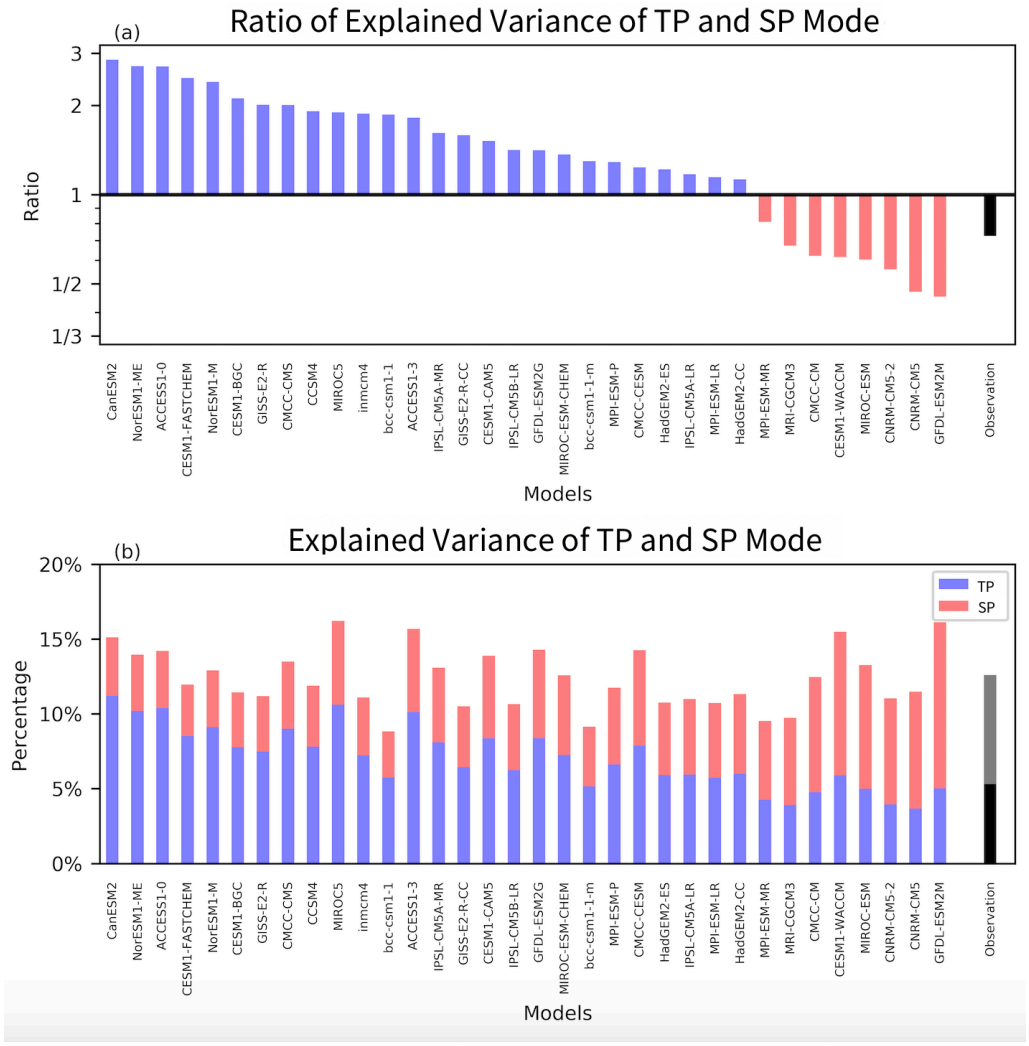

Figure 2.10. (a) The ratio of explained variance of the TP-onset mode to that of the SP-onset mode calculated from the pre-industrial simulations of the 34 CMIP5 models and the observations. The y-axis is in log scale. The blue bars correspond to the TP-dominated models (i.e., ration larger than 1.0), while the red bars correspond to the SP-dominated models. The observational values are indicated by a black bar. (b) The explained variance of the TP-onset and SP-onset modes. The blue (red) bars are the percentages of the TP-onset (SP-onset) modes. The black (gray) bar is the percentage of the TP-onset (SP-onset) mode in the observations.

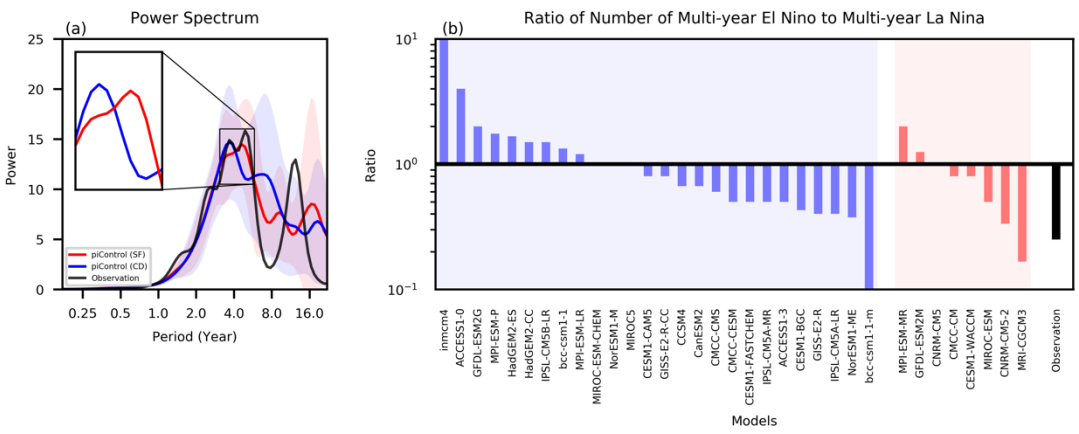

Figure 2.11. (a) Power spectrum of the normalized Niño3.4 index from observations (black), the multi-model mean of the SP-dominated (red) and the TP-dominated (blue) models from last hundred years of the pre-industrial CMIP5 simulations. The shading denotes one standard deviation of each spectrum. (b) The ratio of the number of multi-year El Niño events to the number of multi-year La Niña events. The y-axis is in log10 scale. The blue bars are used for the TP-dominated models, the red bars are used for the SP-dominated simulations, and the black bar is for the observations.

We also compared the El Niño-La Niña asymmetries between these two model groups by examining the ratio of the number of multiyear El Niño events to the number of multiyear La Niña events in the preindustrial simulations. Figure 2.11b shows that most (six out of eight) of the SP-dominated models show a ratio that indicates a preference for more multiyear La Niñas than El Niños. In contrast, the TP-dominated models do not show a preference of having more multiyear El Niño or La Niña events. This result adds some support to the notion that the SP-onset mechanism can increase the El Niño-La Niña asymmetries.

We performed a 15-year sliding lead-lagged correlation between the PCs of the TP-onset and SP-onset modes constructed from the observations and the Niño3.4 index to examine the decadal variations of these two onset mechanisms. As shown in Figure 2.12, the TP-onset mechanism has maintained a relatively stationary correlation with the Niño3.4 index throughout the past six decades, showing positive values when the TP-onset mode leads the Niño3.4 index and negative values when the TP-onset mode lags the Niño3.4. This result indicates that the strength or the contribution of the TP-onset mechanism to ENSO does not exhibit any strong decadal variations during this period. In contrast, the correlation of the SP-onset mechanism with the Niño3.4 index is weak before 1980, which means that the SP-onset mechanism has become important only recently. The correlation intensified in particular after the early 1990s, which implies that ENSO complexity may have become more prominent during the last two decades. This is consistent with Yu et al. (2015), who reported that the SP-onset mechanism intensified after the Atlantic Multidecadal Oscillation switched from a negative to a positive phase in the early 1990s. Lyu and Yu (2017) showed that a positive phase of the Atlantic Multidecadal Oscillation can intensify the eastern Pacific subtropical high enhancing the wind-evaporation-SST feedback strengthening the SP-onset mechanism. Figure 4, in fact, also implies that the SP-onset mechanism is more sensitive than the TP-onset mechanism to changes in Pacific mean state. We note that the SP-onset mechanism may have also changed after 2005, but since this change occurs toward the end of the period examined, more data are needed to confirm this change.

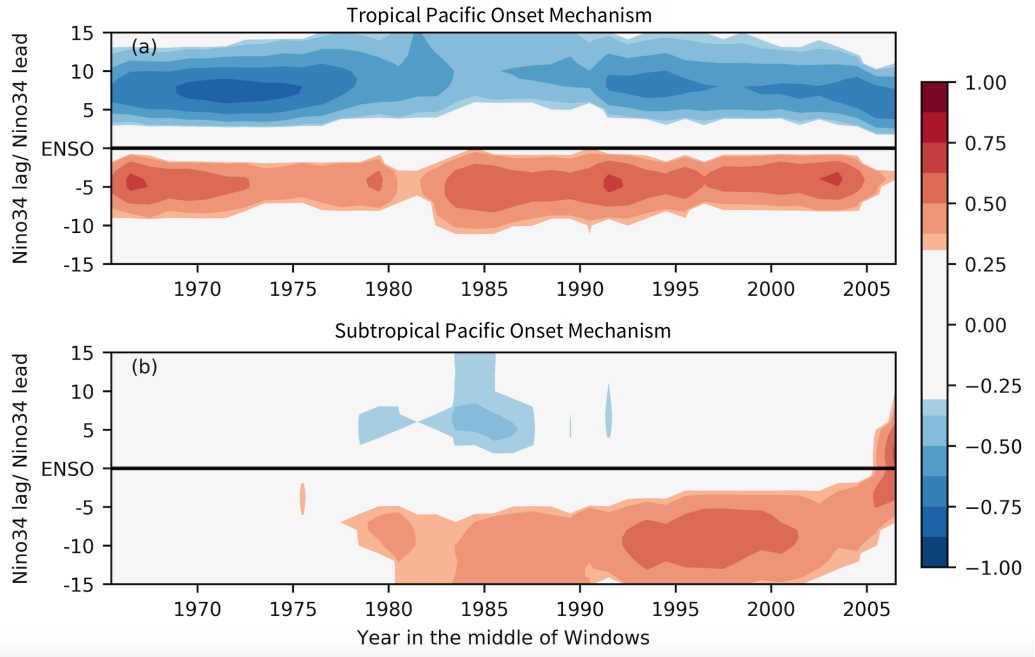

Figure 2.12. 15-year sliding lead/lag correlation values between the Niño 3.4 index and (a) the PCs of the TP-onset mode and (b) the SP-onset mode. Color shaded areas are statistically significant at the 95% confidence level.

2.6 Summary and Discussion

In this chapter, we examined how the onset mechanisms can affect the ENSO complexity. We showed that the SP-onset mechanism is a key source of ENSO complexity and is also capable of importing extratropical influences that can produce multiyear La Niña events as well as El Niño-La Niña asymmetries, a finding that has not previously been emphasized. Our results are consistent with the existing view that stochastic forcing from the extratropics can increase ENSO irregularity (e.g., Alexander et al., 2010; Chang et al., 1996) and diversity (e.g., Capotondi et al., 2015), but we are able to additionally and more specifically describe how the extratropical stochastic forcing works through the SP-onset mechanism to increase ENSO complexity. The analyses of the two

onset mechanisms shed light on the possible sources/causes of the ENSO complexity, which may enable us to better project future changes in ENSO. Our results also indicate that by examining the two ENSO onset mechanisms, we are able to explain the ENSO properties found in a large number of climate models in a novel way.

Chapter 3

The Tropical Regulation of the Subtropical Onset Mechanism

3.1 Abstract

ENSO transitions from one event to another in complex ways. Using observational analyses and forced atmospheric model experiments, we show that a preceding ENSO event can activate a subtropical Pacific forcing mechanism to trigger another ENSO event during the following year. These tropical-subtropical Pacific interactions result in a cyclic ENSO transition if the two ENSO events are of opposite signs or a multi-year ENSO transition if they are of the same sign. The preceding ENSO event should excite deep convection in the tropical Pacific in order to activate the subtropical Pacific mechanism. This requirement enables mean temperatures in the cold tongue and warm pool to respectively control how easily the cyclic and multi-year transitions can occur. A future warmer tropical Pacific is projected to decrease the frequency of occurrence of multi-year ENSO transitions but increase the occurrence of cyclic ENSO transitions.

3.2 Introduction

El Niño-Southern Oscillation (ENSO) is the strongest year-to-year phenomenon in our global climate, causing regional climate extremes and massive ecosystem impacts (McPhaden et al. 2006; Donnelly & Woodruff 2007; Coelho & Goddard 2009; Power et al. 2013). ENSO has recently been observed to exhibit a wide range of complex behaviors (Capotondi et al. 2015; Yu et al. 2017; Timmermann et al. 2018) that impede our understanding of its physical dynamics and results in huge uncertainties in projecting its future changes (Fedorov et al. 2003; Vecchi & Wittenberg 2010;

Collins et al. 2010; Cai et al. 2015; Sohn et al. 2016). One aspect of ENSO complexity is related to the ways that ENSO transitions from one event to another (Yu & Fang 2018; Wang et al. 2019). An El Niño (La Niña) event can be preceded (1) by a La Niña (El Niño) event to become a cyclic ENSO transition; (2) by a neutral event to become an episodic ENSO transition; or (3) by another El Niño (La Niña) event to become a multi-year ENSO transition. Unlike most other studies of ENSO complexity that focus on properties during the peak phase, ENSO transition complexity focuses on ENSO's properties during the onset phase.

Whether an ENSO event goes through a cyclic, episodic, or multi-year transition is affected by its onset (or trigger) mechanism (Yu & Fang 2018)— the process by which the initial ENSO sea surface temperature (SST) anomalies are produced in the equatorial Pacific. Two primary onset mechanisms have been identified by the research community over the past decades (see reviews in Capotondi et al. 2015; Yu et al.; 2017; Wang et al. 2017; Yang et al. 2018). The tropical Pacific onset (TP-onset) mechanism consists of the recharge oscillator (Wyrki 1975; Jin 1997) and delayed oscillator (Battisti & Hirst 1989; Zebiak & Cane 1987) theories. Together, these theories describe how equatorial surface wind anomalies induced by an ENSO event can deepen or shallow the thermocline in the equatorial eastern Pacific over the following months, and onset another ENSO event with an opposite phase. The TP-onset mechanism leads mostly to cyclic ENSO transitions and contributes to reduce ENSO transition complexity (Yu & Fang 2018), although it should be noted that its asymmetric responses between El Niño and La Niña may allow for some complexity (Hu et al. 2017). In contrast, the subtropical Pacific onset (SP-onset) mechanism describes how subtropical Pacific SST anomalies can intrude into the equatorial Pacific to trigger ENSO events (Vimont et al. 2003; Kao & Yu 2009; Yu et al. 2010; Alexander et al. 2010; Anderson & Perez 2015). This onset mechanism has been shown to produce all three transition patterns (Yu & Fang

2018; Fig. 3.1). Therefore, the SP-onset mechanism is a key contributor to ENSO transition complexity and needs to be better understood for projecting future changes in ENSO complexity.

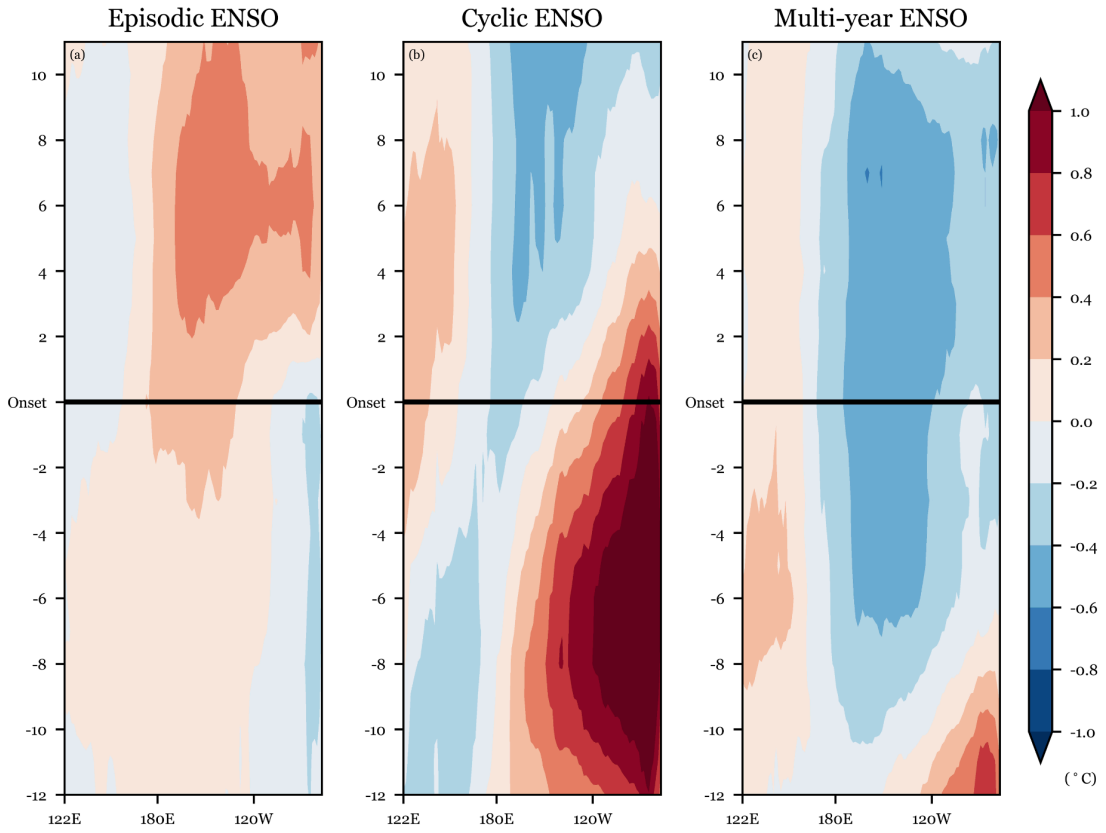

Figure 1. Evolution of equatorial SST anomalies during the three ENSO transition types associated with the subtropical Pacific onset mechanism. a, Equatorial SST anomalies composited from observed episodic El Niño events during 1958-2014 from 12 months before to 12 months after the onset month of El Niño. b, same as a but composited from cyclic ENSO events (specifically El Niño-to-La Niña) months. c, same as a but composited from multi-year La Niña months. The onset month is defined as the month when the SP-onset index becomes larger than 0.7 times its standard deviation.

To trigger an ENSO event, the SP-onset mechanism is initiated by a decrease or increase in trade winds that extends from off the coast of Baja California to the equatorial central Pacific that respectively warms or cools SSTs underneath. The wind and SST anomalies can prolong for several months through a wind-evaporation-SST feedback (WES; Xie & Philander 1994) (aka the Pacific meridional mode (PMM) in Chiang & Vimont (2004) or seasonal footprinting mechanism in Vimont et al. (2003)). The initial trade wind variations are often induced by subtropical atmospheric processes (such as the North Pacific oscillation; NPO) that are non-ENSO related (Vimont et al. 2003). Therefore, it is easy to understand why the SP-onset mechanism can give rise to episodic ENSO transitions. Less attention has been paid in past studies to the possibility that the SP-onset mechanism can also be activated by a preceding ENSO event resulting in either cyclic or multi-year ENSO transitions.

The limited studies on the ENSO-induced SP-onset mechanism have found that extreme El Niño events can activate the SP-onset mechanism to trigger La Niña events during the following year and result in a cyclic El Niño-to-La Niña transition (Yu & Kim 2011; Yu & Fang 2018). Interestingly, the opposite tendency of a cyclic La Niña-to-El Niño transition via the SP-onset mechanism seems to occur less frequently (Yu & Fang 2018). The SP-onset mechanism appears to respond asymmetrically to El Niño and La Niña. What is the cause for this asymmetry and how will this asymmetry change in the future as the earth warms? Answers to these questions are important to project future changes in ENSO transition complexity and are the main focus of this chapter.

3.3 Datasets, Methods, and Model Experiments

Monthly mean values of SST, surface wind, geopotential height, and precipitation, and sea surface height (SSH) during the period of 1958-2014 were used after they were regrided to a common 1.5° × 1° longitude-latitude grid covering the tropical Pacific (20°S–20°N, 122°E–70°W). The SST data is the Hadley Center Sea Ice and Sea Surface Temperature data set (Rayner et al. 2003), the surface wind, geopotential height, and precipitation fields are from the National Centers for Environmental Prediction/National Center for Atmospheric Research (Kalnay et al., 1996), and the SSH data is produced by the German contribution of the Estimating the Circulation & Climate of the Ocean (Köhl, 2015). Anomalies are defined as the deviations from the seasonal cycle averaged over the analysis period after removing the linear trend. The same procedures were applied to the simulations (the last 100 years of the preindustrial simulations and the full periods of the historical, RCP4.5 and RCP8.5 simulations) produced by 28 models of the Coupled Model Intercomparison Project (CMIP5) (Taylor et al. 2012; see Table 3.1). Similar results are obtained when a quadratic trend removal is applied (in place of the linear trend removal).

Several indices were used in the analyses. Indices of the SP- and TP-onset mechanisms were constructed by applying a multi-variate empirical orthogonal function (MEOF) analysis to combined SST, wind, SSH anomalies in the tropical Pacific (Section 2.3; Xue et al. 2000; Yu & Fang 2018). These indices are referred to as the SP-onset index and the TP-onset index. A Niño3.4 index is used to represent the intensity of ENSO events and is defined as the SST anomalies averaged between 5°S–5°N and 170°W–120°W. The equatorial eastern Pacific (EEP) region is defined as the area between 5°S–5°N and 120°W–90°W, whereas the equatorial central Pacific (ECP) region is defined as the area between 5°S–5°N and 160°E–170°W. A series of forced experiments were conducted in this chapter with an atmospheric general circulation model (AGCM).

Model	Modeling Center	Model	Modeling Center
ACCESS1-0	Commonwealth Scientific and Industrial Research Organization (CSIRO) and Bureau of Meteorology (BOM), Australia	GISS-E2-R-CC	NASA Goddard Institute for Space Studies
ACCESS1-3		HadGEM2-CC	Met Office Hadley Centre (additional HadGEM2-ES realizations contributed by Instituto Nacional de Pesquisas Espaciais)
bcc-csm1-1	Beijing Climate Center, China Meteorological Administration	HadGEM2-ES	
bcc-csm1-1-m		inmcm4	Institute for Numerical Mathematics
CanESM2	Canadian Centre for Climate Modelling and Analysis	IPSL-CM5A-LR	Institut Pierre-Simon Laplace
CCSM4	National Center for Atmospheric Research	IPSL-CM5A-MR	
CESM1-BGC	Community Earth System Model Contributors	IPSL-CM5B-LR	
CESM1-CAM5		MIROC-ESM	Japan Agency for Marine-Earth Science and Technology, Atmosphere and Ocean Research Institute (The University of Tokyo), and National Institute for Environmental Studies
CMCC-CM	Centro Euro-Mediterraneo per I Cambiamenti Climatici	MIROC-ESM-CHEM	
CMCC-CMS		MIROC5	Atmosphere and Ocean Research Institute (The University of Tokyo), National Institute for Environmental Studies, and Japan Agency for Marine-Earth Science and Technology
CNRM-CM5	Centre National de Recherches Météorologiques / Centre Européen de Recherche et Formation Avancée en Calcul Scientifique	MPI-ESM-LR	Max-Planck-Institut für Meteorologie (Max Planck Institute for Meteorology)
GFDL-ESM2G	NOAA Geophysical Fluid Dynamics Laboratory	MPI-ESM-MR	
GFDL-ESM2M		MRI-CGCM3	Meteorological Research Institute
GISS-E2-R	NASA Goddard Institute for Space Studies	NorESM1-M	Norwegian Climate Centre

Table 3.1. The names of the 28 CMIP5 models used in chapter 3.

We conducted a series of 4-member forced atmospheric model experiments to examine whether anomalous warming and cooling in the EEP and ECP regions can excite the surface wind anomaly pattern associated with the SP-onset mechanism. The model used is the Community

Atmosphere Model version 6 (CAM6) from the Community Earth System Model version 2 (CESM2). Specifically, the F2000climo component set of CESM2 with the f19_f19_mg17 resolution was used, which means that the standalone CAM6 was run with prescribed seasonal cycles (averaged over 1995-2005) of SSTs and sea-ice extents in the common 1.9x2.5 grid and gx1v7 oceanic resolution for the experiments. The control run is a 7-year simulation with this default model configuration, from which the November conditions of the third year were used as the initial conditions for the experiments. The experiments were integrated from the November initial condition for another three months with warming or cooling added separately to the EEP or ECP region.

In the experiments, we added Gaussian shaped SST anomalies in the EEP or ECP to the climatological SSTs to study the atmospheric responses. The Gaussian forcing has a half-width of 45 degrees in longitude and 10 degrees in latitude and is centered at (175°E, 0°N) when applied to the ECP and at (105°W, 0°N) when applied to the EEP. The forcing was applied throughout the three months from November to January and the maximum amplitude of the anomalies was as follows: -4, -3, -2, -1, +1, +2, +3, and +4°C in each set of EEP and ECP experiments. These different SST amplitudes were designed to mimic the distinct amplitudes of El Niño and La Niña

3.4 Tropical-Induced Subtropical Onset Mechanisms of ENSO

We first examine the anomaly pattern associated with the SP-onset mechanism by regressing SST and surface wind anomalies onto the SP-onset index (Fig. 3.2a). A key feature in the pattern is the overlap of trade wind anomalies with SST anomalies in the northeastern subtropical Pacific. This overlap reflects the subtropical coupled nature of the SP-onset mechanism, which is key to extending the SST anomalies southwestward into the equatorial central Pacific for the ENSO onset.

A negative phase of the SP-onset mechanism (see Fig. 3.2a) can onset a La Niña event, whereas a positive phase of the SP-onset mechanism can onset an El Niño event. As mentioned, the NPO is considered to be a key source for the trade wind anomalies. However, Figure 3.2a indicates that subtropical Pacific wind anomalies may also be related to the large SST anomalies in the equatorial eastern Pacific (EEP) and the equatorial central Pacific (ECP).

The pair of anomalous cyclones straddling the equator to the west of the EEP SST anomalies appears to be a Gill-type response (Gill 1980) to the SST anomalies. The trade wind anomalies over the northeastern subtropical Pacific are associated with the anomalous cyclone to the north. This anomaly structure suggests that the subtropical Pacific trade wind anomalies can be the result of a Gill-type response to the EEP SST anomalies (as illustrated by the red vectors in Fig. 1a) (Wang et al. 2000). An El Niño (La Niña) event in the EEP can activate a negative (positive) phase of the SP-onset mechanism to trigger a subsequent La Niña (El Niño) event, giving rise to a cyclic ENSO transition. On the other hand, the same trade wind anomalies over the northeastern Pacific can also be linked to the ECP SST anomalies through a wave train pattern connecting the two regions (as illustrated by the blue circles in Fig. 3.2a) (Stuecker 2018; Lyu et al. 2017). A La Niña (El Niño) event in the ECP can activate a negative (positive) phase of the SP-onset mechanism to trigger another La Niña (El Niño) event, giving rise to a multi-year ENSO transition. Therefore, the Gill-type response and basin-wide wavetrain enable the SP-onset mechanism to produce cyclic ENSO transitions through the EEP region and multi-year ENSO transitions through the ECP region.

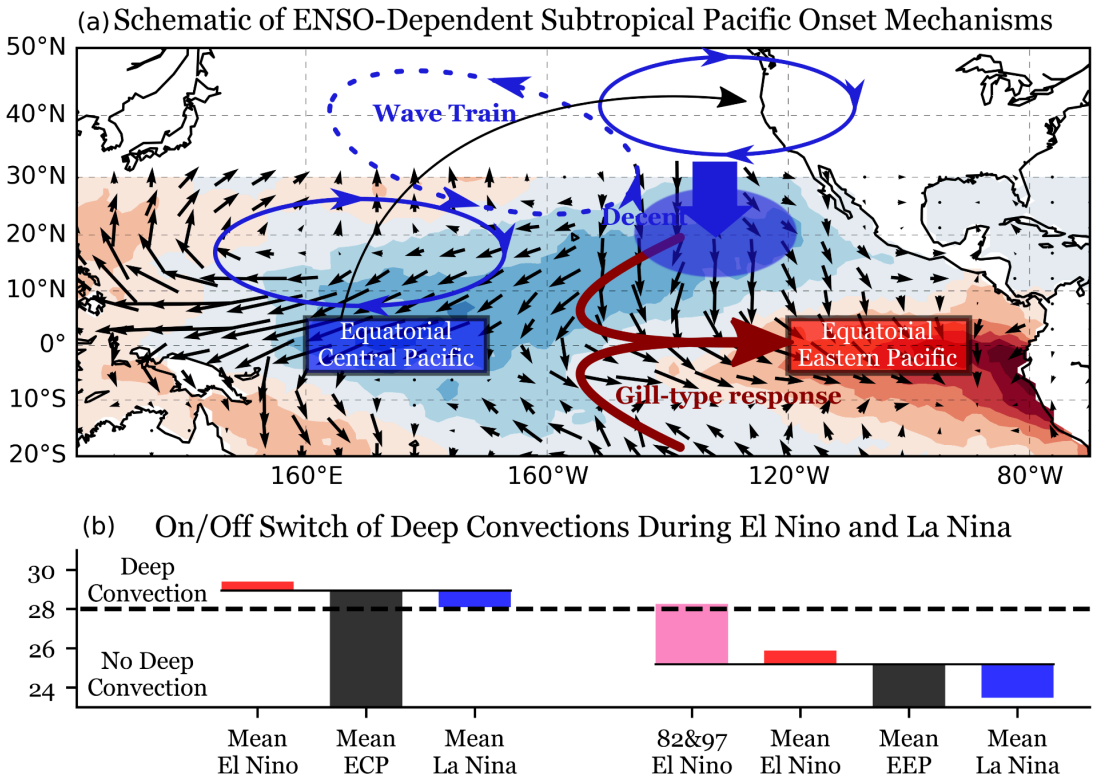

Figure 3.2. (a) Schematic of the processes that enable SST anomalies (color shading) in the equatorial central Pacific (ECP) or equatorial eastern Pacific (EEP) to excite the surface wind anomalies (vectors) associated with the subtropical Pacific onset mechanism via a Gill-type response (brown arrows) and Rossby wave train in the lower troposphere (blue solid and dashed arrows) and the associated descending motions (large blue arrow); (b) the departures of the ECP and EEP SSTs (°C) from the threshold SST value for deep convection (28°C; horizontal thick-dashed line) in their climatological state (horizonal thin-solid lines) and with the values added by the typical SST anomaly values of El Niño (red bars), La Niña (blue bars), and the 1982-83 and 1997-98 extreme El Niño events (pink bar).

In order to excite the Gill-type response and the wavetrain, ENSO events in the EEP and ECP should induce convective heating anomalies. The threshold value for deep convection is around 28°C (Zhang 1993; Sud et al. 1999), which is confirmed for both the EEP and ECP regions by examining the relationships between precipitation anomalies and SSTs over the regions (Figs. 3.3a-b). A composite of all El Niño months when the EEP SSTs are greater than 28°C (the pink dots in Fig. 3.3a) reveals strong evidence of a Gill-type response, which is characterized by a pair of anomalous cyclones in the lower troposphere (Figs. 3.3c-g) and a pair of anticyclones in the upper troposphere (Figs. 3.3h-l). An analysis of the time series of the EEP and SP-onset indices confirms that a negative SP-onset index occurs after the EEP SST index passes the 28°C threshold (Fig. 3.4a). The El Niño-induced anomalous trade winds (and the negative SP-onset mechanism) bring anomalous cold water over the subtropical Pacific toward the tropical central Pacific and switch the composite SST anomalies from El Niño to La Niña condition (Figs. 3.3c-g). In contrast, the Gill-type response is either very weak or absent when we repeat the composite for all El Niño months where the EEP SSTs are lower than 28°C (the red dots in Fig. 3.3a) or with all La Niña months (the blue dots in Fig. 3.3a) (see Fig. 3.5).

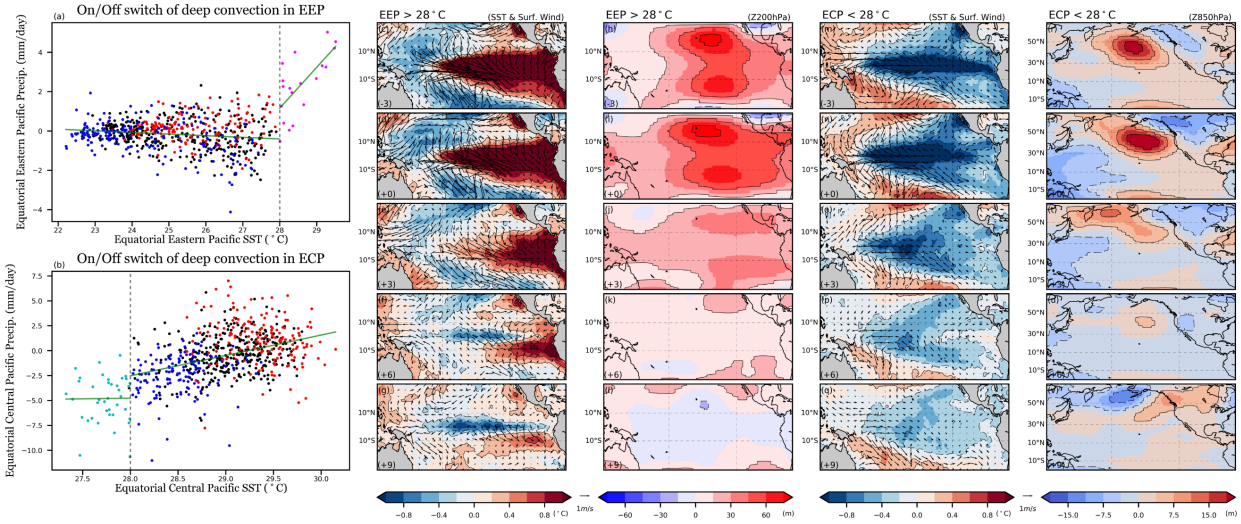

Figure 3.3. Relations between precipitation anomalies and SSTs (a) in the equatorial eastern Pacific (EEP) and (b) the equatorial central Pacific (ECP). Green lines are the linear fits for SSTs greater and less than 28°C. The pink dots are El Niño months when the SST > 28°C; red dots are El Niño months when SST < 28°C; and the blue and light-blue dots are the La Niña months when SST > 28°C and SST < 28°C. Evolution of (c)-(g) SST, surface winds, and (h)-(l) 200hPa geopotential heights anomalies composited for the months in which the EEP SST is greater than 28°C at time lags of -3, 0, +3, +6, +9 months (in the lower left corner of the sub panels). (m)-(v), for the months when ECP SST is lower than 28°C and 850hPa geopotential heights in the right column.

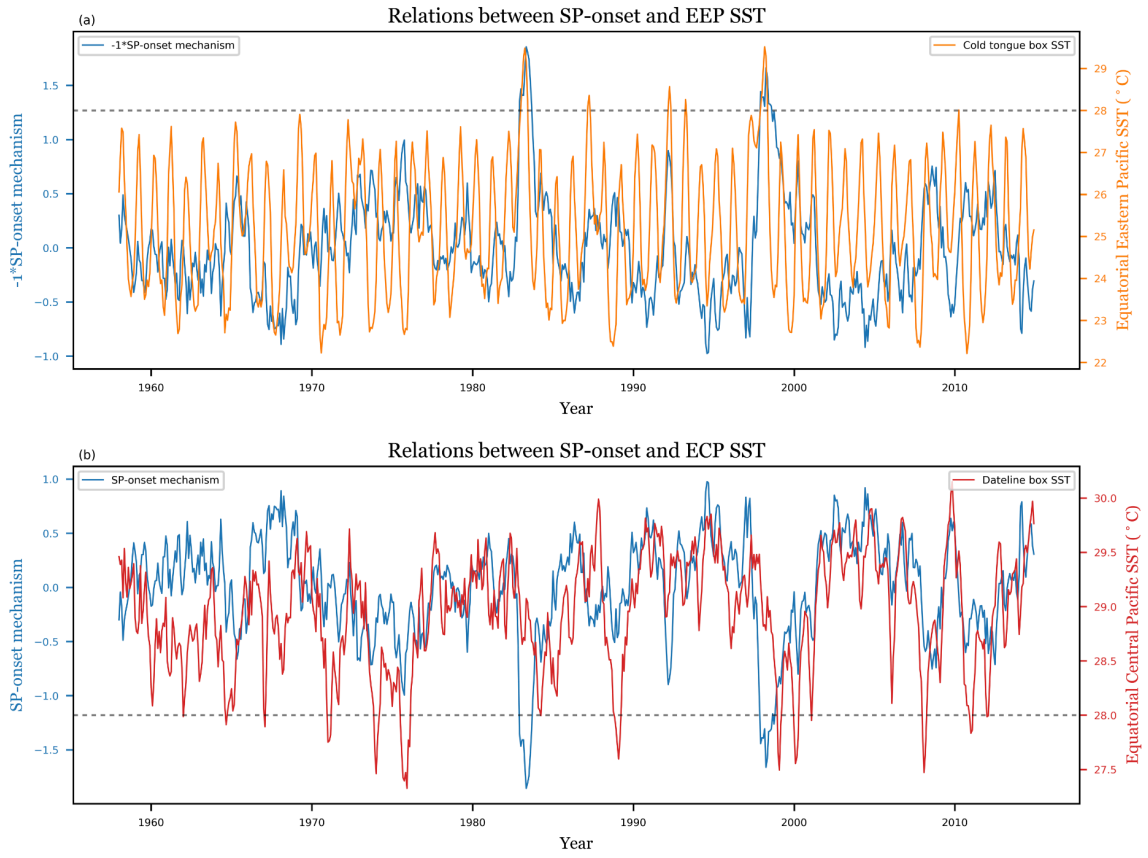

Figure 3.4. Time series of the SP-onset index and equatorial Pacific SSTs. (a) Time series of the reversed SP-onset index (blue) and the equatorial eastern Pacific SST (orange). (b) Time series of the SP-onset index (blue) and the equatorial central Pacific SST (red).

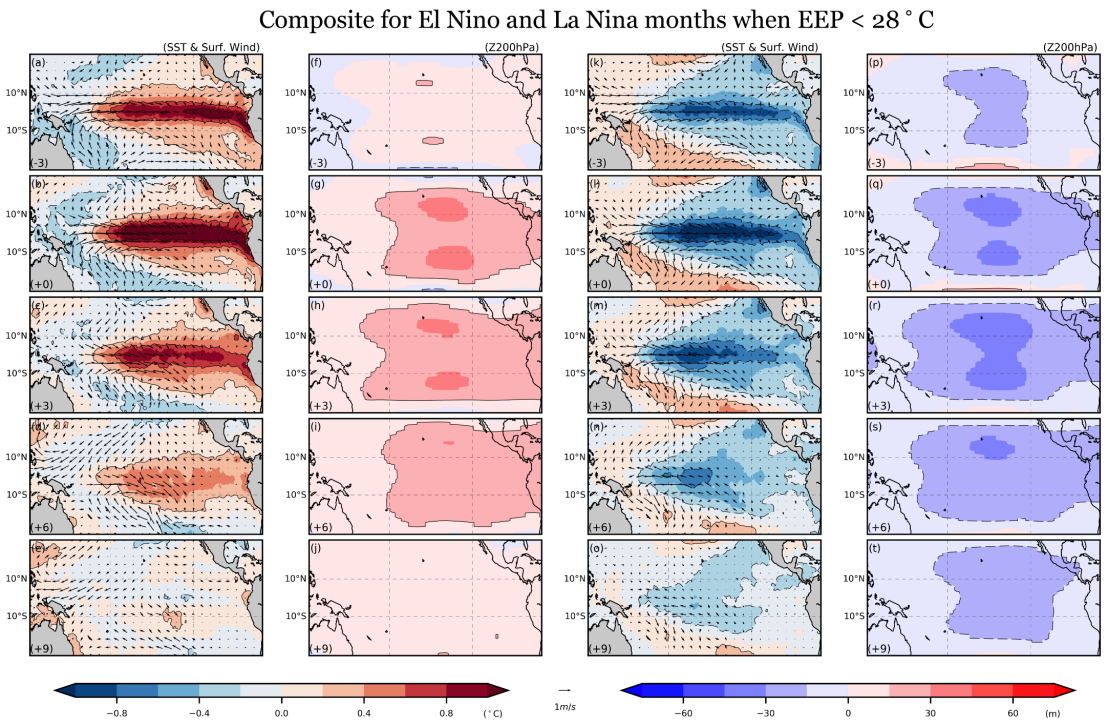

Figure 3.5. Composite for El Niño and La Niña months when the EEP is cooler than 28°C. a-j, Evolution of SST, surface wind (first column), and 200hPa geopotential height (second column) anomalies composited for the El Niño months in which the equatorial eastern Pacific SST is less than 28°C at time lags of -3, 0, +3, +6, +9 months (lag time shown in the lower left corner of the sub panels). k-t, As in a-j, but for La Niña months in which the equatorial eastern Pacific SST is less than 28°C.

Our composite results confirm that only El Niño events that are strong enough to raise EEP SSTs higher than 28°C can activate the SP-onset mechanism to produce the cyclic ENSO transition. Since the climatological SST in the EEP (25.19°C) is lower than the 28°C threshold (Fig. 3.2b), it is impossible for La Niña events to induce anomalous convective heating and activate this mechanism. This explains why the SP-onset mechanism produces more El Niño-to-La Niña than

La Niña-to-El Niño transitions (Yu & Fang 2018). There are only two such very strong El Niños during the analysis period: the 1982-83 and 1997-98 El Niños. We notice that the SP-onset index only becomes strongly negative after the EEP SSTs exceed the 28°C during these two extreme events (Fig. 3.4b). In addition, the SP-onset indices are stronger than the TP-onset indices during these events (lag-0 in Fig. S5a). This confirms that only extreme warming in the EEP can enable the SP-onset mechanism to dominate the TP-onset mechanism and to initiate cooling in the ECP resulting in cyclic transitions (Yu & Kim 2011). Therefore, the climatological SST in the EEP region determines how easily and what type of cyclic ENSO evolution (i.e., El Niño-to-La Niña or La Niña-to-El Niño) can be produced via the SP-onset mechanism. It should be noted that the TP-onset mechanism also contributes to the cyclic transitions in these extreme cases.

Over the ECP region, the climatological SST (28.94°C) is just slightly above the 28°C threshold. Therefore, even moderate La Niña events here can shut off deep convection, resulting in large negative convective heating anomalies (Fig. 3.2b). A composite analysis was performed with the La Niña months that lower the local SSTs below 28°C. The results indicate that a La Niña event that shuts off deep convection in the ECP region can excite wave train responses that extend into the extratropical lower troposphere (Figs. 3.3r-v). The wave train includes an anomalous anti-cyclone off the North American coast that can further induce anomalous descent over the northeastern subtropical Pacific via geostrophic processes (Lyu et al. 2017). The subsidence then enhances the trade winds and initiates a negative phase of the SP-onset mechanism (Fig. 3.3b; Fig. 2.9) to onset another La Niña condition (Figs. 3.3m-q). The negative values of the SP-onset index are confirmed during these events, while the TP-onset index follows its own cycle leading to positive values. (Fig. 3.6b). Therefore, even moderate La Niña events in the ECP region can result in a multi-year La Niña transition through the SP-onset mechanism.

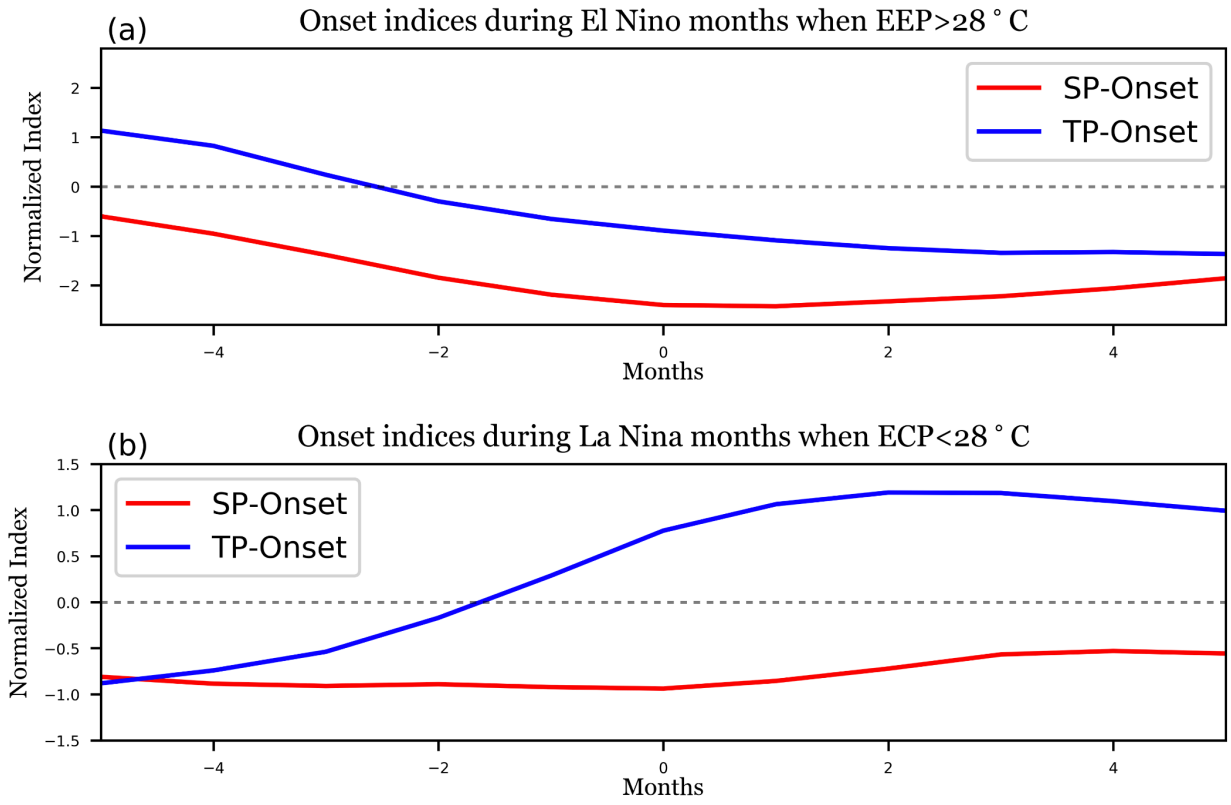

Figure 3.6. Evolutions of the TP-onset and the SP-onset indices composited during (a) those El Niño months that have SSTs in the EEP that are above the deep convection threshold (28°C) and (b) those La Niña months that have SSTs in the ECP that are below the deep convection threshold. The "0" month in the figure marks the time when the local SSTs in the EEP (ECP) first rise above (drop below) the 28°C threshold.

El Niño events in this region can also strengthen deep convection to produce positive convective heating anomalies. However, since most of the central Pacific El Niño (Yu & Kao 2007; Kao & Yu 2009) are of weaker SST anomalies (Lee & McPhaden 2010), the anomalous heating they induce are relatively small. A composite of the El Niño months in the ECP region (Figs. 3.8p-t) indicates that the extratropical wave train pattern excited by warm ECP SST anomalies is

relatively weaker than that excited by cold ECP SST anomalies (cf. Fig. 3.8q and Fig. 3.4b). Also, the evolution of the composite SST anomalies does not show multi-year El Niño transitions (Figs. 3.8k-o). A similar result was obtained in the composite analysis of weak La Niña events that do not lower ECP SSTs to below 28°C (Figs. 3.8a-j).

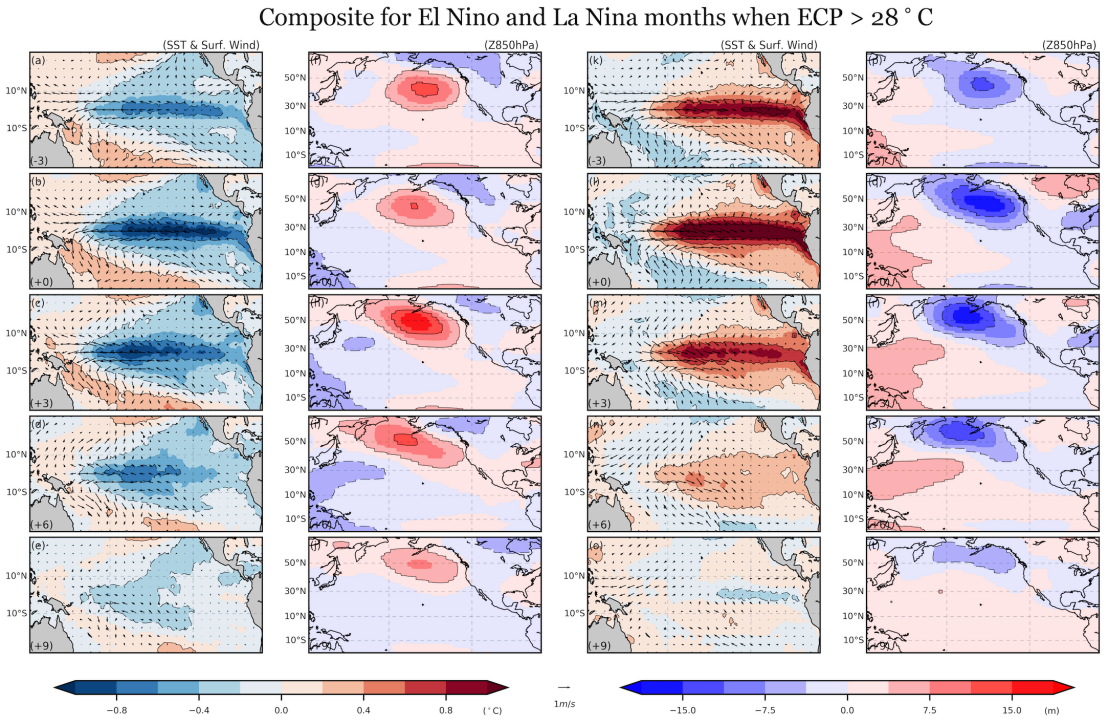

Figure 3.7. Composite of El Niño and La Niña months when the ECP is warmer than 28°C. As in Figure 3.6 but for the El Niño and La Niña months when the equatorial central Pacific is greater than 28°C, except the second and fourth panels are plotted with the 850hPa geopotential heights over the 20°S–65°N.

Our composite analyses indicate that La Niña events in the ECP are more effective than El Niño events in giving rise to multi-year ENSO transitions through the SP-onset mechanism. This explains why the SP-onset mechanism produces more multi-year La Niña transitions than multi-year El Niño transitions (Yu & Fang 2018). Therefore, the climatological SST in the ECP region determines how easily and what type of multi-year transitions (i.e., multi-year La Niña or multi-year El Niño) can be produced via the SP-onset mechanism.

The processes described above were further confirmed by a series of forced AGCM experiments conducted with the Community Earth System Model version 2 (CESM2) (see Section 3.3). In the experiments, Gaussian shaped SST anomalies were prescribed and added onto the climatological SSTs in either the ECP or EEP region with an amplitude that varied from -4°C to +4°C. The EEP experiments confirm that the SST anomalies have to be large enough (+4°C) to raise EEP SSTs above the 28°C threshold to excite deep convection (Fig. 3.9a), induce the Gill-type responses, and enhance the surface trade winds over the northeastern subtropical Pacific for activating a negative SP onset mechanism (Fig. 3.9c). No such response was found in the other EEP experiments (Fig. 3.9a-b). The ECP experiments confirm that large and negative deep convection anomalies can be induced by moderate cold (-1°C SST) anomalies in the region, which can then excite a wave train response in the extratropical atmosphere and enhance the trade winds to activate a negative SP-onset mechanism (Fig. 3.10). In contrast, the wave train response is weaker in the +1°C SST experiment (Fig. 3.10c). In addition, the weak wave train in this experiment emanates from a more eastern part of the ECP region (compared to the -1°C experiment) and results in a surface wind response that is away from the trade wind region.

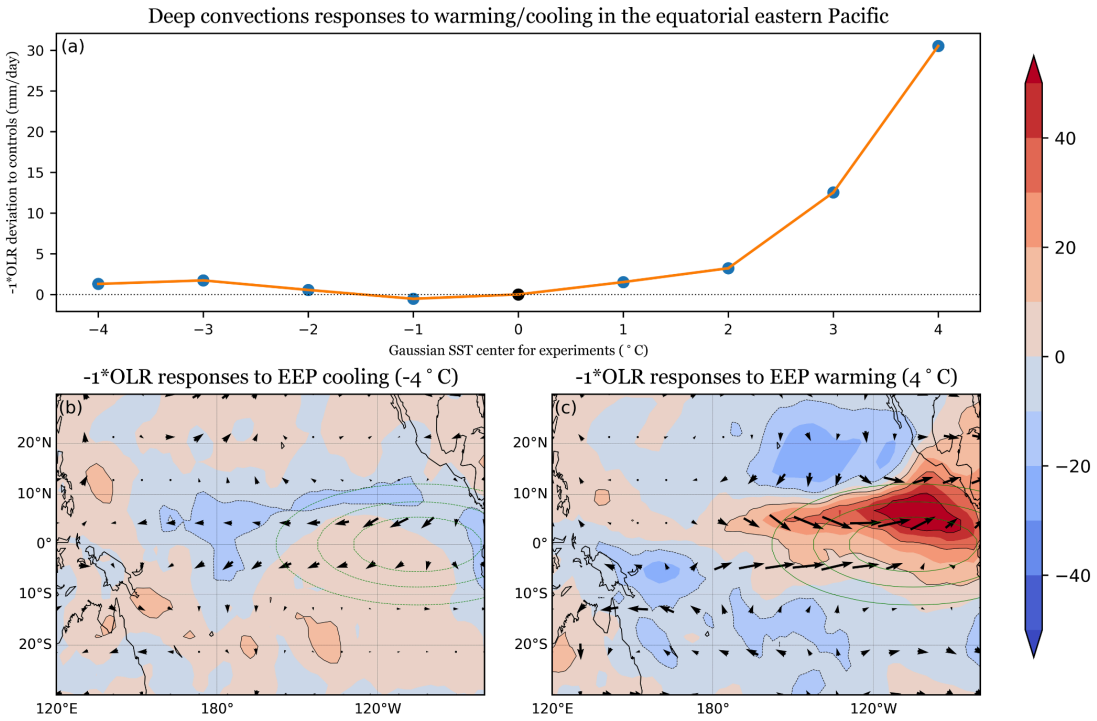

Figure 3.8. Atmospheric responses in model experiments with anomalous warming/cooling in the equatorial eastern Pacific. a, Winter (DJF) Outgoing longwave radiation (-1*OLR; W/m^2) response (i.e., experiment values minus control simulation values) in the 4-member ensemble experiments with -4, -3, -2, -1, +1, +2, +3, +4°C of sea surface temperature anomalies in the equatorial eastern Pacific. b, -1*OLR (shading) and 850mb wind (arrows) responses in the -4°C experiment. c, same as b, but for the +4°C experiment. Green contours are the imposed warming/cooling at a 1°C interval.

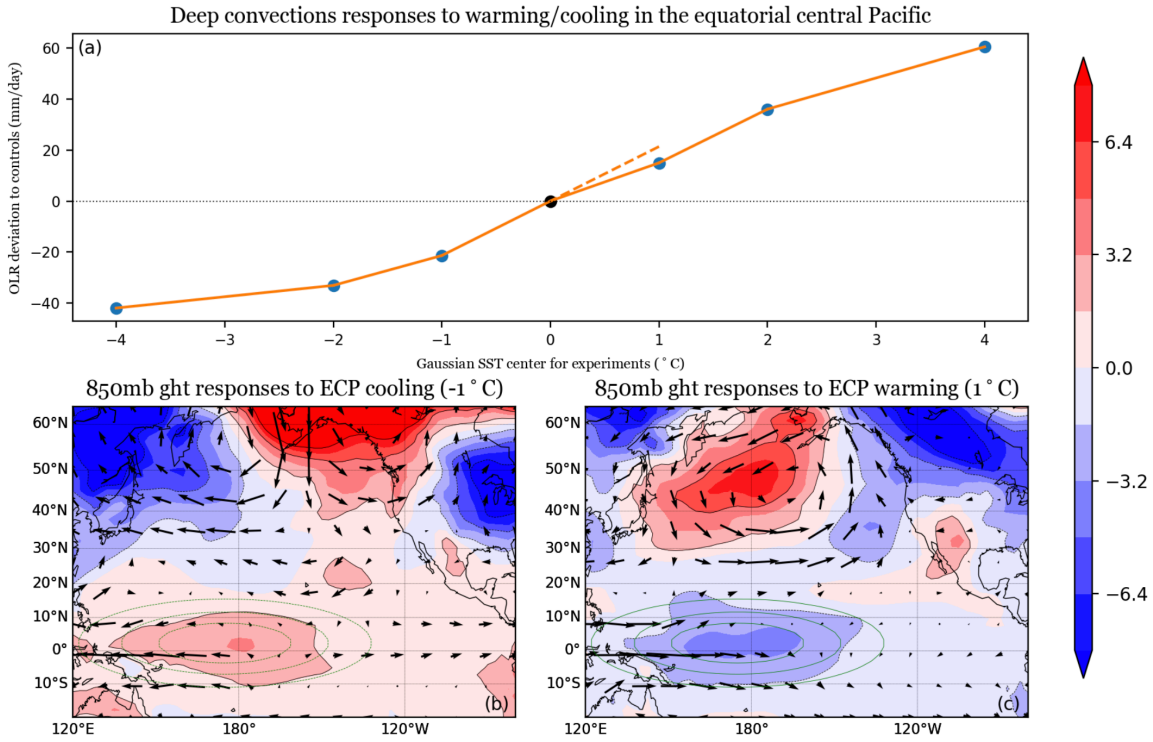

Figure 3.9. Atmospheric responses in model experiments with anomalous warming/cooling in the equatorial central Pacific. As in Figure 3.9, but with the SST anomalies imposed in the equatorial central Pacific experiments (centered at 0°N and 175°E). b and c are the responses of 850mb geopotential heights in the -1°C and +1°C experiments, respectively. Green contours are the imposed warming/cooling at a 0.25°C interval.

3.5 Future Projections on ENSO Transitions

Tropical Pacific mean SSTs are projected to increase in the future (Meehl et al. 2006; Levitus et al. 2009; Kirtman et al. 2013). The multi-model mean (MMM) of the simulations using 28 CMIP5 models (Table 3.1) show that mean SSTs in the EEP are projected to reach 28°C around 2100 (2060) under the RCP4.5 (RCP8.5) scenario (Fig. 3.11a). This tendency should enable El Niño events of any intensity to induce anomalous deep convection in the EEP, activate the negative phase of the SP-onset mechanism, and give rise to cyclic El Niño-to-La Niña transitions.

Conversely, as the mean temperatures increase and exceed the threshold, La Niña events in the EEP will be able to shut off deep convection and lead to a subsequent El Niño event via a positive SP-onset mechanism. The latter process should give rise to cyclic La Niña-to-El Niño transitions. As a result, cyclic ENSO transitions (i.e., both El Niño-to-La Niña and La Niña-to-El Niño) should occur more frequently via the SP-onset mechanism in the future. On the other hand, the projected temperature increases in the ECP region (Fig. 3.3b) will make it harder for La Niña events to reduce ECP SSTs below 28°C and to activate a negative SP-onset mechanism in the region. This should result in fewer multi-year La Niña transitions via the SP-onset mechanism in the future. In other words, the warmer tropical Pacific in the future is expected to increase the occurrence of the cyclic ENSO transition and to reduce the occurrence of the multi-year ENSO transition through the SP-onset mechanism.

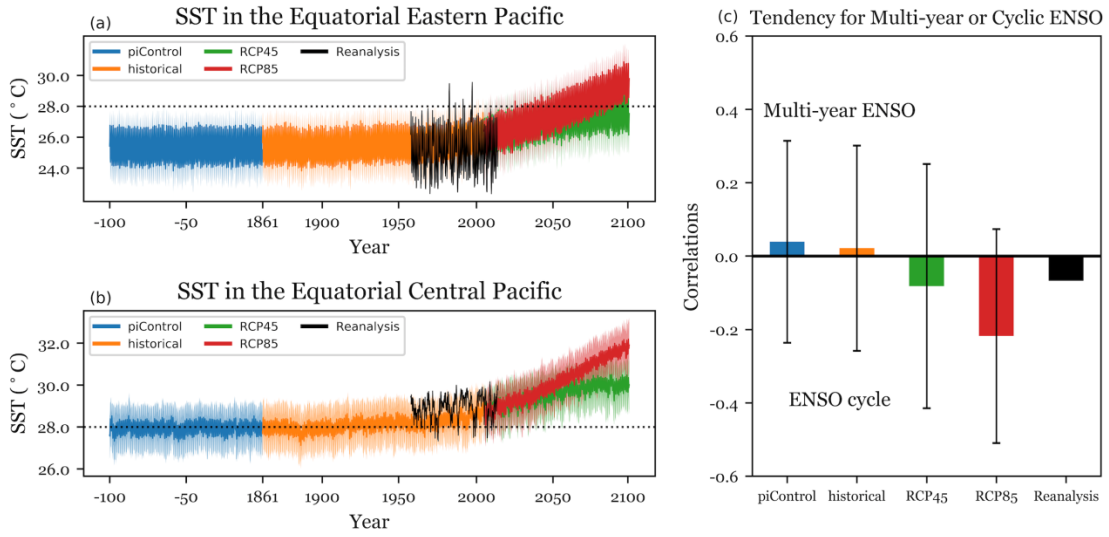

Figure 3.10. CMIP5 model projected SSTs in (a) the equatorial eastern Pacific and (b) equatorial central equatorial Pacific from pre-industrial times to 2100 and (c) the changes in the tendency of the multi-year ENSO versus cyclic ENSO. In (a) and (b), the thick lines are the multi-model means

and the thin lines are the spreads of the projected SSTs from pre-industrial (blue) and historical (orange) to RCP4.5 (green) and RCP8.5 (red) calculated from the 28 models. The black solid lines are based on the reanalysis data. In (c), the tendency is represented by the strongest correlation coefficient when the Niño3.4 index leads the SP-onset index by 1 to 6 months. The multi-model means of the pre-industrial (blue), historical (orange), RCP4.5 (green), RCP8.5 (red) simulations are shown, and the reanalysis is in black. Solid bars are the standard deviations of the model tendency.

It has been suggested that the threshold value for tropical convection may change as the climate warms (Johnson & Xie 2010), which can affect our argument above. To assess this possible impact, we examine the relationships between ENSO SST anomalies and precipitation anomalies over the EEP and ECP regions in the Pre-Industrial, Historical, RCP4.5, and RCP8.5 simulations (Fig. 3.11). We find that, in the EEP region (Figs. S8a-d), the same magnitudes of El Niño SST anomalies induce larger precipitation (i.e., deep convection) anomalies as the region warms (from pre-industrial to RCP8.5 simulations). On the other hand, the La Niña events in the ECP region (Figs. S8e-h) require larger negative anomalies to turn off the deep convection (i.e., reduce the precipitation to zero) in the RCP8.5 simulation than in the pre-industrial simulation. These results indicate that, even if the 28°C threshold may not remain unchanged or other factors may appear to moderate regional deep convection (Back and Bretherton 2009; Sabin et al. 2013), a warmer mean state of the tropical Pacific enables El Niño events to turn on deep convection more easily over the EEP region, but make La Niña events less easily turn off deep convection over the ECP region.

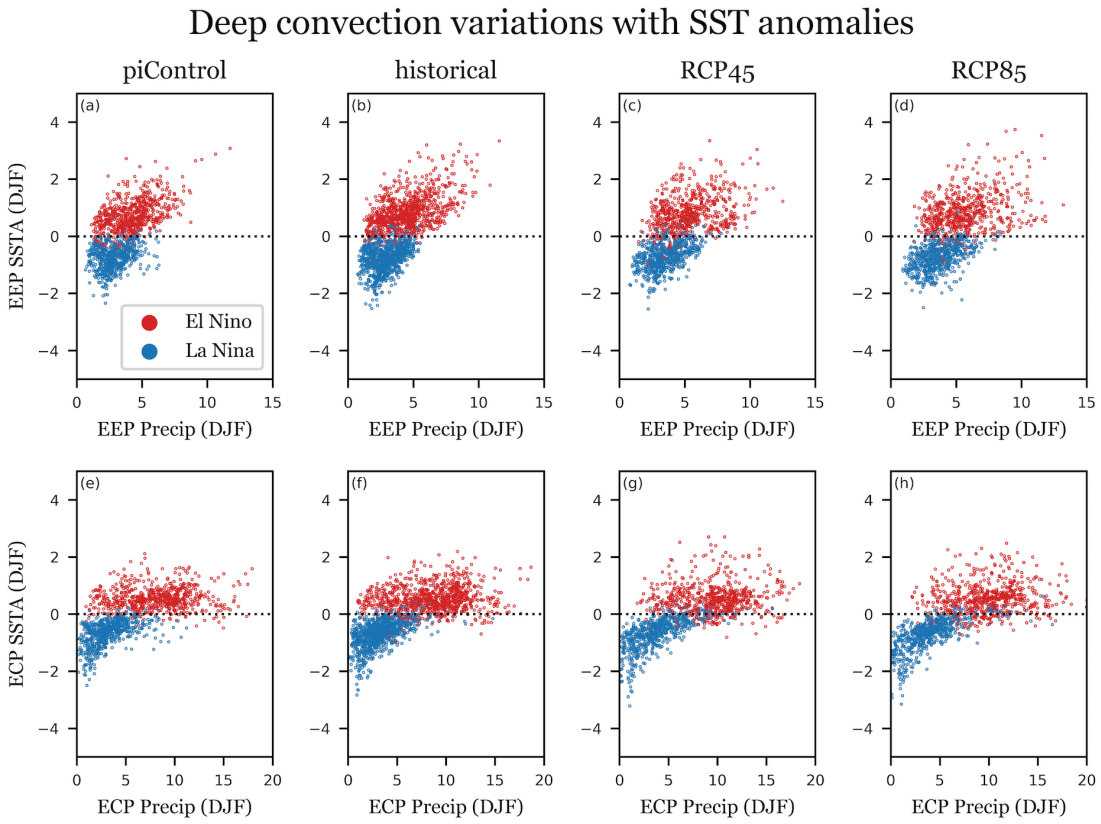

Figure 3.11. Relations between precipitation and SST anomalies in the EEP and ECP regions. (a) The winter SST anomalies and precipitation in the EEP region for El Niño (red) and La Niña (blue) events for the CMIP5 pre-industrial simulations (120 years). (b) to (d) are for the historical (156 years), RCP4.5 (96 years during 2005-2100), and RCP8.5 (96 years during 2005-2100) simulations, respectively. (e) to (h) are for the ECP region.

We further examine if the ENSO transition complexity related to the SP-onset mechanism changes from the pre-industrial to RCP simulations. Figure 3.11c shows the MMM of the strongest lead correlation of the Niño3.4 index with the SP-onset index. A positive correlation implies a multi-year transition via the SP-onset mechanism, since an El Niño (La Niña) event leads to a positive (negative) phase of the SP-onset mechanism and should later develop into another El Niño

(La Niña) event. Conversely, a negative correlation implies a cyclic transition. A weak negative value is found in the reanalysis product, which is consistent with the fact that both multi-year ENSO and cyclic ENSO events are observed (Yu & Fang 2018). In the CMIP5 simulations, the MMM values change from weakly positive in the pre-industrial and historical simulations to strong negatives in the RCP4.5 and RCP8.5 simulations. This tendency indicates that, as the Pacific Ocean warms, the SP-onset mechanism tends to change from a preference for generating multi-year transitions to a preference for cyclic transitions. This future change of ENSO transition complexity is consistent with our projection based on the control of the tropical Pacific mean state on the SP-onset mechanism.

Consistent results can be found by examining the transition patterns of SST anomalies composited for large values of the SP-onset index (Fig. 3.13). Both the positive and negative phases of the SP-onset mechanism produce a transition pattern that changes from being dominated by multi-year ENSO transitions in present-day simulations to being dominated by cyclic ENSO transitions in the RCP simulations. Furthermore, in the pre-industrial and historical simulations, the simulated mean ECP SSTs are colder (around 28°C; see Fig. 3.11b) than the reanalysis SSTs (28.94°C). Therefore, both El Niño and La Niña can enhance or suppress deep convection to give rise to multi-year events. The models with colder ECP SSTs tend to simulate more multi-year El Niños, while the models with warmer ECP SSTs have more multi-year La Niñas as the observations (Fig. 3.14). This CMIP5 model deficiency in simulating too frequent multi-year El Niños in the present-day climate further supports the notion that the mean SSTs in the ECP region control the frequency of occurrence of multi-year ENSO transitions.

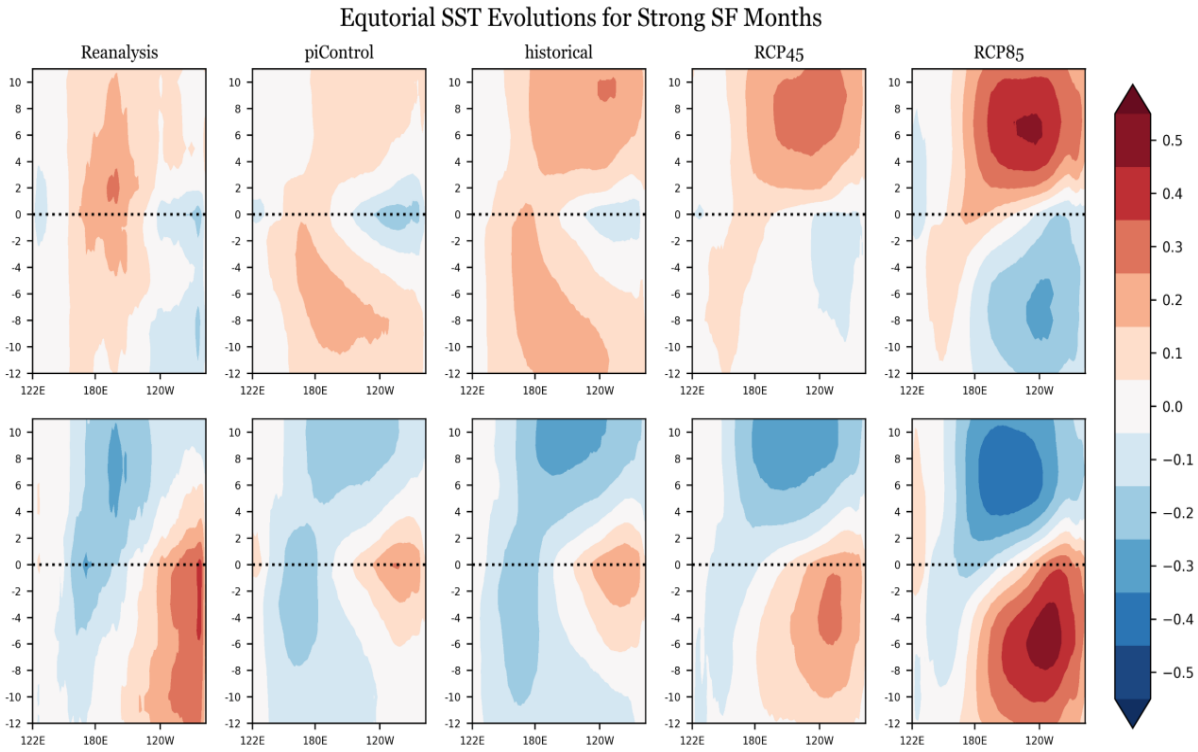

Figure 3.12. Evolution of equatorial SST anomalies associated with the SP-onset mechanism. The values shown are the SST anomalies composited for strong events of the positive (upper panels) and negative (lower panels) phases of the SP-onset mechanism, which were identified respectively as the months in which the SP-onset index is larger than 0.7 times its standard deviation or lower than -0.7 times its standard deviation. The evolution extends from twelve months before to twelve months after the events and is calculated from the reanalysis (first column) and the multi-model means for the pre-industrial (second column), historical (third column), RCP4.5 (fourth column), RCP8.5 (fifth column column). The SSTs are normalized by the standard deviation of their modeled Niño3.4 index before the composites are formed and the color bar for the reanalysis panel is two times larger than those of the other panels (shown on the right in °C).

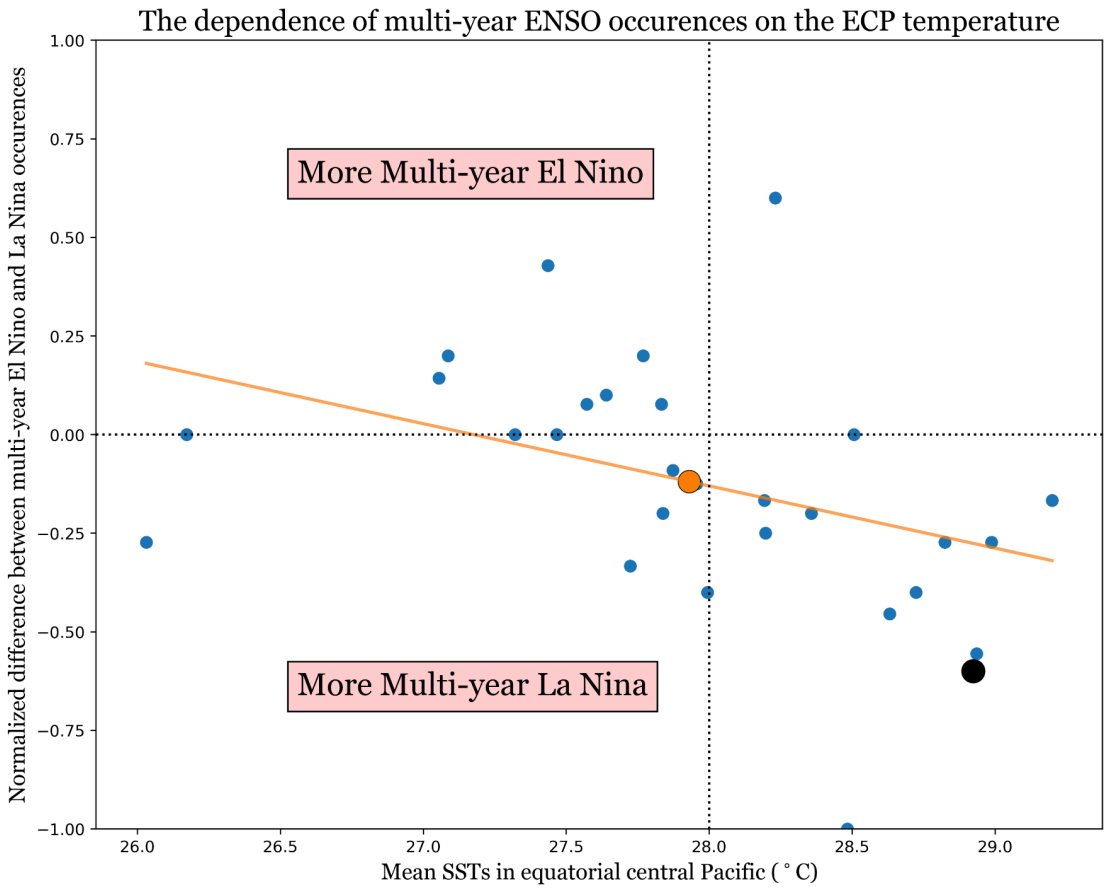

Figure 3.13. The dependence of multi-year ENSO occurrences on the mean surface temperature in the equatorial central Pacific. The y-axis is the difference between the occurrences of multi-year El Niño and La Niña, which are normalized by the total occurrences of the multi-year El Niño and La Niña in each CMIP5 pre-industrial simulation. A multi-year event is identified by having a prior ENSO with same phase or an ENSO event is longer than 18 months. The orange dot is the multi-model-mean of pre-industrial simulations and the black dot is the reanalysis product. The orange line is their linear fit.

3.6 Summary and Discussion

We have, in this chapter, shown that the tropical Pacific mean SSTs control the ENSO transition complexity produced by the SP-onset mechanism. Since the SP-onset mechanism is a key source of the transition complexity, our finding offers a way to use tropical Pacific mean states to assess future or past ENSO transition complexities. More interestingly, we find the mean SSTs in different parts of the equatorial Pacific matter for different ENSO transition patterns. The mean SSTs in the EEP region affect how frequently cyclic ENSO transitions can occur, whereas the mean SSTs in the ECP affect how frequently multi-year transitions can occur. We find these relationships are useful to link CMIP5 model deficiencies in simulating ENSO transition complexity and tropical Pacific mean state simulations. Finally, the control of the tropical mean state can also explain why the SP-onset mechanism responds differently to El Niño and La Niña, which is a key source of El Niño-La Niña asymmetries that has not yet been fully explored nor understood.

Chapter 4

Model Diagnosis on ENSO Transition Complexity

4.1 Abstract

The observed El Niño and La Niña exhibit different complexities in their event-to-event transition patterns. The El Niño is dominated in order by episodic, cyclic, and multi-year transitions, but the reversed order is found in the La Niña. A subtropical Pacific onset mechanism is used to explain this difference. This mechanism triggers El Niño/La Niña events via subtropical processes and is responsible for producing multi-year and episodic transitions. Its nonlinear responses to the tropical Pacific mean state result in more multi-year transitions for La Niña than El Niño and more episodic transitions for El Niño than La Niña. The CMIP5/6 models realistically simulate the observed transition complexity of El Niño but fail to simulate the transition complexity of La Niña. This deficiency arises from a weaker than observed subtropical onset mechanism and a cold bias in the tropical Pacific mean sea surface temperatures in the models.

4.2 Introduction

El Niño-Southern Oscillation (ENSO) is a complex phenomenon that involves wide ranges of different patterns, amplitudes and temporal evolutions (Kao and Yu 2009; Capotondi et al. 2015; Wang et al. 2017; Yu et al. 2017; Timmermann et al. 2018; Yu & Fang 2018). One important part of the complexity appears in the way that one ENSO event transitions to another. An El Niño (La Niña) event can be preceded by a La Niña (El Niño) event to result in a cyclic transition, by another El Niño (La Niña) event to become a multi-year transition, or by a neutral (non-ENSO) condition

to become an episodic transition (Yu & Fang 2018). ENSO onset mechanisms control how anomalies in sea surface temperature (SST) are established in the equatorial Pacific and play critical roles in controlling transition patterns (Yu & Fang 2018; Wang et al. 2019).

Two primary onset mechanisms of ENSO have been identified: a tropical Pacific onset (TP-onset) mechanism and a subtropical Pacific onset (SP-onset) mechanism (Wang et al. 2017; Yu et al. 2017; Yu & Fang 2018). The TP-onset mechanism invokes equatorial thermocline variations to initiate the sea surface temperature (SST) anomalies associated with ENSO, such as those described by the recharged oscillator (Wyrtki 1975; Jin 1997) and delayed oscillator theories (Battisti & Hirst 1989; Suarez & Schopf 1988; Zebiak & Cane 1987). This mechanism typically produces ENSO SST anomalies first in the eastern equatorial Pacific, where the thermocline is the shallowest and SSTs are most sensitive to thermocline variations. Yu & Fang (2018) find that the TP-onset mechanism generates mostly the cyclic transition and contributes to reduce ENSO transition complexity, although some complexity may arise from its asymmetric responses to El Niño and La Niña (Hu et al. 2017).

On the other hand, the SP-onset mechanism invokes subtropical Pacific processes to trigger ENSO events (Yu et al. 2010; Yu & Kim 2011). The subtropical processes include those described by the seasonal footprinting mechanism (Vimont et al. 2003; Kao & Yu 2009; Alexander et al. 2010), trade wind charging (Anderson et al. 2013; Anderson & Perez 2015), wind-evaporation-SST feedback (Xie & Philander 1994) and Pacific meridional mode (PMM; Chiang & Vimont 2004). This mechanism typically results in ENSO SST anomalies that first appear in the central equatorial Pacific, where the northeastern Pacific trade winds approach the equator (Yu et al. 2010). Yu & Fang (2018) find that the SP-onset mechanism can result in all three transition patterns and is a key source of ENSO transition complexity.

Recent studies (Yu & Fang 2018; Fang & Yu 2020) reveal that the SP-onset mechanism responds differently to El Niño and La Niña. Therefore, it is possible that transition complexity can be different between these two ENSO phases. The goals of this chapter are to compare the transition complexity between El Niño and La Niña in the observations, and to examine whether the CMIP5/6 models can reproduce the observed complexities, and, if not, to identify model deficiencies and their causes.

4.3 Datasets and Methods

Monthly mean values of SST, surface wind, and sea surface heights (SSH) were regridded to a common grid of 1.5°-longitude by 1°-latitude for analysis. The anomalies were defined as the deviations from the seasonal cycles (calculated from the analysis period 1948-2016) with their linear trends removed. The SST, surface wind, and SSH data are downloaded respectively from the Hadley Center Sea Ice and Sea Surface Temperature data set (HadISST) (Rayner et al. 2003), the National Centers for Environmental Prediction–National Center for Atmospheric Research (NCEP–NCAR) reanalysis (Kalnay et al. 1996), and the German contribution of the Estimating the Circulation and Climate of the Ocean project (Köhl, 2015). The same procedures were applied to the last one hundred years of the pre-industrial simulations produced by 34 CMIP5 models (Taylor et al. 2012; see Table 4.1 for the details of the models) and 20 CMIP6 models (see Table 4.2).

	Model	Modeling Center		Model	Modeling Center
1	ACCESS1-0	Commonwealth Scientific and Industrial Research Organization (CSIRO) and Bureau of Meteorology (BOM), Australia	18	HadGEM2-CC	Met Office Hadley Centre
2	ACCESS1-3		19	HadGEM2-ES	
3	CCSM4	National Center for Atmospheric Research Community Earth System Model Contributors	20	IPSL-CM5A-LR	Institut Pierre-Simon Laplace
4	CESM1-BGC		21	IPSL-CM5A-MR	
5	CESM1-CAM5		22	IPSL-CM5B-LR	
6	CESM1-FASTCHEM		23	MIROC-ESM	Japan Agency for Marine-Earth Science and Technology, Atmosphere and Ocean Research Institute, and National Institute for Environmental Studies
7	CESM1-WACCM		24	MIROC-ESM-CHEM	
8	CMCC-CESM	Centro Euro-Mediterraneo per I Cambiamenti Climatici	25	MIROC5	
9	CMCC-CM		26	MPI-ESM-LR	Max-Planck-Institut für Meteorologie (Max Planck Institute for Meteorology)
10	CMCC-CMS		27	MPI-ESM-MR	
11	CNRM-CM5	Centre National de Recherches Météorologiques	28	MPI-ESM-P	
12	CNRM-CM5-2		29	MRI-CGCM3	Meteorological Research Institute
13	CanESM2	Canadian Centre for Climate Modelling and Analysis	30	NorESM1-M	Norwegian Climate Centre
14	GFDL-ESM2G	NOAA Geophysical Fluid Dynamics Laboratory	31	NorESM1-ME	
15	GFDL-ESM2M		32	bcc-csm1-1	Beijing Climate Center, China Meteorological Administration
16	GISS-E2-R	NASA Goddard Institute for Space Studies	33	bcc-csm1-1-m	
17	GISS-E2-R-CC		34	inmcm4	Institute for Numerical Mathematics

Table 4.1. The names of the 34 CMIP5 models used in this chapter.

	Model	Modeling Center
1	AWI-CM-1-1-MR	Alfred Wegener Institute, Helmholtz Centre for Polar and Marine Research (AWI), in Bremerhaven
2	BCC-CSM2-MR	Beijing Climate Center, China Meteorological Administration
3	BCC-ESM1	Beijing Climate Center, China Meteorological Administration
4	CAMS-CSM1-0	Chinese Academy of Meteorological Sciences
5	CESM2	Community Earth System Model Contributors
6	CESM2-FV2	
7	CESM2-WACCM	National Center for Atmospheric Research
8	CESM2-WACCM-FV2	
9	CNRM-CM6-1	Centre National de Recherches Météorologiques
10	CNRM-ESM2-1	
11	CanESM5	Canadian Centre for Climate Modelling and Analysis
12	E3SM-1-0	U.S. Department of Energy
13	EC-Earth3-Veg	European EC-Earth consortium
14	GFDL-CM4	Geophysical Fluid Dynamics Laboratory
15	GISS-E2-1-G	NASA Goddard Institute for Space Studies
16	GISS-E2-1-H	
17	HadGEM3-GC31-LL	Met Office Hadley Centre
18	IPSL-CM6A-LR	Institut Pierre-Simon Laplace
19	MIROC6	Atmosphere and Ocean Research Institute (The University of Tokyo), National Institute for Environmental Studies, and Japan Agency for Marine-Earth Science and Technology
20	SAM0-UNICON	Seoul National University

Table 4.2. The names of the 20 CMIP5 models used in this chapter.

A TP-onset index and a SP-onset index were constructed from the combined SST, surface wind, and SSH anomalies using a multivariate empirical orthogonal function analysis (Xue et al. 2000; Yu & Fang 2018; see Section 2.3 for details). We identify the transition pattern (i.e., cyclic, multi-year, or episodic) for every El Niño and La Niña event observed during the analysis period based on the ENSO condition during the previous year (Fig. 4.1; Table 4.3). An El Niño (La Niña) event occurs when the 3-month average of Niño3.4 index (SST anomalies averaged between 5°S-5°N and 170°W-120°W) are larger (smaller) than 0.7 (-0.7) standard deviation for 6 or more consecutive months. The onset and termination of an El Niño (La Niña) event are defined as the months when the averaged Niño3.4 index first goes above or drops below the threshold, respectively. A cyclic ENSO transition is one in which an ENSO event is preceded (within 12 months) by an event of the opposite phase. Similarly, a multi-year ENSO transition is identified the one in which the preceding and the current events are of the same phase. All other transitions are classified as episodic. An event that is longer than 18 months is considered to be two separate events and the second event is identified as a multi-year ENSO event (and additional multi-year events are identified for each additional 12 months that event persists). The same classification methodology was applied to the CMIP5/6 model simulations. The effectiveness of this classification method is verified by examining the evolution of the Niño3.4 index (SST anomalies averaged between 5°S-5°N and 170°W-120°W) for each of the transition patterns (see Fig. 4.1 for the observations, Fig. 4.2 for CMIP5 models, and Fig. 4.3 for CMIP6 models)

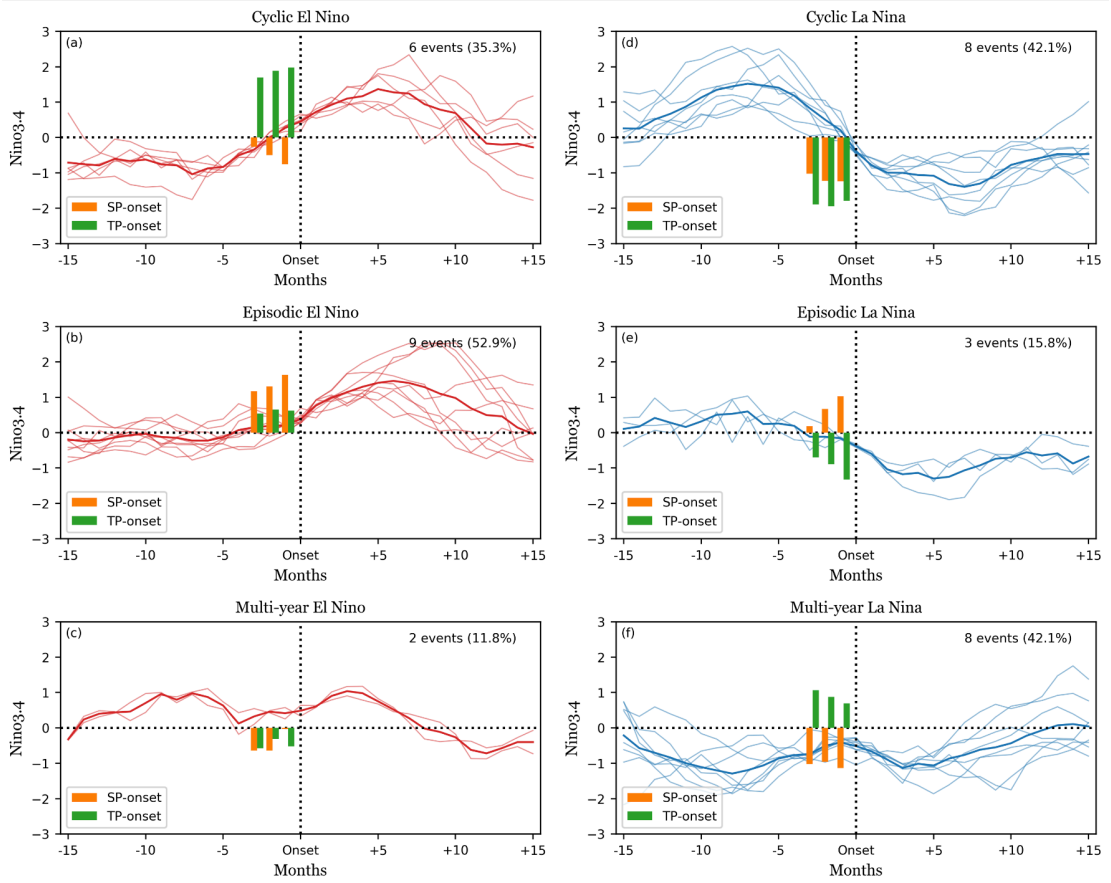

Figure 4.1. Evolutions of the Niño3.4 index during the cyclic, episodic, and multi-year transitions of (a-c) El Niño and (d-f) La Niña. Each thin line represents the evolution of the Niño3.4 index during an individual ENSO event. Thick lines are the mean evolutions of all events in the panel. The evolutions are displayed from 12 months before the ENSO onset month to 12 months after. The mean strengths of the SP-onset index (orange) and TP-onset index (green) during the pre-onset months are shown by the bars for the three months before the ENSO onset month.

El Niño	Transition	Onset (Mon)	La Niña	Transition	Onset (Mon)
1951	Cyclic	6	1949	Episodic	9
1957	Cyclic	4	1954	Episodic	5
1963	Episodic	6	1955	Multi-year	2
1965	Cyclic	5	1956	Multi-year	6
1968	Episodic	10	1964	Cyclic	4
1969	Multi-year	8	1970	Cyclic	6
1972	Cyclic	5	1973	Cyclic	5
1976	Cyclic	8	1975	Multi-year	3
1977	Multi-year	8	1983	Cyclic	9
1982	Episodic	4	1984	Multi-year	9
1986	Episodic	8	1988	Cyclic	4
1991	Episodic	9	1995	Cyclic	8
1994	Episodic	8	1998	Cyclic	6
1997	Episodic	4	1999	Multi-year	8
2002	Episodic	6	2000	Multi-year	9
2009	Cyclic	7	2007	Episodic	7
2015	Episodic	3	2008	Multi-year	10
			2010	Cyclic	5
			2011	Multi-year	7

Table 4.3. Classification of ENSO transitions in the reanalysis.

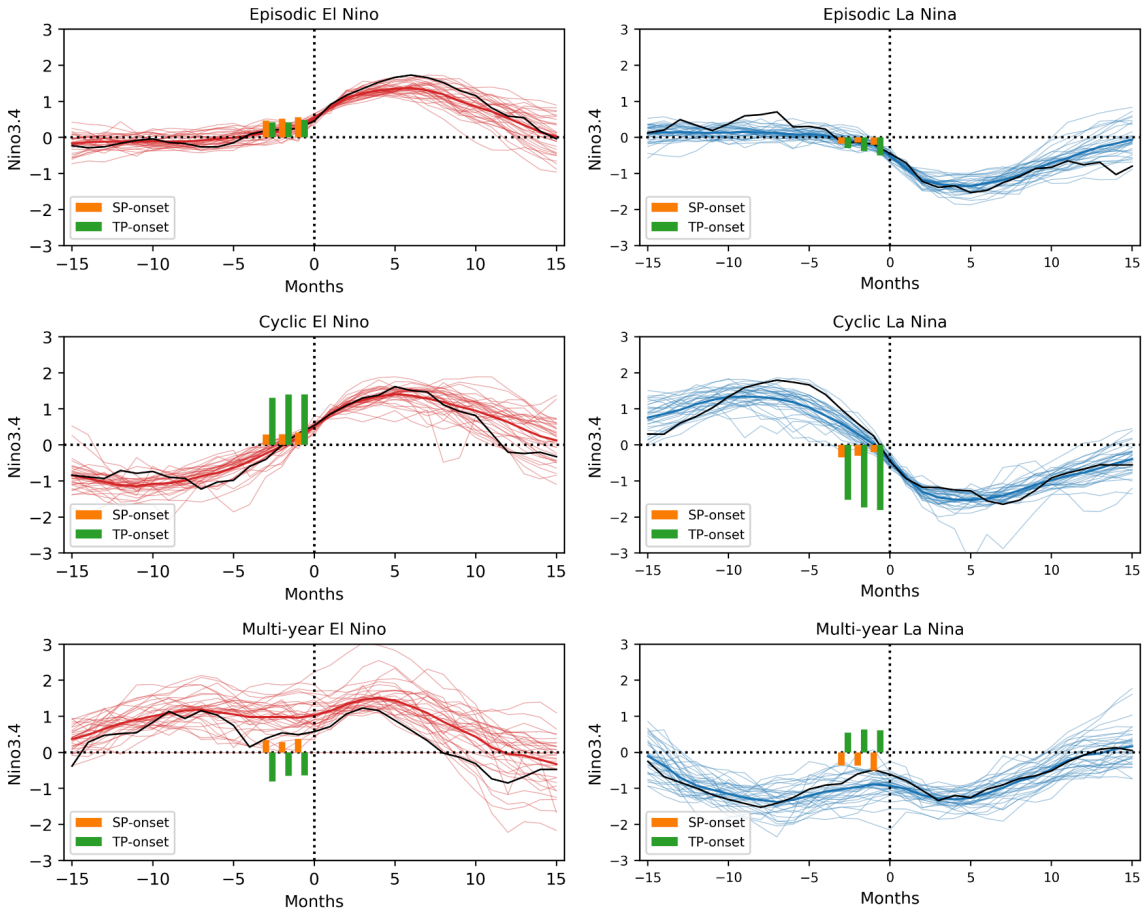

Figure 4.2. Same as Figure 4.1 but for the CMIP5 models. Thin lines represent the mean evolutions of normalized Niño3.4 index of individual CMIP5 models and the thick line represents their multi-model mean. Black lines are the mean evolutions calculated from the reanalysis. The bars are the multi-model means of the SP-onset index and TP-onset index during the pre-onset months.

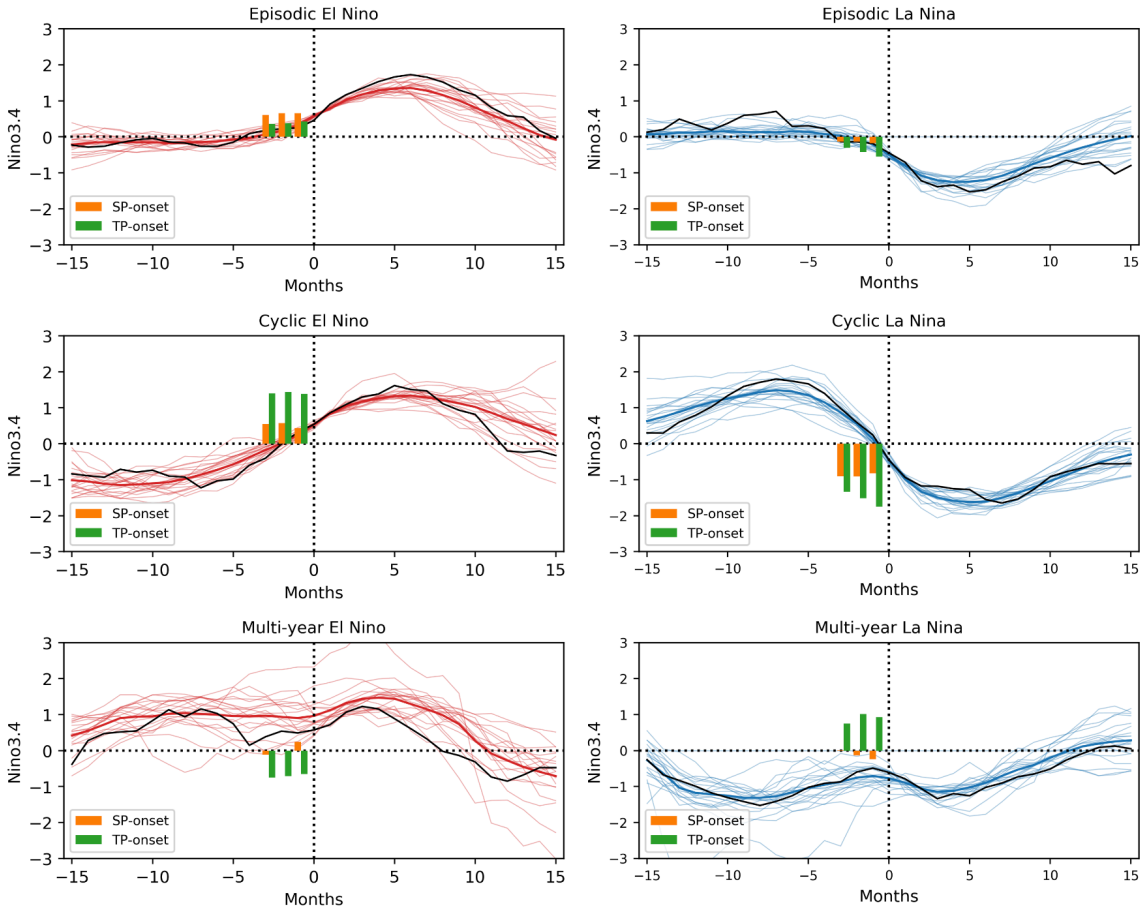

Figure 4.3. As in Figure 4.2, but for the CMIP6 models.

4.4 The Reversed Dominance of ENSO Transitions for El Niño and La Niña

Figure 4.4a shows that, during the analysis period of 1948-2016, El Niño events are dominated by episodic transitions (52.9%; 9 events), followed by cyclic transitions (35.3%; 6 events), and the least by multi-year transitions (11.8%; 2 events). However, the opposite is true for La Niña events whose transitions are most frequently multi-year (42.1%; 8 events) and cyclic (42.1%; 8 events), and episodic transitions become the least (15.8%; 3 events). The transition complexity is thus asymmetric between the El Niño and La Niña phases of the ENSO. The asymmetry comes from

the very distinct dominances of the episodic and multi-year transitions, while the cyclic transition accounts for similar percentages in El Niño and La Niña.

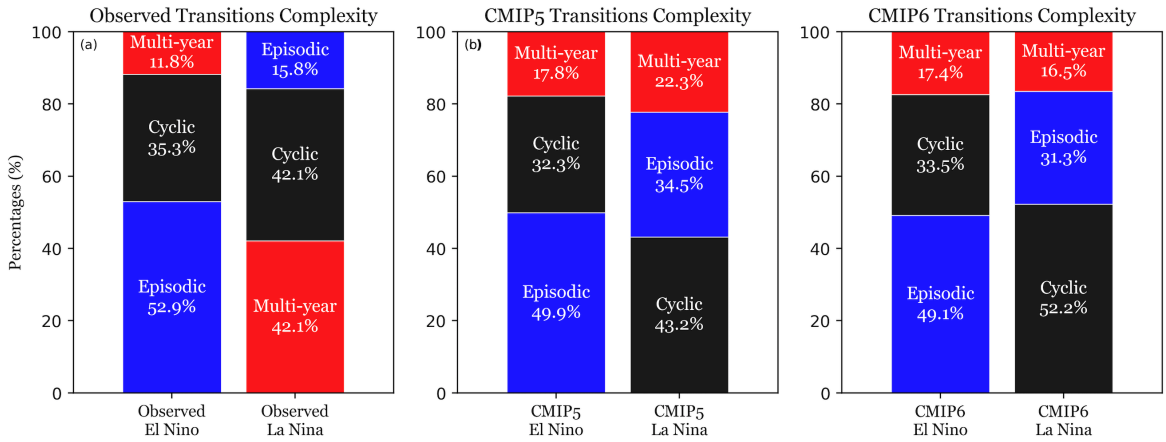

Figure 4.4. The transition complexity of El Niño (left bars) and La Niña (right bars) in (a) the observations, (b) the multi-model mean from thirty-four CMIP5 models, and (c) the multi-model mean from twenty CMIP6 models. The percentages of the transitions are ordered from highest (bottom) to lowest (top).

To understand the cause of the asymmetry, we contrast the evolutions of equatorial (5°S-5°N) SST anomalies composited for the three transition patterns of El Niño and La Niña (Figs. 4.5a-f). As expected, ENSO SST anomalies in the cyclic, episodic, and multi-year transitions were preceded by opposite-signed, near-neutral, and same-signed anomalies in the previous year, respectively. It is important to note that the onset locations (during months -3 to 0) of the ENSO SST anomalies are different. The anomalies first appear in the eastern equatorial Pacific for both the cyclic El Niño and La Niña and in the central equatorial Pacific for both the multi-year El Niño and La Niña; whereas the SST anomalies show up in the central equatorial Pacific for the episodic El Niño but in the eastern equatorial Pacific for the episodic La Niña.

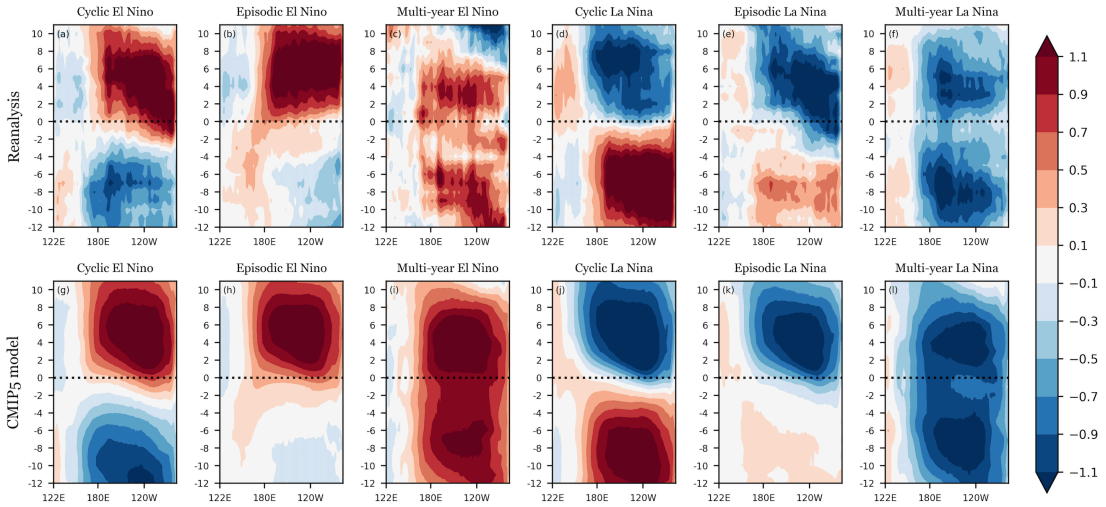

Figure 4.5. Evolutions of equatorial (5°S-5°N) Pacific SST anomalies composited for the cyclic, episodic, and multi-year transitions of (a)-(c) El Niño and (d)-(f) La Niña in the reanalysis and (g)-(i) for the simulated El Niños and (j)-(l) La Niñas in the multi-model mean of CMIP5 simulations. Shadings are SST anomalies from 12 months before the ENSO onset month to 12 months after.

As mentioned, the TP-onset mechanism triggers ENSO events in which anomalies appear first in the eastern equatorial Pacific; whereas the SP-onset mechanism triggers ENSO events in which anomalies appear first in the central equatorial Pacific. The locations of SST anomalies in Figs. 4.5a-f suggest that the onset mechanisms are the same for the cyclic transition (the TP-onset mechanism) and multi-year transition (the SP-onset mechanism) of El Niño and La Niña, but are different for the episodic El Niño and La Niña. While the SP-onset mechanism is more associated with the episodic El Niño, the TP-onset mechanism is more associated with the episodic La Niña. The values of the TP-onset and SP-onset indices during the onset period of each transition (see months -3 to month 0 in Figs. 4.11a-f) confirm this. Therefore, the causes of the asymmetric transition complexity are related to how these different mechanisms result in more frequent

episodic El Niños than episodic La Niñas and how the SP-onset mechanism results in more multi-year La Niñas than El Niños.

Figure 4.5e shows that the episodic La Niña is preceded by weak warming. This evolution pattern is similar to that of the cyclic La Niña, except that in the episodic La Niña the warming is not strong enough to be classified as an El Niño. Their similarity can also be seen in their associated thermocline evolutions (represented by the SSH anomalies; Figs. 4.6d and e), confirming the contribution of the TP-onset mechanism to the episodic La Niña. One-third of episodic El Niño events are also more associated with the TP-onset mechanism (Fig. 4.7e-f), even though the majority of episodic El Niños are associated with the SP-onset mechanism. These results indicate that the TP-onset mechanism can generate both episodic El Niños and La Niñas, but the episodic El Niño can also be additionally produced by the SP-onset mechanism. The fact that the SP-onset mechanism favors to produce episodic El Niños but not La Niñas can explain why episodic events account for a larger percentage of El Niños (52.9%) than La Niñas (15.8%).

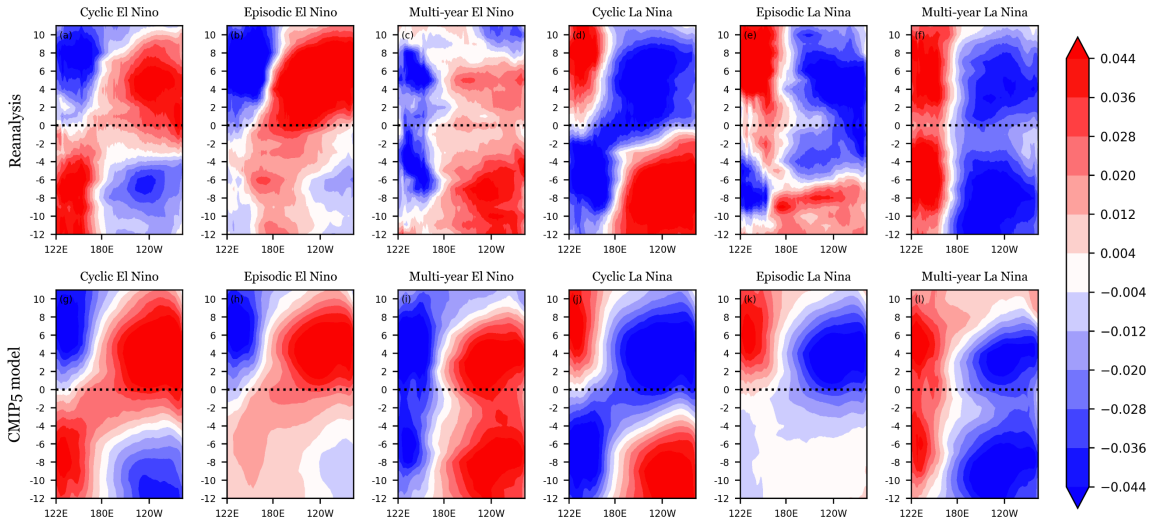

Figure 4.6. As in Figure 4.5, but for equatorial SSH anomalies (meters).

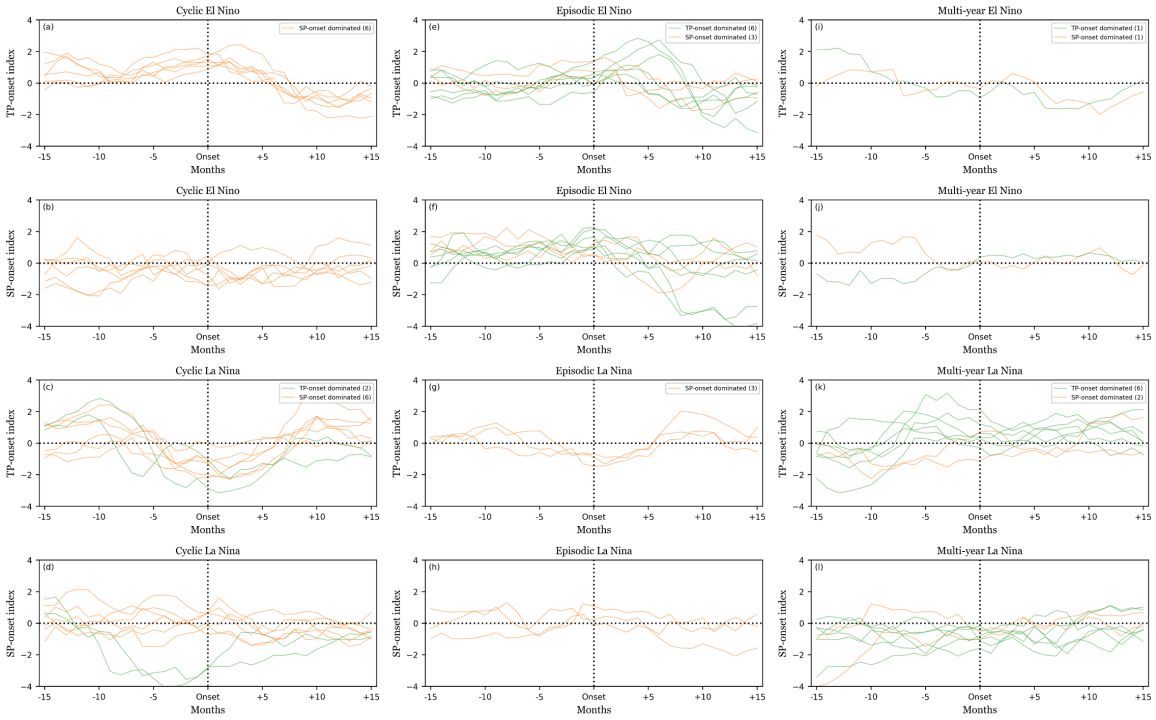

Figure 4.7. The evolution of the normalized TP-onset and SP-onset indices for the three transition patterns of El Niño and La Niña event during the analysis period 1948-2016. Panels (a)-(d) are for the cyclic transition; panels (e)-(h) are for the episodic transition; and panels (i)-(l) are for the multi-year transition. The first row is the TP-onset for El Niño; the second row is the SP-onset for El Niño; the third row is the TP-onset for La Niña; the last row is the SP-onset for La Niña. Each thin line represents the mean evolution of the normalized index and thick lines are the multi-model means. The green lines show transitions that are dominated by the TP-onset mechanism; defined as events where the values of the TP-onset index during the pre-onset months (3 months before the onset months) of El Niño (La Niña) are more positive (negative) than those of the SP-onset index. The orange lines illustrate the transitions that are dominated by the SP-onset mechanism.

Previous studies have shown that the SP-onset mechanism is more capable of producing episodic El Niño events than episodic La Niña events (e.g., Larson & Kirtman 2013). One explanation for this is that an anomalous warming induced by the mechanism in the central equatorial Pacific can excite a stronger atmospheric feedback than an anomalous cooling induced by the same mechanism in the same region (Chen et al. 2019). Therefore, the initial warming triggered by the SP-onset mechanism has a larger chance to develop into an episodic El Niño, but the initial equatorial cooling triggered by the SP-onset mechanism has a smaller chance to develop into an episodic La Niña.

As for the reason why the SP-onset mechanism produces more multi-year La Niñas than multi-year El Niños, Fang & Yu (2020) have offered an explanation. They find the occurrence frequencies of the multi-year El Niño and La Niña are controlled by the mean SSTs in the equatorial central Pacific. With a mean SST there that is slightly higher than the threshold temperature (28°C) for deep convection, a La Niña cooling in the region can abruptly turn off the deep convection. This generates a strong heating anomaly that excites a stronger wavetrain response than a comparable El Niño warming in this region (Lyu et al. 2017; Stuecker 2018; Fang & Yu 2020). The stronger (weaker) wavetrain response is more (less) capable of activating the SP-onset mechanism and to onset another La Niña (El Niño) in the following year. Therefore, present-day mean SSTs in the equatorial Pacific favor more multi-year La Niña transitions than multi-year El Niño transitions.

4.5 Model Deficiencies on ENSO Transition Complexity

We next examine whether CMIP5 models can simulate the differences in transition frequencies between El Niño and La Niña described above. Pre-industrial simulations produced by thirty-four

CMIP5 models were analyzed (Table 4.1). Their multi-model means (MMM) (Fig. 4.4b) show that the simulated El Niño has a similar transition complexity as in the observations. Episodic El Niño transitions account for the highest percentage (49.93%), followed by cyclic El Niño transition (32.27%), with multi-year El Niño transitions least frequent (17.80%). However, the CMIP5 models cannot reproduce the observed frequency of occurrence of the La Niña transition patterns. While the multi-year La Niña transition accounts for the highest observed percentage, it accounts for the least of the simulated La Niña transitions (22.3%). The leading transition pattern for the simulated La Niña is the cyclic transition (43.18%) followed by the episodic transition (34.5%).

We further examine the transition complexity in each individual CMIP5 model and present the results using an ENSO Transition Complexity (ETC) diagram (Fig. 4.8). In the diagram, the x- and y-axis values are, respectively, the percentages of episodic and multi-year transitions in each model. The percentage of cyclic transitions is represented by the circle size (larger dots for higher percentages). Based on the values of the x and y axis, we can divide the ETC diagram into regions where cyclic, episodic, and multi-year transitions dominate. Figure 4.8a shows that all but two CMIP5 models realistically produce more episodic El Niños than multi-year El Niños (i.e., below the dashed line of x=y), and that all but five models have El Niño transitions that are dominated by the episodic type. The observed transition complexity of El Niños is realistically reproduced in most of the CMIP5 models. The ETC diagram for La Niña (Fig. 4.8b) reveals a completely different story. Only five CMIP5 models produce more multi-year La Ninas than episodic La Niñas (i.e., above the dashed line of x=y). The CMIP5 models have a tendency to simulate too many episodic La Niñas and too few multi-year La Niñas, failing to reproduce the observed transition complexity of La Niña.

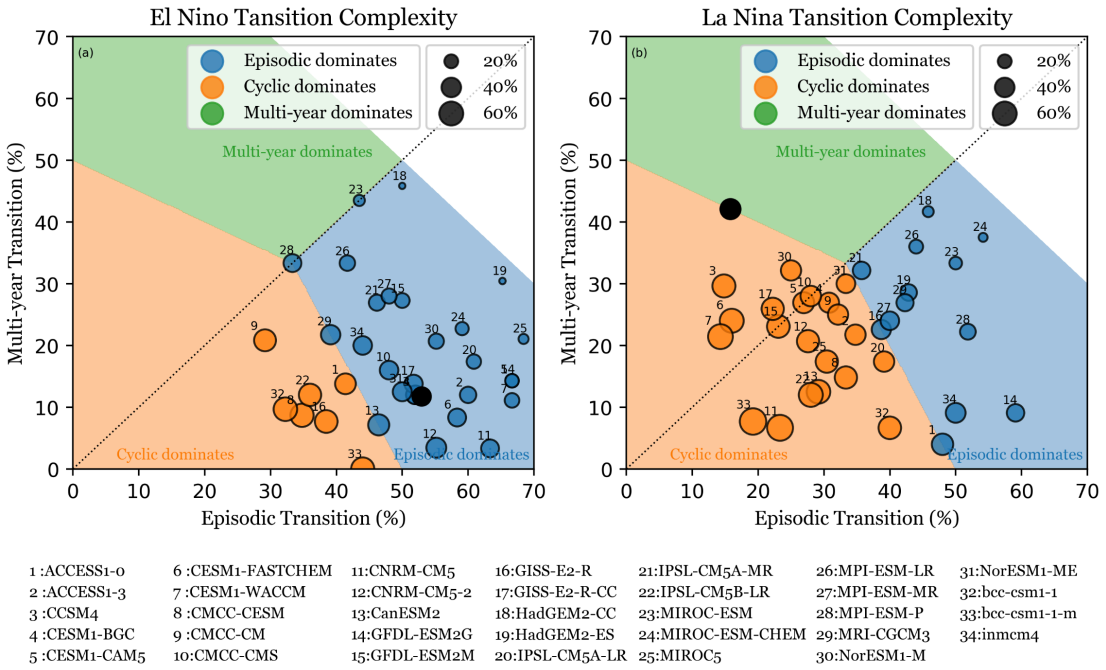

Figure 4.8. ENSO transition complexity (ETC) diagrams for (a) the simulated El Niño and (b) the La Niña in CMIP5 models in CMIP5 models. The x-axis and y-axis are, respectively, the percentage of episodic transitions and multi-year transitions in each model. The size of the circles is proportional to the percentage of cyclic transitions. The color of the circle indicates the highest percentage of transitions: orange for cyclic, blue for episodic, and green for multi-year transition. The same color scheme is used in the background shadings to indicate the regions of the diagram where each of the three transitions is most frequent. The black dot is the observations and the CMIP5 models are labeled with their corresponding numbers.

To identify the sources of these model deficiencies, we examine the MMM evolutions of the equatorial SST anomalies during the three transitions (Figs. 4.5g-l). Overall, all three transitions for the simulated El Niño and La Niña have onset locations similar to those in the observations. This similarity implies that the underlying transition dynamics in the models are similar to those in the observations. The relative strengths of the TP-onset and the SP-onset indices in the models

also confirm this assertion (Fig. 4.2). However, we notice that the episodic El Niños in the models also show an onset signature in the eastern equatorial Pacific which is absent in the observations. This difference suggests that the models have an overly strong TP-onset mechanism. We find that in about half of the CMIP5 models (16/34) the episodic El Niño is more associated with the TP-onset mechanism (Fig. 4.9e-f). This is consistent with Yu & Fang (2018) who find most CMIP5 models have stronger than observed TP-onset mechanisms and weaker than observed SP-onset mechanisms. Since the episodic El Niño can be generated by both mechanisms, the frequency of occurrence of the episodic El Niño in the models may not be much different from observations in spite of the weaknesses noted in the simulations of the two onset mechanisms. In contrast, the episodic La Niña is produced primarily by the TP-onset mechanism, leading to an overestimation of episodic La Niña events in the models (34.5% vs 15.8% in the observations).

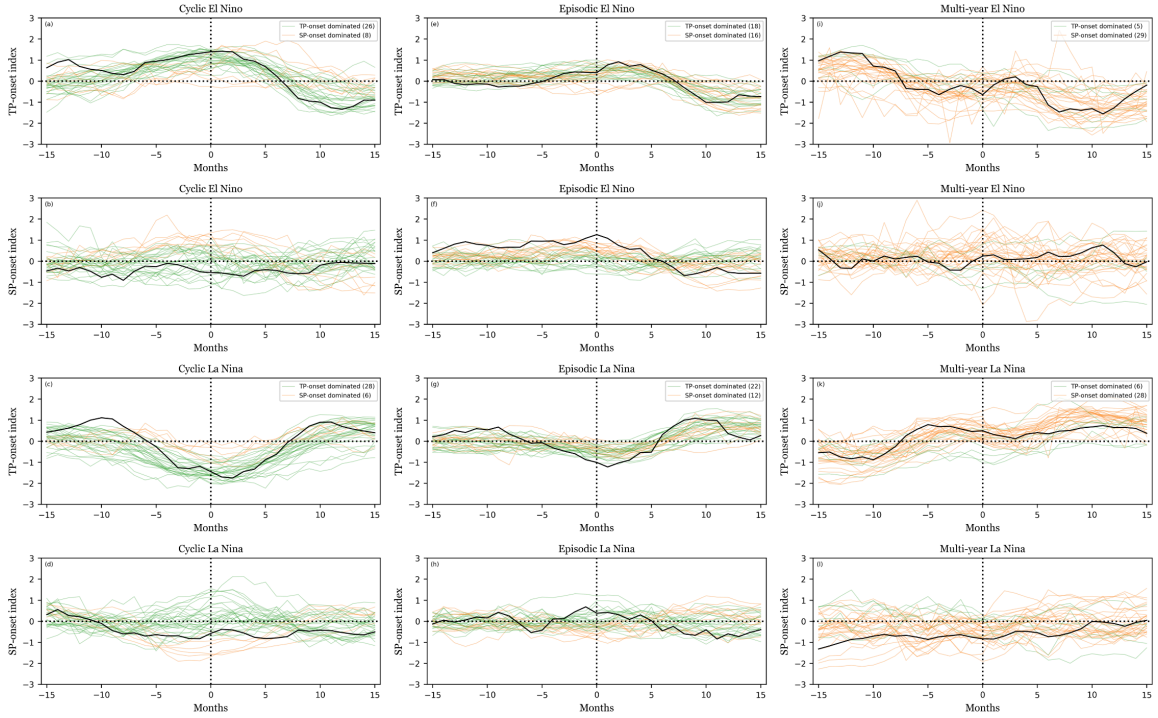

Figure 4.9. As in Figure 4.7, except the thin lines represent the mean evolutions in the individual CMIP5 models and the thick lines are the multi-model means. The black lines are the mean evolutions for the reanalysis. The green lines show transitions that are dominated by the TP-onset mechanism; defined as events where the values of the TP-onset index during the pre-onset months (3 months before the onset months) of El Niño (La Niña) are more positive (negative) than those of the SP-onset index. The orange lines illustrate the transitions that are dominated by the SP-onset mechanism.

As mentioned above, the fact that mean SSTs are close to 28°C in the equatorial central Pacific is the reason why the SP-onset mechanism produces more multi-year La Niñas than multi-year El Niños in the observations. The fact that the CMIP5 models produce a smaller asymmetry between the numbers of multi-year El Niños and La Niñas (22.3% vs. 17.8%; see Fig. 4.4b) implies that the mean SSTs in the models are different from the observations. To examine this possibility, we contrast in Figure 4.10 the mean SSTs in the tropical Pacific between the five models that produce the most multi-year La Niñas and the five models that produce most multi-year El Niños (see Fig. 4.11 for the models). The group with more multi-year La Niñas (Fig. 4.10b) has mean SSTs that are similar to the observations (Fig. 4.10a), slightly warmer than the 28°C in the equatorial central Pacific (red boxes in Fig. 4.10). In contrast, the group with more multi-year El Niños (Fig. 4.10c) shows much colder mean SSTs in the equatorial central Pacific (27.3°C). This is consistent with the suggestion of Fang & Yu (2020) that a warmer (colder) mean SST in the equatorial central Pacific favors more multi-year La Nina (El Niño) events.

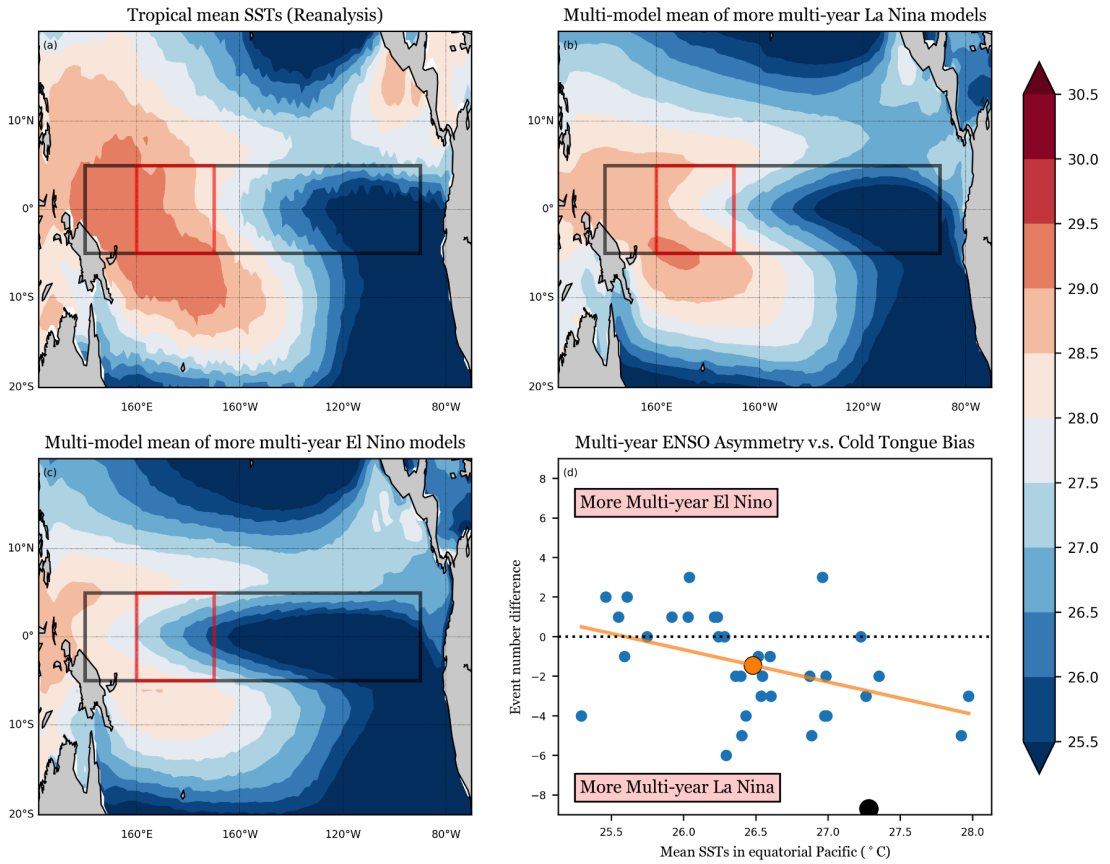

Figure 4.10. (a) Mean SSTs in the tropical Pacific calculated from (a) the observations during 1948-2016, (b) the five CMIP5 models with the most multi-year El Niños in Fig. S7, and (c) the five CMIP5 models with the most multi-year La Niñas. The red box denotes the equatorial central Pacific region (5°S-5°N and 160°E-170°W). Panel (d) displays the relationship between the event number difference and the mean SST across the equatorial Pacific (5°S-5°N and 140°E-120°W; the black box). The black dot is the reanalysis value (scaled to event numbers in 100 years as in model simulation), and the orange dot is the multi-model mean value with the orange line representing the linear regression (passing 99% significance test).

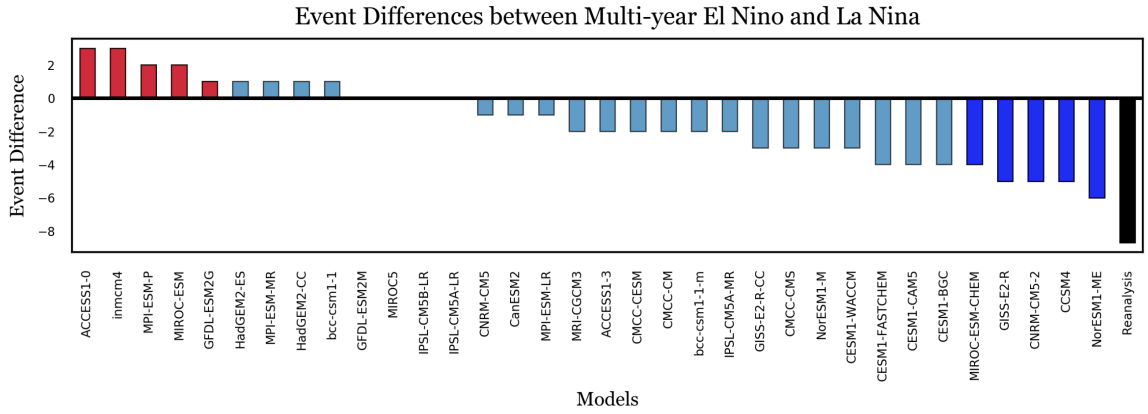

Figure 4.11. The difference in the numbers of multi-year El Niño and multi-year La Niña events. The five models with the largest positive difference (i.e., more multi-year El Niños) are shown in red and the five with the largest negative difference (i.e., more multi-year La Niñas) are shown in blue. The black bar is the reanalysis (scaled to event numbers in 100 years for comparison with 100 year long model simulations).

Contemporary models are known to have a tendency to produce a lower than observed mean SSTs in the central equatorial Pacific associated with a cold tongue that extends further westward than observed (Davey et al. 2001; Misra et al. 2008; Vannière et al. 2012; Li et al. 2016). We therefore examine in Figure 4.10d the relationship between the model differences in multi-year transitions and the model mean SSTs across the equatorial Pacific (5°S-5°N and 140°E-120°W; black boxes in Fig. 4.10). A significant (at 99% level) linear relationship exists between these two quantities. The colder the mean equatorial SSTs in the model, the stronger tendency to have more multi-year El Niños. The MMM value of the mean SST (26.5 °C) is colder than the observed value (27.3 °C), leading to the tendency for more multi-year La Niñas in the models. The well-known cold bias in the equatorial Pacific is a key reason why the CMIP5 models cannot reproduce the observed El Niño-La Niña asymmetry in multi-year transitions.

We repeat the analyses performed using the thirty-four CMIPS models with twenty CMIP6 models (Fig. 4.3) and obtain similar results without significant improvements (Fig. 4.4c). As for the CMIP5 models, the CMIP6 models also reproduce the observed transitions frequencies for El Niño but fail to reproduce the La Niña transitions (Fig. 4.12a). The underlying dynamics is also well-simulated in the CMIP6 models (Figs. 4.12b-g and 4.13). The TP-onset mechanism is also overestimated in the CMIP6 models, where the relative strengths between the two onset mechanisms is not dominated by the SP-onset mechanism for the episodic El Niño (Fig. 4.14). However, the relation between the cold tongue bias and the tendency for multi-year La Niñas is weaker in the CMIP6 models (Figs. 4.15 and 4.16). This entails that the differences between CMIP5 and CMIP6 models need to be further investigated with more CMIP6 models in the futureThe CMIP6 models does not show any significant improvement over CMIP5 models in the simulation of the ENSO transition complexity. Both sets of models fail to reproduce the observed transition complexity for La Niña.

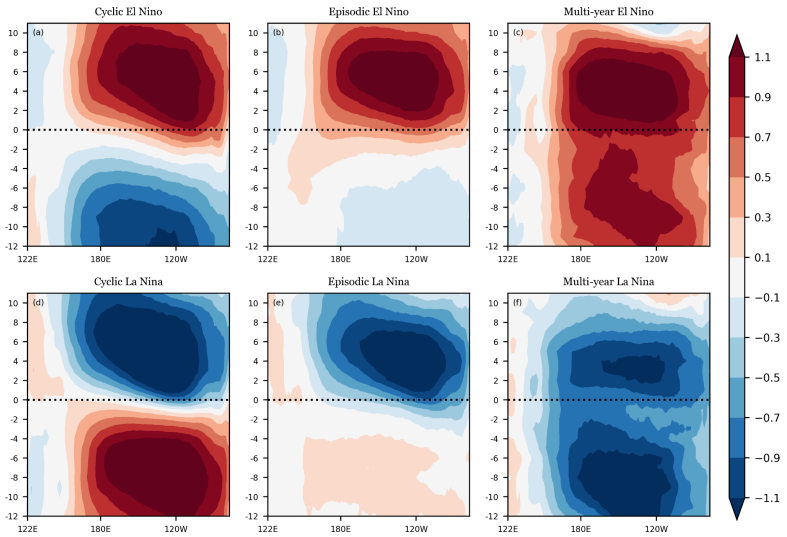

Figure 4.12. As in Fig. 4.5, except for the CMIP6 models.

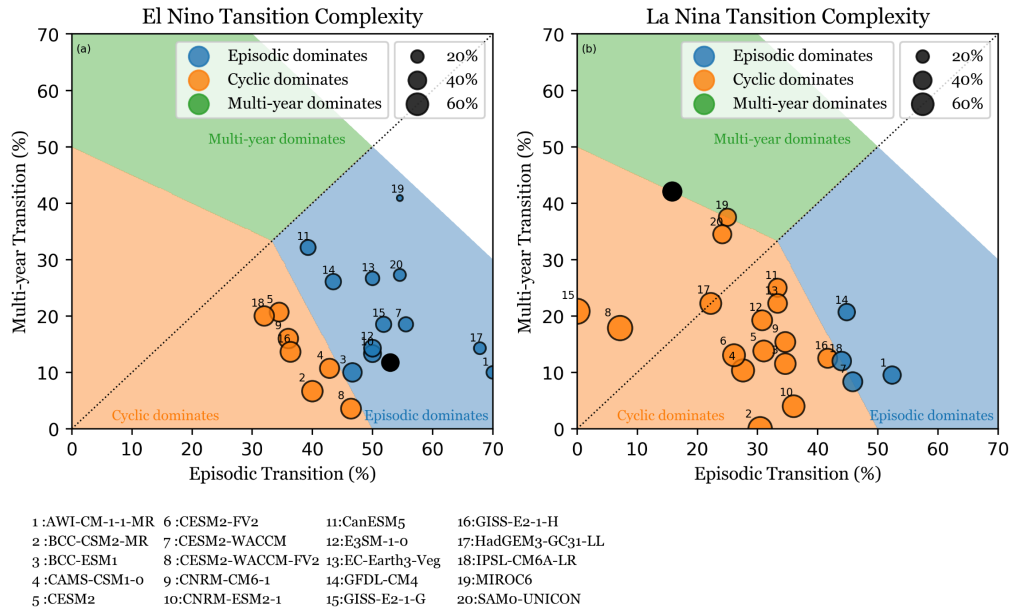

Figure 4.13. Same as Figure 4.8 but for 20 CMIP6 models.

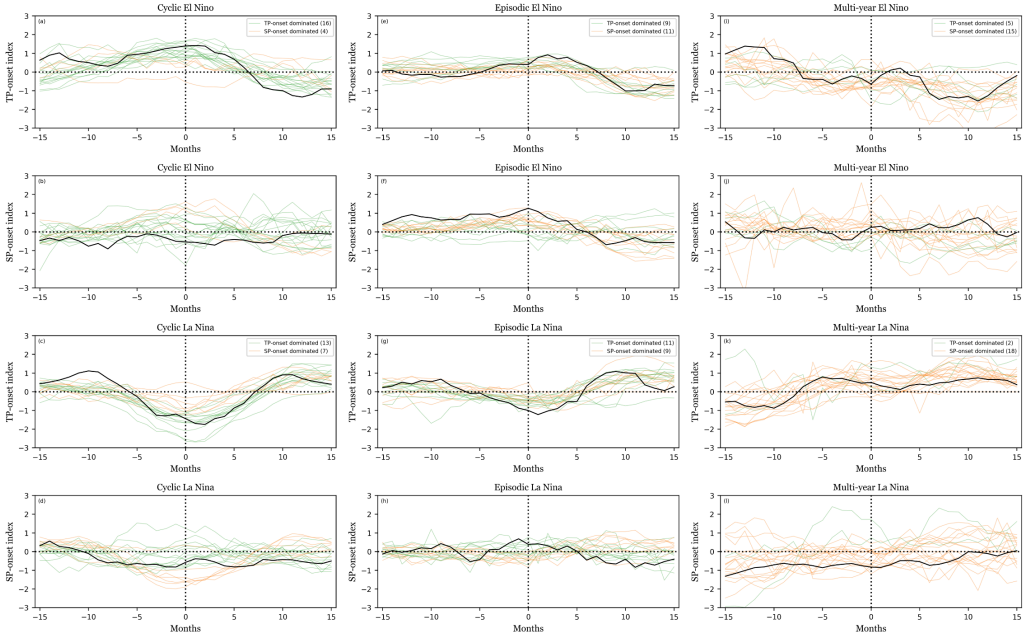

Figure 4.14. As in Figure 4.9 but for CMIP6 models.

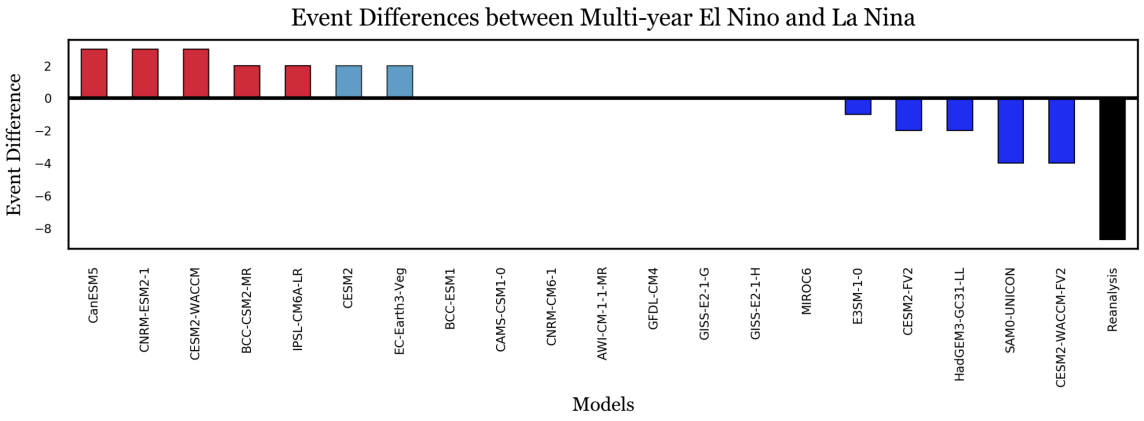

Figure 4.15. As in Figure 4.11, except for CMIP6 models.

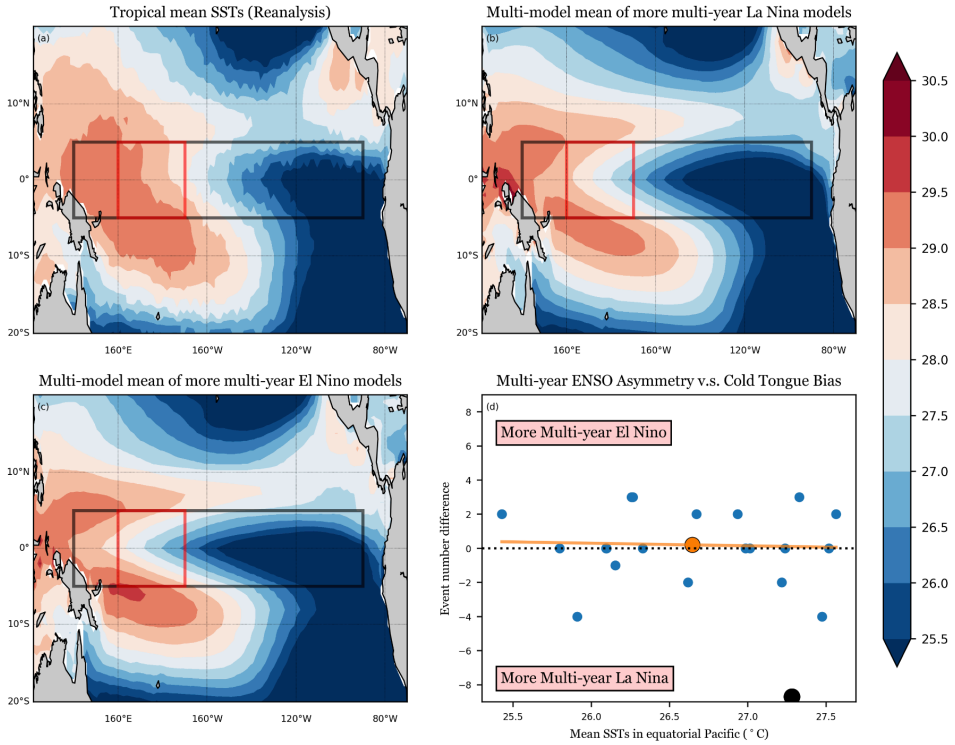

Figure 4.16. As in Figure 4.10, except for CMIP6 models.

4.6 Summary and Discussion

In this chapter, we find that there are more episodic El Niños than La Niñas and more multi-year La Niñas than El Niños in the observations. This difference is the result of the nonlinear characteristics of the SP-onset mechanism. Our findings further confirm the critical roles of the SP-onset mechanism in determining the ENSO transition complexity and the transition asymmetry between the El Niño and La Niña. We find that the CMIP5 and CMIP6 models can reproduce the transition complexity for El Niño but not for La Niña. The models tend to produce too many episodic La Niña events and too few multi-year La Niña events. We are able to link the former deficiency to a weaker than observed SP-onset mechanism in the CMIP5/6 models and the latter to a cold bias in mean state SSTs in the equatorial Pacific in the models. To achieve better simulations of ENSO transition complexity, further efforts are to improve the model deficiencies in simulating the SP-onset mechanism and mean SSTs in the equatorial Pacific.

Chapter 5

Conclusions and Future Directions

5.1 Summary of Results

In this dissertation, a dynamical framework is developed to study El Niño-Southern Oscillation (ENSO) transition complexity with a focus on the onset mechanisms of ENSO. The study is conducted with multiple reanalysis products and simulations from state-of-the-art global climate models.

Chapter 2 lays the foundation of our dynamical framework for studying ENSO transition complexity. Unlike previous ENSO studies focusing more on properties and dynamics of ENSO during the development and peak phases, our dynamical framework for ENSO transition complexity focuses on the onset phase and studies the characteristics and complexity within event-to-event transitions (Fig. 5.1). The key requirement of this framework is to obtain the intensity of distinct ENSO onset mechanisms, so that we can compare the relative importance of those onset mechanisms during different ENSO transitions. We found that the two ENSO onset mechanisms, the Tropical Pacific onset (TP-onset) and Subtropical Pacific onset (SP-onset) mechanisms, can be simultaneously represented by the two leading modes from the multi-variate empirical orthogonal function (MEOF) analysis (Xue et al. 2000). The MEOF analysis is using the combined anomalies of sea surface temperature (SST), surface wind, and sea surface height (SSH) in the tropical Pacific and can represent the surface-subsurface coupled dynamics of ENSO. The MEOF analysis is applied to reanalysis products and preindustrial runs of 34 Climate Model Intercomparison Project version 5 (CMIP5) model simulations.

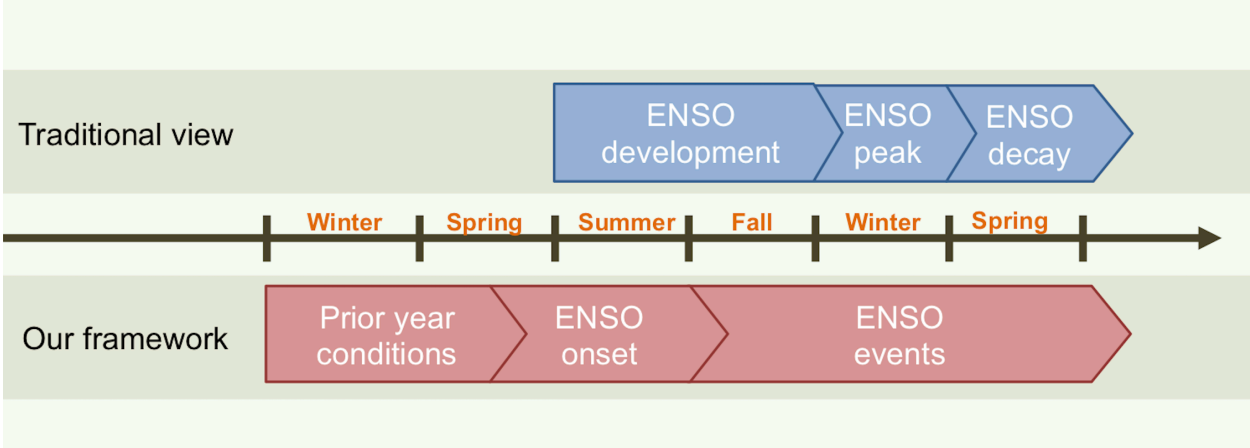

Figure 5.1. Schematic of viewpoints for ENSO complexity. The top is the traditional viewpoint and the bottom is our framework for studying ENSO transition complexity.

The two ENSO onset mechanisms, along with their statistical modes, are then used to investigate the control of onset mechanisms on the ENSO transition complexity. The TP-onset mechanism invokes equatorial thermocline variations to initiate the SST anomalies in the eastern Pacific and further triggers ENSO events. Due to its oscillatory nature, the TP-onset mechanism gives rise mostly to the cyclic ENSO transition (i.e., El Niño-to-El Niño and La Niña-to-La Niña) and contributes to a reduction in ENSO transition complexity. In contrast, the SP-onset mechanism brings subtropical Pacific SST anomalies into the equatorial central Pacific through a series of subtropical coupling and onsets an ENSO event. The SP-onset can generate all three patterns of ENSO transitions and contributes to an increase of transition complexity. These results highlight the importance of the SP-onset mechanism in ENSO transition complexity. Furthermore, the importance of the SP-onset mechanism in triggering ENSO events has increased since the 1990s, while the TP-onset mechanism has remained stable over the past six decades. The changes of ENSO properties or the increase of ENSO complexity observed in recent decades can thus be understood from the changes in the relative importance of two ENSO onset mechanisms.

Chapter 3 seeks to obtain a deeper understanding of the SP-onset mechanism with a focus on how its varying contributions to the cyclic, episodic, and multi-year ENSO transitions are established. The SP-onset mechanism is found to generate all these three transitions (in chapter 2), but only the physical process leading to the episodic transition (i.e., neutral-to-ENSO) is well studied. We find that distinct locations of ENSO SST anomalies are responsible for generating cyclic and multi-year transitions through the SP-onset mechanism. The equatorial eastern Pacific (EEP) is the key location to enable the mechanism to produce the cyclic transition; while the equatorial central Pacific (ECP) is responsible for producing the multi-year transition through the SP-onset mechanism. The El Niño warming in the EEP, for instance, can incite a Gill-type response to activate the negative phase of SP-onset mechanism to onset another La Niña event (resulting in a cyclic transition); whereas, the El Niño warming in the ECP can incite a wavetrain response to activate the positive phase of SP-onset mechanism to onset another El Niño event (resulting in a multi-year transition). Such atmospheric responses are confirmed by composite analysis in observations and by conducting atmospheric model experiments. The discovery of the two processes explains how three ENSO transitions can all be generated by the SP-onset mechanism.

We further show in chapter 3 that how frequently the cyclic and multi-year transitions can be produced by the SP-onset mechanism. Such frequency, indeed, is controlled by the mean SST-state in the tropical Pacific and is used to project the future changes of the two transitions. Why can the tropical mean SST affect the cyclic and multi-year transitions? As mentioned, these two transitions require the preceding-year ENSO events to activate the SP-onset mechanism and onset another ENSO event in the following year. Whether or not an ENSO event can activate the SP-onset mechanism depends on whether the event can induce/reduce local deep convection to

produce anomalous heating leading to its atmospheric response of each region. This is where the tropical Pacific mean-SSTs play a role in the ENSO transitions.

It is known that the total SSTs (i.e., the mean SSTs plus the SST anomalies of the ENSO event) have to exceed a threshold temperature (28°C) to excite deep convection. Since the mean SST is much lower than the convection threshold in the EEP (Fig. 3.2), only extreme El Niño events can incite convective heating to result in a cyclic La Niña (extreme El Niño-to-La Niña). Weak El Niño and all La Niña events cannot turn on the SP-onset mechanism to produce the cyclic transitions. On the other hand, the mean SSTs in the ECP are just slightly higher than the convective threshold. La Niña events here can turn-off deep convections to produce large anomalous cooling. As a result, La Niña events are more capable than El Niño events to activate the SP-onset mechanism. Through this mean state control, the SP-onset mechanism tends to produce more multi-year La Niña events than multi-year El Niño events. The results further explain why La Niña prefers to continue its cooling and forms a multi-year transition, but El Niño is easily to produce cyclic transition in the following year. Furthermore, with a future warmer climate, both EEP and ECP regions are expected to be warmer, where EEP will become closer to the convective threshold and ECP will become farer from the threshold. Therefore, we can project that cyclic transitions will increase (due to easier inducing deep convection) but multi-year transitions will decrease (due to harder reducing deep convection) in the RCP4.5 and RCP8.5 simulations of CMIP5 models.

Chapter 4 further contrasts the transition complexity between El Niño and La Niña by the classification developed for three ENSO transitions. We examined if the observed contrast can be reproduced in CMIP5/6 model simulations, and, if not, what sources of model deficiencies are. We find that the observed El Niño has the most occurrence for the episodic transition, followed by

the cyclic transition, and has the least for the multi-year transition. The reversed order is found for La Niña, which the multi-year transition and the cyclic transition have the most percentages, followed by the least frequency for the episodic transition. This El Niño-La Niña asymmetry in transition complexity is found to be related to the SP-onset mechanism. The SP-onset mechanism is more capable to produce the episodic El Niño than the episodic La Niña due to the nonlinear growth of the equatorial wind anomalies it induces; and the SP-onset mechanism is more preferable in generating the multi-year La Niña than the multi-year El Niño as described in chapter 3 of the nonlinear responses to the mean SSTs in the ECP. To our knowledge, this is the first time that the El Niño-La Niña asymmetry has even been documented and related to all three ENSO transitions.

Chapter 4 further shows that CMIP5/6 models fails to simulate this reversed transition complexity between El Niño and La Niña. CMIP5/6 models simulate a realistic order of the El Niño transitions (episodic, cyclic, and then multi-year transition) when compared to observations. However, the models erroneously produce a similar order (rather than the observed reversed order) of transition patterns for La Niña. Compared to observations, CMIP5/6 models produce too many episodic La Niñas and too few multi-year La Niñas. The key model deficiency is a cold bias in the tropical Pacific, which has been a well-known bias in contemporary climate models. Through the mean state control, this cold bias cause CMIP5/6 models to produce too few multi-year La Niñas. These results provide evidence of why CMIP5/6 models cannot simulate the observed ENSO transition complexity.

In brief, this dissertation has developed a novel dynamical framework to study ENSO transition complexity. This framework has been shown effective in explaining the observed ENSO transition

complexity and El Niño-La Niña asymmetries, assessing contemporary model performance in ENSO transition complexity, and projecting future changes in ENSO transition and its complexity.

5.2 Implications of Future Researches

The dynamical framework we develop in this dissertation offers a new perspective to understand ENSO dynamics. The possible implications of this framework are described in the following four research topics.

5.2.1 Understanding Other ENSO Complexities Arise from the Two ENSO Onset Mechanisms

In addition to the transition complexity, our framework can be further applied to study other complex behaviours of ENSO. For example, the zonal propagations of SST anomalies are distinct between El Niño and La Niña (Chen et al. 2016). La Niña tends to produce only westward propagation, while El Niño can produce both eastward and westward propagation of warming, due to their nonlinear growth of the equatorial wind anomalies it induces (Santoso et al. 2013). However, the propagation direction may also depend on where the anomalous SSTs are initiated. It is possible that the TP-onset mechanism initiates the SST anomalies in the eastern Pacific. Therefore, the SST anomalies only can propagate westward. In contrast, the SP-onset mechanism initiates the anomalies in the central Pacific, which forces the SSTs to only propagate to the east. Whether the two onset mechanisms can determine ENSO propagation may also contribute to the asymmetry in ENSO propagations. Furthermore, the ENSO onset mechanisms can also be combined with the existing understanding of ENSO complexity in order to explain more complex behaviours. As mentioned in chapter 1, for instance, ENSO is known to have two types: the eastern

Pacific type and the central Pacific type of ENSO. What ENSO transitions can generate which types of ENSO? Or how the two ENSO onset mechanisms can produce the two types of ENSO.

5.2.2 Classifying ENSO Impacts Based on the Transitions

The global impacts of ENSO are mostly studied when the ENSO SST anomalies are the largest (during its peak phase). On the contrary, ENSO impacts during other seasons are more difficult to investigate due to the weak amplitude of ENSO. Our view of ENSO transitions may provide a way to study ENSO teleconnections during these seasons. For example, Jong et al. (2020) compare the summer precipitation in the U.S. between the cyclic La Niña and multi-year La Niña. The different transitions of ENSO can be used as a classification method to separate the different global or regional climate impacts when ENSO is weak. Furthermore, as mentioned in the chapter 3, ENSO events in the EEP and ECP can induce distinct atmospheric responses through their nonlinear deep convection responses to the mean SST-state. Whether the nonlinear convective heating responses to ENSO events can also impact regional climates distinctly can also be interesting. As stated in the chapter 3, future projections on of ENSO teleconnections/impacts can also be made.

5.2.3 Improving Model Simulations and Enhancing ENSO Predictions

Throughout the entire dissertation, the SP-onset mechanism is shown to have a critical rule in ENSO transition complexity. However, we find that contemporary climate models underestimate the SP-onset mechanism and overestimate the TP-onset mechanism. Thus, the question is why do models underestimate the SP-onset mechanism? Additionally, what parameters or physical processes control the relative importance of the two onset mechanisms? By investigating these

questions, the model representation of ENSO transition complexity can improve, which may also improve the ENSO predictions using better model parameterization.

We also find in chapter 4 that the cold tongue bias can control the frequency of multi-year El Niño and multi-year La Niña. The stronger cold tongue bias, the more multi-year El Niños are produced. However, more multi-year La Niñas than multi-year El Niños is found in observations. A detailed study on the asymmetry between multi-year El Niño and La Niña may not only simulate the observed tendency of more multi-year La Niña but also help solving the cold tongue bias issue, since both quantities are significantly related.

5.2.4 Simulations of the Past and Future ENSO

This dissertation develops a novel framework to compare the ENSO transition complexity between observations and state-of-art climate model simulations. The same technique, indeed, can be applied to projecting past and future simulations of ENSO. For instance, by applying our framework to the Paleoclimate Modelling Intercomparison Project (PMIP) simulations, we can investigate whether the different mean climate states (e.g., Last Glacial Maximum, Mid-Holocene, and Little Ice Age) can produce distinct ENSO transition complexity. We can also examine whether their transition complexity is consistent with our current knowledge of ENSO dynamics. On the other hand, we can apply our framework to future RCP simulations. Although we made a simple projection of the future cyclic and multi-year transition in chapter 4, the projection did not include the episodic transition and the possible changes for the TP-onset mechanism. ENSO transition complexity should be further projected based on a more comprehensive discussion on the changes of all three transitions.

BIBLIOGRAPHY

Alexander, M. A., Vimont, D. J., Chang, P., & Scott, J. D. (2010). The impact of extratropical atmospheric variability on ENSO: Testing the seasonal footprinting mechanism using coupled model experiments. *Journal of Climate*, *23*(11), 2885-2901.

Amaya, D. J. (2019). The Pacific Meridional Mode and ENSO: a Review. *Current Climate Change Reports*, 1-12.

An, S. I., & Kim, J. W. (2017). Role of nonlinear ocean dynamic response to wind on the asymmetrical transition of El Niño and La Niña. *Geophysical Research Letters*, *44*(1), 393-400.

An, S. I., & Kim, J. W. (2018). ENSO transition asymmetry: Internal and external causes and intermodel diversity. *Geophysical Research Letters*, *45*(10), 5095-5104.

Anderson, B. T., Perez, R.C. & Karspeck, A.. (2013). Triggering of El Niño onset through trade wind–induced charging of the equatorial Pacific. *Geophysical Research Letters,* 40.6, 1212-1216.

Anderson, B. T., & Perez, R. C. (2015). ENSO and non-ENSO induced charging and discharging of the equatorial Pacific. *Climate Dynamics*, *45*(9-10), 2309-2327.

Ashok, K., Behera, S. K., Rao, S. A., Weng, H., & Yamagata, T. (2007). El Niño Modoki and its possible teleconnection. *Journal of Geophysical Research: Oceans*, *112*(C11).

Back, L. E. & Bretherton C. S. (2009). On the relationship between SST gradients, boundary layer winds, and convergence over the tropical oceans. *Journal of Climate* 22(15), 4182-4196.

Balmaseda, M. A., Mogensen, K., & Weaver, A. T. (2013). Evaluation of the ECMWF ocean reanalysis system ORAS4. *Quarterly Journal of the Royal Meteorological Society*, *139*(674), 1132-1161.

Barnston, A. G., Leetmaa, A., Kousky, V. E., Livezey, R. E., O'Lenic, E. A., Van den Dool, H., ... & Unger, D. A. (1999). NCEP forecasts of the El Niño of 1997–98 and its US impacts. *Bulletin of the American Meteorological Society*, *80*(9), 1829-1852.

Battisti, D. S. & Anthony C. H. (1989) Interannual variability in a tropical atmosphere–ocean model: Influence of the basic state, ocean geometry and nonlinearity. *Journal of the atmospheric sciences,* 46.12, 1687-1712.

Bjerknes, J. (1969). Atmospheric teleconnections from the equatorial pacific 1. *Monthly Weather Review*, *97*(3), 163-172.

Cai, W., Wang, G., Santoso, A., McPhaden, M. J., Wu, L., Jin, F. F., ... & England, M. H. (2015). Increased frequency of extreme La Niña events under greenhouse warming. *Nature Climate Change*, *5*(2), 132-137.

Cai, W., Santoso, A., Wang, G., Yeh, S. W., An, S. I., Cobb, K. M., ... & Lengaigne, M. (2015). ENSO and greenhouse warming. *Nature Climate Change*, *5*(9), 849-859.

Capotondi, A., Wittenberg, A. T., Newman, M., Di Lorenzo, E., Yu, J. Y., Braconnot, P., ... & Jin, F. F. (2015). Understanding ENSO diversity. *Bulletin of the American Meteorological Society*, *96*(6), 921-938.

Capotondi, A., & Sardeshmukh, P. D. (2015). Optimal precursors of different types of ENSO events. *Geophysical Research Letters*, *42*(22), 9952-9960.

Chang, P., L. Ji, H. Li, and M. Flugel (1996), Chaotic dynamics versus stochastic processes in El Niño–Southern Oscillation in coupled ocean-atmosphere models, *Physica D*, **98**, 301–320.

Chang, P., Ji, L., & Li, H. (1997). A decadal climate variation in the tropical Atlantic Ocean from thermodynamic air-sea interactions. *Nature*, *385*(6616), 516.

Chang, P., L. Zhang, R. Saravanan, D. J. Vimont, J. C. H. Chiang, L. Ji, H. Seidel, and M. K. Tippett (2007). Pacific meridinal mode and El Niño-Southern Oscillation. *Geophys. Res. Lett.*, **34**, L16608, doi:10.1029/2007GL030302.

Chen, C., Cane, M. A., Henderson, N., Lee, D. E., Chapman, D., Kondrashov, D., & Chekroun, M. D. (2016). Diversity, Nonlinearity, Seasonality, and Memory Effect in ENSO Simulation and Prediction Using Empirical Model Reduction. *Journal of Climate*, *29*(5), 1809-1830.

Chen, C., Cane, M. A., Wittenberg, A. T., & Chen, D. (2017). ENSO in the CMIP5 Simulations: Life Cycles, Diversity, and Responses to Climate Change. *Journal of Climate*, *30*(2), 775-801.

Chen, D., Lian, T., Fu, C., Cane, M. A., Tang, Y., Murtugudde, R., ... & Zhou, L. (2015). Strong influence of westerly wind bursts on El Niño diversity. *Nature Geoscience*, *8*(5), 339-345.

Chen, H. C., Sui, C. H., Tseng, Y. H., & Huang, B. (2015). An analysis of the linkage of Pacific subtropical cells with the recharge–discharge processes in ENSO evolution. *Journal of Climate*, *28*(9), 3786-3805.

Chen, M., Li, T., Shen, X., & Wu, B. (2016). Relative roles of dynamic and thermodynamic processes in causing evolution asymmetry between El Niño and La Niña. *Journal of Climate*, *29*(6), 2201-2220.

Chen, N., & Majda, A. J. (2016). Simple dynamical models capturing the key features of the Central Pacific El Niño. *Proceedings of the National Academy of Sciences*, *113*(42), 11732-11737.

Chen, N., Thual, S., & Stuecker, M. F. (2019). El Niño and the Southern Oscillation: Theory. Book Chapter in *Reference Module in Earth Systems and Environmental Sciences.*

Chiang, J. C., & Vimont, D. J. (2004). Analogous Pacific and Atlantic meridional modes of tropical atmosphere–ocean variability. *Journal of Climate*, *17*(21), 4143-4158.

Choi, K. Y., Vecchi, G. A., & Wittenberg, A. T. (2013). ENSO transition, duration, and amplitude asymmetries: Role of the nonlinear wind stress coupling in a conceptual model. *Journal of Climate*, *26*(23), 9462-9476.

Coelho, C. A., & Goddard, L. (2009). El Niño–induced tropical droughts in climate change projections. *Journal of Climate*, *22*(23), 6456-6476.

Collins, M., An, S. I., Cai, W., Ganachaud, A., Guilyardi, E., Jin, F. F., ... & Vecchi, G. (2010). The impact of global warming on the tropical Pacific Ocean and El Niño. *Nature Geoscience*, *3*(6), 391.

Davey, M. et al. (2002) STOIC: a study of coupled model climatology and variability in tropical ocean regions. *Climate Dynamics,* 18.5, 403-420.

Dewitte, B., Vazquez-Cuervo, J., Goubanova, K., Illig, S., Takahashi, K., Cambon, G., ... & Ortlieb, L. (2012). Change in El Nino flavours over 1958–2008: Implications for the long-term trend of the upwelling off Peru. *Deep Sea Research Part II: Topical Studies in Oceanography*, *77*, 143-156.

Di Lorenzo, E., Cobb, K. M., Furtado, J. C., Schneider, N., Anderson, B. T., Bracco, A., ... & Vimont, D. J. (2010). Central pacific El Nino and decadal climate change in the North Pacific ocean. *Nature Geoscience*, *3*(11), 762.

DiNezio, P. N., & Deser, C. (2014). Nonlinear controls on the persistence of La Niña. *Journal of Climate*, *27*(19), 7335-7355.

DiNezio, P. N., Deser, C., Okumura, Y., & Karspeck, A. (2017). Predictability of 2-year La Niña events in a coupled general circulation model. *Climate Dynamics*, *49*(11-12), 4237-4261.

Dommenget, D., Bayr, T., & Frauen, C. (2013). Analysis of the non-linearity in the pattern and time evolution of El Niño southern oscillation. *Climate dynamics*, *40*(11-12), 2825-2847.

Donnelly, J. P., & Woodruff, J. D. (2007). Intense hurricane activity over the past 5,000 years controlled by El Niño and the West African monsoon. *Nature*, *447*(7143), 465.

Fang, S.-W. & Yu, J.-Y. (2020). A Control of ENSO Transition Complexity by Tropical Pacific Mean SSTs through Tropical-Subtropical Interaction. *Geophysical Research Letters* (In press).

Fedorov, A. V., Harper, S. L., Philander, S. G., Winter, B., & Wittenberg, A. (2003). How predictable is El Niño?. *Bulletin of the American Meteorological Society*, *84*(7), 911-920.

Frauen, C., & Dommenget, D. (2010). El Niño and La Niña amplitude asymmetry caused by atmospheric feedbacks. *Geophysical Research Letters*, *37*(18).

Gill, A. (1980). Some simple solutions for heat-induced tropical circulation. *Quarterly Journal of the Royal Meteorological Society*, *106*(449), 447-462.

Graf, H. F., & Zanchettin, D. (2012). Central Pacific El Niño, the "subtropical bridge," and Eurasian climate. *Journal of Geophysical Research: Atmospheres*, *117*(D1).

Ham, Y. G., & Kug, J. S. (2012). How well do current climate models simulate two types of El Nino?. *Climate dynamics*, *39*(1-2), 383-398.

Ham, Y. G., Kug, J. S., Park, J. Y., & Jin, F. F. (2013). Sea surface temperature in the north tropical Atlantic as a trigger for El Niño/Southern Oscillation events. *Nature Geoscience*, *6*(2), 112-116.

Hu, Z. Z., Kumar, A., Xue, Y., & Jha, B. (2014). Why were some La Niñas followed by another La Niña?. *Climate dynamics*, *42*(3-4), 1029-1042.

Hu, Z. Z., Kumar, A., Huang, B., Zhu, J., Zhang, R. H., & Jin, F. F. (2017). Asymmetric evolution of El Niño and La Niña: the recharge/discharge processes and role of the off-equatorial sea surface height anomaly. *Climate Dynamics*, *49*(7-8), 2737-2748.

Jin, F. F. (1997a). An equatorial ocean recharge paradigm for ENSO. Part I: Conceptual model. *Journal of the Atmospheric Sciences*, *54*(7), 811-829.

Jin, F. F. (1997b). An equatorial ocean recharge paradigm for ENSO. Part II: A stripped-down coupled model. *Journal of the Atmospheric Sciences*, *54*(7), 830-847.

Jin, F. F., An, S. I., Timmermann, A., & Zhao, J. (2003). Strong El Niño events and nonlinear dynamical heating. *Geophysical research letters*, *30*(3), 20-1.

Johnson, N. C., & Xie, S. P. (2010). Changes in the sea surface temperature threshold for tropical convection. *Nature Geoscience*, *3*(12), 842.

Jong, B. T., Ting, M., Seager, R., & Anderson, W. B. (2020). ENSO teleconnections and impacts on US summertime temperature during multi-year La Niña life-cycle. *Journal of Climate*, (2020).

Kalnay, E., Kanamitsu, M., Kistler, R., Collins, W., Deaven, D., Gandin, L., ... & Zhu, Y. (1996). The NCEP/NCAR 40-year reanalysis project. *Bulletin of the American meteorological Society*, *77*(3), 437-471.

Kao, H. Y., & Yu, J. Y. (2009). Contrasting eastern-Pacific and central-Pacific types of ENSO. *Journal of Climate*, *22*(3), 615-632.

Kim, S. T., & Yu, J. Y. (2012). The two types of ENSO in CMIP5 models. *Geophysical Research Letters*, *39*(11).

Kim, S. T., Cai, W., Jin, F. F., Santoso, A., Wu, L., Guilyardi, E., & An, S. I. (2014). Response of El Niño sea surface temperature variability to greenhouse warming. *Nature Climate Change*, *4*(9), 786.

Kirtman, B. P. (1997). Oceanic Rossby wave dynamics and the ENSO period in a coupled model. *Journal of climate*, *10*(7), 1690-1704.

Kirtman, B., Power, S. B., Adedoyin, A. J., Boer, G. J., Bojariu, R., Camilloni, I., ... & Prather, M. (2013). Near-term climate change: projections and predictability.

Kobayashi, S., Ota, Y., Harada, Y., Ebita, A., Moriya, M., Onoda, H., ... & Miyaoka, K. (2015). The JRA-55 reanalysis: General specifications and basic characteristics. *Journal of the Meteorological Society of Japan. Ser. II*, *93*(1), 5-48.

Köhl, A. (2015). Evaluation of the GECCO2 ocean synthesis: transports of volume, heat and freshwater in the Atlantic. *Quarterly Journal of the Royal Meteorological Society*, *141*(686), 166-181.

Kug, J. S., Jin, F. F., & An, S. I. (2009). Two types of El Niño events: cold tongue El Niño and warm pool El Niño. *Journal of Climate*, *22*(6), 1499-1515.

Larkin, N. K., & Harrison, D. E. (2005). Global seasonal temperature and precipitation anomalies during El Niño autumn and winter. *Geophysical Research Letters*, *32*(16).

Larson, S., & Kirtman, B. (2013). The Pacific Meridional Mode as a trigger for ENSO in a high-resolution coupled model. *Geophysical Research Letters*, *40*(12), 3189-3194.

Larson, S. M., & Kirtman, B. P. (2014). The Pacific meridional mode as an ENSO precursor and predictor in the North American multimodel ensemble. *Journal of Climate*, *27*(18), 7018-7032.

Lee, T., & McPhaden, M. J. (2010). Increasing intensity of El Niño in the central-equatorial Pacific. *Geophysical Research Letters*, *37*(14).

Lee, S. K., Mapes, B. E., Wang, C., Enfield, D. B., & Weaver, S. J. (2014). Springtime ENSO phase evolution and its relation to rainfall in the continental US. *Geophysical Research Letters*, *41*(5), 1673-1680.

Lee, S. K., DiNezio, P. N., Chung, E. S., Yeh, S. W., Wittenberg, A. T., & Wang, C. (2014). Spring persistence, transition, and resurgence of El Niño. *Geophysical Research Letters*, *41*(23), 8578-8585.

Lee, R. W. K., Tam, C. Y., Sohn, S. J., & Ahn, J. B. (2018). Predictability of two types of El Niño and their climate impacts in boreal spring to summer in coupled models. *Climate dynamics*, *51*(11-12), 4555-4571.

Levitus, S., Antonov, J. I., Boyer, T. P., Locarnini, R. A., Garcia, H. E., & Mishonov, A. V. (2009). Global ocean heat content 1955–2008 in light of recently revealed instrumentation problems. *Geophysical Research Letters*, *36*(7).

Li, G., Xie, S. P., Du, Y., & Luo, Y. (2016). Effects of excessive equatorial cold tongue bias on the projections of tropical Pacific climate change. Part I: The warming pattern in CMIP5 multi-model ensemble. *Climate dynamics*, *47*(12), 3817-3831.

Li, W., Zhang, P., Ye, J., Li, L., & Baker, P. A. (2011). Impact of two different types of El Niño events on the Amazon climate and ecosystem productivity. *Journal of Plant Ecology*, *4*(1-2), 91-99.

Li, X., Li, C., Ling, J., & Tan, Y. (2015). The Relationship between Contiguous El Niño and La Niña Revealed by Self-Organizing Maps. *Journal of Climate*, *28*(20), 8118-8134.

Linkin, M. E., & Nigam, S. (2008). The North Pacific Oscillation–west Pacific teleconnection pattern: Mature-phase structure and winter impacts. *Journal of Climate*, *21*(9), 1979-1997.

Lyu, K. and J.-Y. Yu (2017). Climate impacts of the Atlantic Multidecadal Oscillation simulated in the CMIP5 models: a re-evaluation based on a revised index, *Geophysical Research Letters*, 44, DOI: 10.1002/2017GL072681.

McGregor, S., Ramesh, N., Spence, P., England, M. H., McPhaden, M. J., & Santoso, A. (2013). Meridional movement of wind anomalies during ENSO events and their role in event termination. *Geophysical Research Letters*, *40*(4), 749-754.

McPhaden, M. J., & Zhang, X. (2009). Asymmetry in zonal phase propagation of ENSO sea surface temperature anomalies. *Geophysical Research Letters*, *36*(13).

McPhaden, M. J., Zebiak, S. E., & Glantz, M. H. (2006). ENSO as an integrating concept in earth science. *science*, *314*(5806), 1740-1745.

Meehl, G. A., Washington, W. M., Santer, B. D., Collins, W. D., Arblaster, J. M., Hu, A., ... & Strand, W. G. (2006). Climate change projections for the twenty-first century and climate change commitment in the CCSM3. *Journal of climate*, *19*(11), 2597-2616.

Misra, V., Marx, L., Brunke, M., & Zeng, X. (2008). The equatorial Pacific cold tongue bias in a coupled climate model. *Journal of climate*, *21*(22), 5852-5869.

Nakagawa, M., Tanaka, K., Nakashizuka, T., Ohkubo, T., Kato, T., Maeda, T., ... & Teo, S. (2000). Impact of severe drought associated with the 1997–1998 El Nino in a tropical forest in Sarawak. *Journal of Tropical Ecology*, *16*(3), 355-367.

Newman, M., Shin, S. I., & Alexander, M. A. (2011). Natural variation in ENSO flavors. *Geophysical Research Letters*, *38*(14).

Newman, M., Alexander, M. A., Ault, T. R., Cobb, K. M., Deser, C., Di Lorenzo, E., ... & Schneider, N. (2016). The Pacific decadal oscillation, revisited. *Journal of Climate*, *29*(12), 4399-4427.

Ñiquen, M., & Bouchon, M. (2004). Impact of El Niño events on pelagic fisheries in Peruvian waters. *Deep sea research part II: topical studies in oceanography*, *51*(6-9), 563-574.

North, G. R., 1984: Empirical orthogonal functions and normal modes. *Journal of the Atmospheric Science*,41, 879–887.

Ohba, M., & Watanabe, M. (2012). Role of the Indo-Pacific interbasin coupling in predicting asymmetric ENSO transition and duration. *Journal of climate*, *25*(9), 3321-3335.

Ohba, M., & Ueda, H. (2009). Role of nonlinear atmospheric response to SST on the asymmetric transition process of ENSO. *Journal of Climate*, *22*(1), 177-192.

Okumura, Y. M., & Deser, C. (2010). Asymmetry in the duration of El Niño and La Niña. *Journal of Climate*, *23*(21), 5826-5843.

Okumura, Y. M., DiNezio, P., & Deser, C. (2017). Evolving impacts of multiyear La Niña events on atmospheric circulation and US drought. *Geophysical Research Letters*, *44*(22), 11-614.

Okumura, Y. M., Ohba, M., Deser, C., & Ueda, H. (2011). A proposed mechanism for the asymmetric duration of El Niño and La Niña. *Journal of climate*, *24*(15), 3822-3829.

Paek, H., Yu, J.-Y., & Qian. C. (2017). Why were the 2015/2016 and 1997/1998 extreme El Niños different?. *Geophys. Res. Lett*., 44.

Picaut, J., Masia, F., & Du Penhoat, Y. (1997). An advective-reflective conceptual model for the oscillatory nature of the ENSO. *Science*, *277*(5326), 663-666.

Pillai, P. A., Rao, S. A., George, G., Rao, D. N., Mahapatra, S., Rajeevan, M., ... & Salunke, K. (2017). How distinct are the two flavors of El Niño in retrospective forecasts of Climate Forecast System version 2 (CFSv2)?. *Climate Dynamics*, *48*(11-12), 3829-3854.

Power, S., Delage, F., Chung, C., Kociuba, G., & Keay, K. (2013). Robust twenty-first-century projections of El Niño and related precipitation variability. *Nature*, *502*(7472), 541.

Quiroz, R. S. (1983). The climate of the "El Niño" winter of 1982–83—A season of extraordinary climatic anomalies. *Monthly Weather Review*, *111*(8), 1685-1706.

Rayner, N. A., Parker, D. E., Horton, E. B., Folland, C. K., Alexander, L. V., Rowell, D. P., ... & Kaplan, A. (2003). Global analyses of sea surface temperature, sea ice, and night marine air temperature since the late nineteenth century. *Journal of Geophysical Research: Atmospheres*, *108*(D14).

Ren, H. L., & Jin, F. F. (2013). Recharge oscillator mechanisms in two types of ENSO. *Journal of Climate*, *26*(17), 6506-6523.

Sabin, T. P., Babu, C. A., & Joseph, P. V. (2013). SST–convection relation over tropical oceans. *International journal of climatology*, *33*(6), 1424-1435.

Santoso, A., McGregor, S., Jin, F. F., Cai, W., England, M. H., An, S. I., ... & Guilyardi, E. (2013). Late-twentieth-century emergence of the El Niño propagation asymmetry and future projections. *Nature*, *504*(7478), 126-130.

Santoso, A., Mcphaden, M. J., & Cai, W. (2017). The defining characteristics of ENSO extremes and the strong 2015/2016 El Niño. *Reviews of Geophysics*, *55*(4), 1079-1129.

Schneider, E. K., Huang, B., & Shukla, J. (1995). Ocean wave dynamics and El Nino. *Journal of climate*, *8*(10), 2415-2439.

Smith, T. M., Reynolds, R. W., Peterson, T. C., & Lawrimore, J. (2008). Improvements to NOAA's historical merged land–ocean surface temperature analysis (1880–2006). *Journal of Climate*, *21*(10), 2283-2296.

Sohn, S. J., Tam, C. Y., & Jeong, H. I. (2016). How do the strength and type of ENSO affect SST predictability in coupled models. *Scientific reports*, *6*, 33790.

Stuecker, M. F. (2018). Revisiting the Pacific meridional mode. *Scientific reports*, *8*(1), 1-9.

Suarez, M. J., & Schopf, P. S. (1988). A delayed action oscillator for ENSO. *Journal of the atmospheric Sciences*, *45*(21), 3283-3287.

Sud, Y. C., Walker, G. K., & Lau, K. M. (1999). Mechanisms regulating sea-surface temperatures and deep convection in the tropics. *Geophysical research letters*, *26*(8), 1019-1022.

Takahashi, K., Montecinos, A., Goubanova, K., & Dewitte, B. (2011). ENSO regimes: Reinterpreting the canonical and Modoki El Niño. *Geophysical Research Letters*, *38*(10).

Taylor, K. E., Stouffer, R. J., & Meehl, G. A. (2012). An overview of CMIP5 and the experiment design. *Bulletin of the American Meteorological Society*, *93*(4), 485-498.

Thomas, E. E., & Vimont, D. J. (2016). Modeling the mechanisms of linear and nonlinear ENSO responses to the Pacific meridional mode. *Journal of Climate*, *29*(24), 8745-8761.

Thual, S., Majda, A. J., Chen, N., & Stechmann, S. N. (2016). Simple stochastic model for El Niño with westerly wind bursts. *Proceedings of the National Academy of Sciences*, *113*(37), 10245-10250.

Timmermann, A., An, S. I., Kug, J. S., Jin, F. F., Cai, W., Capotondi, A., ... & Stein, K. (2018). El Niño–southern oscillation complexity. *Nature*, *559*(7715), 535-545.

Vannière, B., Guilyardi, E., Madec, G., Doblas-Reyes, F. J., & Woolnough, S. (2013). Using seasonal hindcasts to understand the origin of the equatorial cold tongue bias in CGCMs and its impact on ENSO. *Climate dynamics*, *40*(3-4), 963-981.

Vecchi, G. A., & Wittenberg, A. T. (2010). El Niño and our future climate: Where do we stand?. *Wiley Interdisciplinary Reviews: Climate Change*, *1*(2), 260-270.

Vimont, D. J., Wallace, J. M., & Battisti, D. S. (2003). The seasonal footprinting mechanism in the Pacific: Implications for ENSO. *Journal of Climate*, *16*(16), 2668-2675.

Wang, B., Wu, R., & Fu, X. (2000). Pacific–East Asian teleconnection: how does ENSO affect East Asian climate?. *Journal of Climate*, *13*(9), 1517-1536.

Wang, B. et al. (2019). Historical change of El Niño properties sheds light on future changes of extreme El Niño.. *Proceedings of the National Academy of Sciences,* 116.45, 22512-22517.

Wang, C., Weisberg, R. H., & Virmani, J. I. (1999). Western Pacific interannual variability associated with the El Niño-Southern Oscillation. *Journal of Geophysical Research: Oceans*, *104*(C3), 5131-5149.

Wang, C. (2000). On the atmospheric responses to tropical Pacific heating during the mature phase of El Niño. *Journal of the atmospheric sciences*, *57*(22), 3767-3781.

Wang, C., & Wang, X. (2013). Classifying El Niño Modoki I and II by different impacts on rainfall in southern China and typhoon tracks. *Journal of Climate*, *26*(4), 1322-1338.

Wang, C., Deser, C., Yu, J. Y., DiNezio, P., & Clement, A. (2017). El Niño and Southern Oscillation (ENSO): A Review. In *Coral Reefs of the Eastern Tropical Pacific* (pp. 85-106). Springer Netherlands.

Wang, L., Yu, J. Y., & Paek, H. (2017). Enhanced biennial variability in the Pacific due to Atlantic capacitor effect. *Nature Communications*, *8*, 14887.

Wang, S. Y., L'Heureux, M., & Chia, H. H. (2012). ENSO prediction one year in advance using western North Pacific sea surface temperatures. *Geophysical Research Letters*, *39*(5).

Wang, S. Y., L'Heureux, M., & Yoon, J. H. (2013). Are greenhouse gases changing ENSO precursors in the western North Pacific?. *Journal of Climate*, *26*(17), 6309-6322.

Weisberg, R. H., & Wang, C. (1997). A western Pacific oscillator paradigm for the El Niño-Southern Oscillation. *Geophysical research letters*, *24*(7), 779-782.

Widlansky, M. J., Timmermann, A., & Cai, W. (2015). Future extreme sea level seesaws in the tropical Pacific. *Science advances*, *1*(8), e1500560.

Wu, X., Okumura, Y. M., & DiNezio, P. N. (2019). What Controls the Duration of El Niño and La Niña Events?. *Journal of Climate*, *32*(18), 5941-5965.

Wyrtki, K. (1975). El Niño—the dynamic response of the equatorial Pacific Oceanto atmospheric forcing. *Journal of Physical Oceanography*, *5*(4), 572-584.

Xie, S. P. (1999). A dynamic ocean–atmosphere model of the tropical Atlantic decadal variability. *Journal of Climate*, *12*(1), 64-70.

Xie, S. P., & Philander, S. G. H. (1994). A coupled ocean-atmosphere model of relevance to the ITCZ in the eastern Pacific. *Tellus A*, *46*(4), 340-350.

Xu, K., Tam, C. Y., Zhu, C., Liu, B., & Wang, W. (2017). CMIP5 projections of two types of El Niño and their related tropical precipitation in the twenty-first century. *Journal of Climate*, *30*(3), 849-864.

Xue, Y., Leetmaa, A., & Ji, M. (2000). ENSO prediction with Markov models: The impact of sea level. *Journal of Climate*, *13*(4), 849-871.

Yang, S., Li, Z., Yu, J. Y., Hu, X., Dong, W., & He, S. (2018). El Niño–Southern oscillation and its impact in the changing climate. *National Science Review*, *5*(6), 840-857.

Yeh, S. W., Kug, J. S., Dewitte, B., Kwon, M. H., Kirtman, B. P., & Jin, F. F. (2009). El Niño in a changing climate. *Nature*, *461*(7263), 511.

Yeh, S. W., Kirtman, B. P., Kug, J. S., Park, W., & Latif, M. (2011). Natural variability of the central Pacific El Niño event on multi-centennial timescales. *Geophysical Research Letters*, *38*(2).

Yeh, S. W., Kug, J. S., & An, S. I. (2014). Recent progress on two types of El Niño: Observations, dynamics, and future changes. *Asia-Pacific Journal of Atmospheric Sciences*, *50*(1), 69-81.

Yu, J-Y, & Fang S-W. (2018). The Distinct Contributions of the Seasonal Footprinting and Charged-Discharged Mechanisms to ENSO Complexity. *Geophysical Research Letters,* 45.13, 6611-6618.

Yu, J. Y., & Kao, H. Y. (2007). Decadal changes of ENSO persistence barrier in SST and ocean heat content indices: 1958–2001. *Journal of Geophysical Research: Atmospheres*, *112*(D13).

Yu, J. Y., Kao, H. Y., & Lee, T. (2010). Subtropics-related interannual sea surface temperature variability in the central equatorial Pacific. *Journal of Climate*, *23*(11), 2869-2884.

Yu, J. Y., & Kim, S. T. (2011). Relationships between extratropical sea level pressure variations and the central Pacific and eastern Pacific types of ENSO. *Journal of Climate*, *24*(3), 708-720.

Yu, J. Y., Lu, M. M., & Kim, S. T. (2012). A change in the relationship between tropical central Pacific SST variability and the extratropical atmosphere around 1990. *Environmental Research Letters*, *7*(3), 034025.

Yu, J. Y., Kao, P. K., Paek, H., Hsu, H. H., Hung, C. W., Lu, M. M., & An, S. I. (2015). Linking emergence of the central Pacific El Niño to the Atlantic multidecadal oscillation. *Journal of Climate*, *28*(2), 651-662.

Yuan, Y., & Yang, S. (2012). Impacts of different types of El Niño on the East Asian climate: Focus on ENSO cycles. *Journal of Climate*, *25*(21), 7702-7722.

Yu, J. Y., Kao, P. K., Paek, H., Hsu, H. H., Hung, C. W., Lu, M. M., & An, S. I. (2015). Linking emergence of the central Pacific El Niño to the Atlantic multidecadal oscillation. *Journal of Climate*, *28*(2), 651-662.

Yu, J.-Y., X. Wang, S. Yang, H. Paek, and M. Chen (2017). Changing El Niño-Southern Oscillation and Associated Climate Extremes, Book Chapter in *Climate Extremes: Patterns and Mechanisms*, Wang, S.-Y., Jin-Ho Yoon, Chris Funk, and R. R. Gillies (Ed.), AGU Geophysical Monograph Series, Vol. 226, Pages 3-38.

Zebiak, S. E., & Cane, M. A. (1987). A model El Niño–southern oscillation. *Monthly Weather Review*, *115*(10), 2262-2278.

Zhang, C. (1993). Large-scale variability of atmospheric deep convection in relation to sea surface temperature in the tropics. *Journal of Climate*, *6*(10), 1898-1913.

Zhang, W., Jin, F. F., Li, J., & Ren, H. L. (2011). Contrasting impacts of two-type El Niño over the western North Pacific during boreal autumn. *Journal of the Meteorological Society of Japan. Ser. II*, *89*(5), 563-569.

Zhang, H., Clement, A., & Di Nezio, P. (2014). The South Pacific meridional mode: A mechanism for ENSO-like variability. *Journal of Climate*, *27*(2), 769-783.